SAPIENZA
UNIVERSITÀ DI ROMA

PhD Course in Molecular Medicine

XXXVII cycle

Coordinator Prof. Giuseppe Giannini

Targeted therapies for Malignant Mesothelioma.

Candidate

Valentina Angiolini
Matricola 1679872

Tutor

Prof.ssa Laura Masuelli

A.A. 2023-2024

SOMMARIO

ABSTRACT

Malignant mesothelioma (MM) is an aggressive neoplasia arising from mesothelial cells that line serous cavities, such as pleura, peritoneum, pericardium, and vaginal tunic. It is defined as an occupational disease because it is related to asbestos exposure. It mainly affects people between 50 and 70 years of age, with a male to female mortality ratio of 4:1. Despite traditional multidisciplinary treatment, involving the combination of chemotherapy, radiotherapy and surgery, prognosis remains poor. This is partly due to the delay of the diagnosis and partly due to the inadequacy of therapeutic approaches. The aim of this project is to find new therapeutic strategies for the treatment of MM based on a molecular targeted approach.

In this study the *in vitro* and *in vivo* anticancer effects of Bortezomib (Bor), the first selective and reversible proteasome inhibitor, on MM have been investigated. Bor was able to inhibit cell growth in a dose- and time-dependent manner; to induce apoptosis in treated cell lines, both human (H-Meso-1, MM-F1 and MM-B1) and murine (#40a); to modulate the expression of several molecules deregulated in MM, such as EGFR, ErbB2 and AKT; to induce Unfolded Protein Response, altering the expression of Grp78, CHOP and BiP. *In vivo* studies on C57BL/6 murine MM model have shown that Bor inhibited tumor growth and increased mice overall survival. Moreover, Bor treatment was able to modulate tumor immune microenvironment [1].

The ErbB receptor family is often overexpressed in MM patients and the use of EGFR-targeted drugs can inhibit MM cell proliferation. It is described that the use of a specific unitarget drugs can induce drug-resistance leading to the activation of different deregulated signaling pathways, such as those mediated by ErbB family receptor, Hedgehog, Axl, Wnt [2]. Recent studies in our laboratory, investigated the *in vitro* and *in vivo* effects of a specific inhibitor of ErbB family receptor, Afatinib (AFA), in combination with a multitarget molecule, Curcumin (CUR). CUR was able to enhance AFA effects increasing the AFA-induced reduction of the proliferation rate and pro-apoptotic effects *in vitro*. Indeed, i*n vivo*

AFA-antitumor activity was enhanced by its combination with CUR significantly increasing mice overall survival [3].

In another study from our laboratory the effects of inhibitors of Hh- (GANT-61) and ErbB receptors (AFA)-mediated signaling pathways, involved in neoplastic transformation and progression, were evaluated. The combined treatment with two inhibitors was more effective than the single treatments in reducing MM growth in vitro and in vivo, overcame the occurrence of drug resistance.

Based on these results, we are currently studying whether combined treatment using three different molecular targeted drugs, used at low doses, is more effective than single and dual treatments in inhibiting tumor growth in MM. Specifically, we are testing the combination of AFA, with Y15, a FAK inhibitor, and TP-0903, an Axl inhibitor.

Our preliminary data showed an increase of cell proliferation inhibition, with a proportional increase in cell death, in all cell lines treated with the triple combination compared to single and dual treatments in a time-dependent manner. Moreover, the use of 3D cultures has made possible to study the antitumor effects of these three inhibitors on systems that are more complex and more representative of *in vivo* tumor models. Spheroids treated with AFA, Y15 or TP-0903, used alone or in double combination, showed a significant inhibition of growth compared to control spheroids, and the triple combination significantly decreases spheroid growth compared to control, single or double treated spheroids. Finally, the triple combination reduced cell viability in treated spheroids compared to control ones.

In conclusion, targeted therapy offers significant promise in achieving better treatment outcomes with fewer side effects than conventional therapies. This study could be helpful in developing new personalized therapies that are more effective for MM patient.

INTRODUCTION

1. MALIGNANT MESOTHELIOMA

Malignant mesothelioma (MM) is a rare and aggressive neoplasia that originates from mesothelium cells lining serous cavities such as pleura, pericardium, peritoneum, and tunica vaginalis [4]. In adults, mesothelium is a type of monolayer squamous epithelium that lines the surfaces of all coelomic organs. Histologically, it is marked by its apical and basal lateral polarity, robust cell-cell adhesion, and the presence of a basal membrane [5].

The most common MM is malignant pleural mesothelioma (MPM) which originates from both visceral and parietal pleura and involves about 70-90% of diagnosed cases [5, 6]; in other cases, they typically occur in peritoneum, while pericardium and tunica vaginalis are affected more rarely [7].

The development of this disease is associated with a multifactorial etiology and consists of a multistep process that begins with cellular DNA damage and the subsequent promotion phase in which the genetically modified mesothelial cells overproliferate. Then, a tumor progression phase follows, in which cells develop a more aggressive phenotype, and eventually acquire the ability to metastasize and invade other tissues [8, 9].

The "World Health Organization Classification of Tumors of the Lung, Pleura, Thymus, and Heart" defines this disease as diffuse MM to distinguish it from other localized tumors of pleura that have different characteristics and clinical course. In fact, besides MM, several benign tumors can develop in this tissue, including adenomatoid tumors and benign cystic mesothelioma [6].

MM is a professional neoplastic lesion that predominantly affects men between 50 and 70 years old, with a male to female mortality ratio of 4:1 [8, 10]. It can occasionally affect children [10]. There is a higher incidence of MM in industrialized countries than in non-industrialized countries, reflecting the past use and production of asbestos [10, 11].

Each year about 2,000 to 3,000 cases of MM are diagnosed in the United States, partly related to asbestos exposure. For males born between 1945 and 1950 in Western Europe, researchers have predicted an increase in the peak of incidence of mesothelioma during the period from 2015 to 2025, especially MPM, due to asbestos exposure in this population [12, 13].

In Italy, the Seventh Report of the National Mesothelioma Registry (ReNaM), dated December 2020, reports information on 31,572 MM cases diagnosed from 1993 to 2018 [14]. The percentage of cases with an age at diagnosis of less than 45 years is equal to or just less 2% of the total. 35% of patients with MM are between 65 and 74 years old, and 50% of cases are between 61 and 76 years old. Up to 45 years of age, the disease is very rare (only 1.4% of registered cases). The mean age at diagnosis is 70 years with no appreciable differences by gender [14]. The average survival of patients without treatment is around 9-12 months [15], but even following classic therapy, the survival does not exceed 22 months. Nevertheless, with current multimodal therapy, 5-year survival is achieved in only 5% of patients [16].

The main risk factor implicated in the pathogenesis of this tumor is asbestos exposure (about 80% of MM) [17]. Although such exposure is a recognized etiologic factor for pleural and peritoneal MM, its role in the development of pericardial MM is controversial [18].

Other causes have been related to the occurrence of MM and include mineral fibers other than asbestos, such as erionite found only in Cappadocia and Turkey, ionizing radiation, all conditions leading to the formation of scarring processes of the pleura, and exposure to biological agents, including SV-40 virus [19].

2. ASBESTOS

The term "asbestos" identifies mineral fibers with an asbestiform crystalline structure, composed of silicate of magnesium, calcium and iron. Asbestos occurs naturally combined with other minerals; it is extracted from quarries and mines by crushing the parent rock, from which the purified fiber is obtained [10, 20].

There are two distinct geometric types of asbestos fibers: (i) amphibole, consisting of straight, stiff and brittle fibers, includes amosite (brown asbestos), crocidolite (blue

asbestos), anthophyllite, actinolite and tremolite; (ii) serpentine consisting of short, flexible fibers which is mainly represented by chrysotile (white asbestos) [20].

Chrysotile is the most widely used type but, in general, the former type of fibers is more widespread and still used in different regions of the world carrying a higher risk of MM [21, 22].

Asbestos was widely used in the 1980s and 1990s for the fabrication of a many products in industrial and civil sectors due to its numerous properties, including resistance to high temperatures, mechanical insults, chemical and biological agents, and flexibility [21].

These, together with the low cost of production and broad availability in nature, have made this mineral an extremely versatile material for use in many industries, from transportation sector to construction, automotive industry, etc. [10, 23].

Several studies have demonstrated the ability of asbestos to flake and reduce into very fine airborne and inhalable fibers [10]. For this reason, they have been classified as carcinogenic for humans by the International Agency for Research on Cancer (IARC) [24].

Although strict legislation has been implemented to prevent asbestos exposure through bans and mine closures in many countries, to date a decrease in the incidence of MM has not been observed. This is due to the long latency period from the time of asbestos exposure to the onset of the neoplasia, ranging from 13 to 50 years [25-27].

In Italy, the use of asbestos began to spread extensively during the World Wars in several sectors, particularly in the textile industry, construction, shipyards, and transportation [28].

Historically, asbestos mining has been one of the most important industrial activities in northern Italy. In particular, the Balangero mine located in Piedmont was the largest chrysotile quarry in Europe. Starting in the 1930s, numerous industries emerged in Piedmont, Apulia, and Lombardy that used asbestos for the production of asbestos-cement. In fact, the incidence of MM in these areas is still high today [29].

Italy was the first European country to enforce the prohibition of the mining, production and marketing of asbestos with the legislation of National Law No. 257 of March 27, 1992, as a transposition of European Directive EEC 91/382 [30].

In 2002, the ISPESL (High Institute for Occupational Prevention and Safety) established a register reporting established cases of mesothelioma related to asbestos exposure, with the aim of estimating the incidence, impact and spread of MM in Italy, and the identification of unknown sources of environmental contamination (DPCM 308/2002) [24].

Moreover, the National Mesothelioma Registry (ReNaM) has carried out surveillance work on mesothelioma cases, establishing an archive comprising 5,173 cases (3,746 males and 1,427 females) [24, 31].

2.1 Molecular mechanism of cancerogenesis

Asbestos-induced mesothelioma carcinogenesis is associated with a persistent inflammatory response initiated by ROS, cytokines, chemokines, growth factors, and pro-inflammatory factors [32, 33]. It is unclear whether asbestos fibers act on mesothelial cells directly or indirectly [34]. Nevertheless, the current state of knowledge has identified several mechanisms of action of asbestos-induced carcinogenesis [35].

A first mechanism is the occurrence of frustrated phagocytosis suggesting that inhaled asbestos fibers can induce prolonged cycles of damage, repair, and local inflammation resulting in their entrapment between the visceral and parietal pleura. Specifically, the fibers repeatedly scratch the mesothelial surface, damaging its integrity and leading to the activation of macrophages [32]. Macrophages, failing to phagocyte the fibers, go to death thus triggering the inflammatory process associated with a massive production of reactive oxygen species (ROS) and inflammatory cytokines. This phenomenon induces reiterated damage of the mesothelial cells, promoting DNA mutations and promoting neoplastic transformation [32, 36].

A second mechanism is called Fenton reaction, that was hypothesized by Upadhyay and Kamp, who demonstrated how asbestos fibers can generate tissue inflammation and promote ROS production into the tissues themself [37].

Asbestos fibers have iron (II) ions (Fe^{2+}) on their surface, which promote the production of ROS that interacting with cellular components, induce DNA mutations and neoplastic transformation [36]. Indeed, through Fenton reaction, free Fe(II) converts hydrogen peroxide (H_2O_2) into hydroxyl radicals (●OH), which oxidize DNA, free nucleic acids, proteins and lipids [38]. This process induces cytokines release, including tumor necrosis factor-alpha (TNF-α) released by macrophages and high mobility group box-1 (HMGB-1) proteins released by necrotic cells, amplifying the inflammatory response and increasing the number of cells undergoing oxidative damage (Fig. 1) [39].

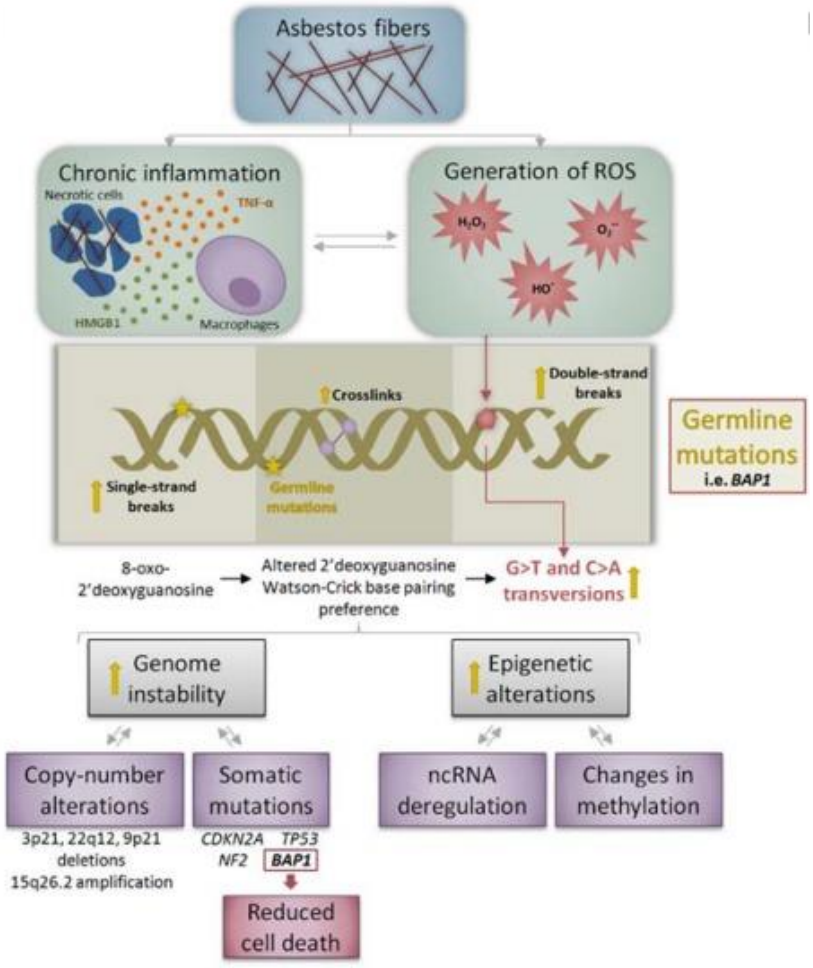

Figure 1. Molecular outcomes of exposure to asbestos fibers. *Asbestos-related carcinogenic effects mainly occur through two mechanisms: activation of chronic inflammation and generation of reactive oxygen species (ROS) [25].*

Oxidative DNA damage, if not adequately repaired, is highly mutagenic and can trigger to genomic instability, promoting carcinogenesis [25]. Major oxidative lesions include oxidized DNA bases, abasic sites, DNA single-strand breaks (SSBs), DNA double-strand breaks (DSBs), and intra- and inter-chain DNA cross-links [25].

In addition, asbestos fibers induce constitutive activation of epidermal growth factor receptor (EGFR) and hepatocyte growth factor receptor (MET), which are involved in cell survival and proliferation. Both EGFR and MET are receptors tyrosine kinase (RTK) that undergo activating mutations or gene amplifications resulting in activation of intracellular transduction pathways of the MAP kinase cascade and the phosphatidylinositol-3-kinase (PI3K)/AKT/mTOR cascade [34]. In turn, these pathways culminate in the activation of activator transcription factor protein-1 (AP-1) and nuclear transcription factor k-B (NF - kB), which play a pivotal role in regulating the expression of genes involved in inflammation, proliferation and apoptosis [35, 40].

In addition, asbestos can induce the production of cytokines and growth factors in mesothelial cells and resident macrophages. These include transforming growth factor-beta (TGF-β), tumor necrosis factor-alpha (TNF-α), and platelet-derived growth factor (PDGF) [41].

Finally, in tissue cultures it has been shown that asbestos can physically interact with the mitotic spindle and induce aneuploidy or other chromosomal damage [42].

Among the genetic alterations found in MM, we find mutations at the 3p21 chromosomal region that contains the BRCA1-associated protein 1 (BAP-1) gene locus, which is important in epigenetic regulation, and homozygous deletion of the 22q12 locus of the neurofibromatosis type 2 (NF2) gene. This gene encodes for the Merlin protein, an oncosuppressor inactivated in 40% of MM, and this loss of function promotes the invasiveness of the neoplasm itself [25, 43].

Again, deletion of the 9p21 locus containing the CDKN2A gene, which encodes for the oncosuppressor p16INK4a, has been described. This alteration results in loss of cell cycle control and is present in 80% of MM [34].

3. SIMIAN VIRUS 40

Simian Virus 40 (SV-40) belongs to the family *Polyomaviridae* and has an oncogenic potential both in humans and rodents blocking oncosuppressor genes. It is a small heat-resistant virus with a highly icosahedral capsid [44, 45]. It has a covalently closed double-stranded DNA genome of 5kbp that can be divided into two different regions:

1. The early region encoding for three "early" non-structural proteins: large T-antigen (T-ag), small t-antigen (t-ag), 17K T-ag (17KT);
2. A late region encoding for three "late" structural proteins: VP1, VP2, VP3 and a maturation protein: LP1 or agnoprotein.

The late region is not involved in the cell immortalization process; in contrast, the early region is responsible for the transforming properties of the virus itself. Specifically, the T-ag binds to viral and cellular DNA inducing its replication. In addition, it has mutagenic and clastogenic properties resulting in cellular chromosomal alterations, such as aneuploidies, chromosome rearrangements, and point mutations [44].

The mechanism of action of T-ag is based on its ability to bind several important cellular oncosuppressors that prevent proliferation when DNA damage occurs, including p53, pRb, p130 / Rb2, p107, p400 and p300. By inhibiting p53, T-ag interferes with DNA repair before the cell can move into the S phase for continuation of the cell cycle. Usually, if the cell does not repair DNA damages, it goes into apoptosis, but T-ag-mediated inhibition of p53 allows its mitosis and the mutations propagation. T-ag also has several functions to increase the transforming potential [44, 46].

SV-40 is able to infect different cell types in different ways. In 2004, H. Pass et *al*. performed *in vitro* experiments on infected mesothelial cells and fibroblasts to specifically demonstrate

the sensitivity of mesothelial cells to SV-40 transformation. Their comparison showed that mesothelial cells survived SV-40 infection and acquired a transformed phenotype; in contrast, fibroblasts were completely lysed [46]. These results highlight the peculiar tropism of SV-40 to infect and transform mesothelial cells, but also to cause genetic and epigenetic alterations when present in human MM cells [47].

4. HISTOLOGICAL CLASSIFICATION AND TNM STAGING

According to the 2021 classification made by the World Health Organization (WHO), mesothelioma can be divided into benign and preinvasive mesothelial cancers, adenomatoid cancer, MM in situ, well-differentiated papillary MM, localized MM, and diffuse MM. The latter can be subdivided into three different histotypes, based on the presence of cells with epithelial- or spindle-like morphology in the tumor tissue: (i) epithelioid; (ii) sarcomatoid; and (iii) mixed or biphasic [48].

The **epithelioid** histotype is characterized by a diffuse growth of globular or polygonal cells on the pleural surface. Heterogeneity of morphologic *patterns* often coexists in the same tumor tissue, correlating with different prognosis [49].

Cytoarchitectural patterns include papillary, tubulo-papillary, trabecular, solid, micropapillary clear cell, transitional, adenomatoid/microcystic, and deciduoid. In most of these patterns, cells have a large eosinophilic cytoplasm with nuclear atypia and few mitoses [50]. In the less differentiated forms, nuclei are hyperchromic, with a prominent nucleolus, and there is the presence of giant cells [51]. These tumor types represent a critical issue for differential diagnosis with other types of neoplasms with an epithelial origin. For this reason, it is necessary the use of immunohistochemical techniques for their discrimination [52] (Fig. 2).

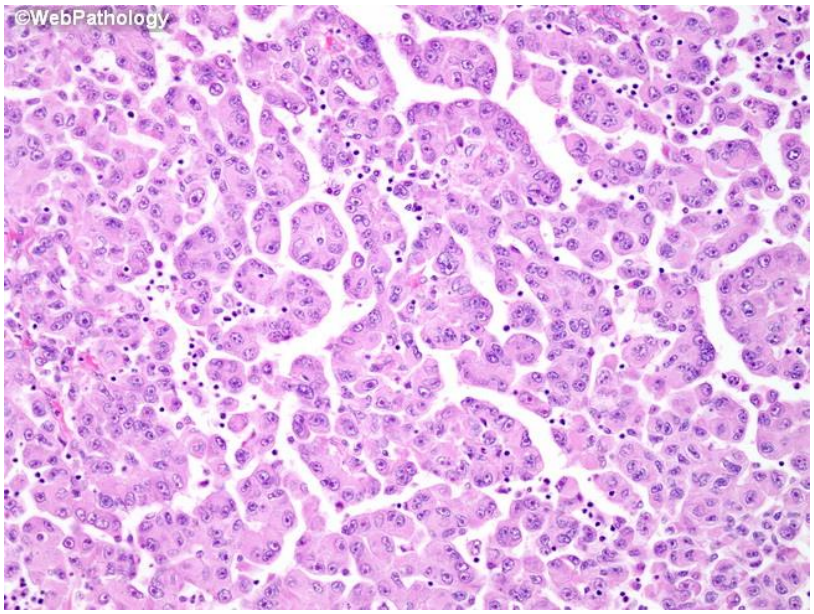

Figure 2. Malignant mesothelioma epithelioid histotype *[53].*

On the contrary, the **sarcomatoid** histotype is characterized by the proliferation of fusiform or mesenchymal-like cells, bundle-organized or arranged in a disordered manner that infiltrate the soft tissues of the parietal pleura [49]. Desmoplastic variant is rare, difficult-to-diagnose with an incidence of 2% and causes distant metastasis [51]. The MM cells can exhibit varying degrees of atypia, ranging from mild to severe, and may display pleomorphic characteristics such as atypical giant cells, bizarre nuclei, and the presence of abnormal mitotic spindles. In addition, there is the presence of tumor necrosis foci [50] (Fig. 3).

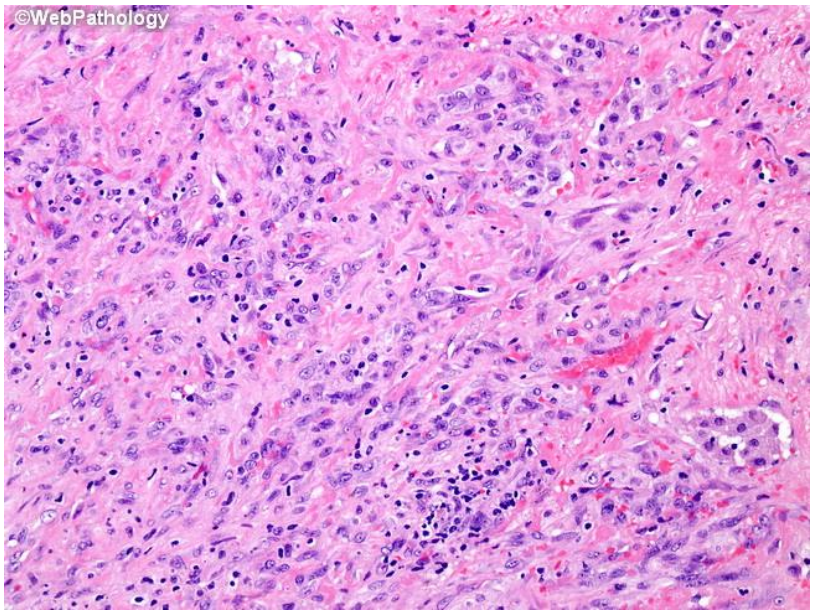

Figure 3. Malignant mesothelioma sarcomatoid histotype *[53].*

Finally, the **biphasic** histotype is characterized by the mixture of the epithelioid and sarcomatoid pattern with the presence of at least 10% of cells one of the two components [49, 50]. Some studies have shown the importance of sarcomatoid elements for diagnosis as a high percentage of this component results in a poorer prognosis [50] (Fig. 4).

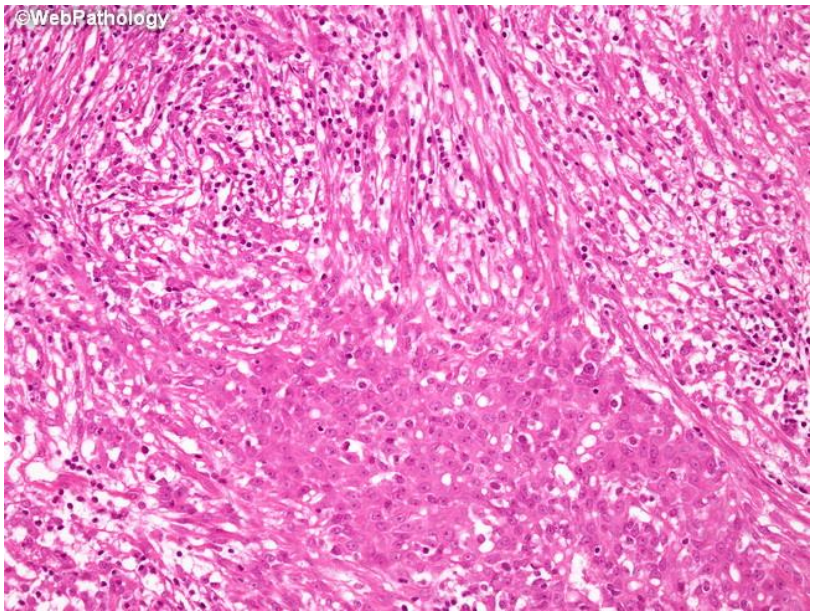

Figure 4. ***Malignant mesothelioma biphasic histotype*** *[53].*

Among the three different histological types, the epithelioid type has a more favorable prognosis, in contrast, the sarcomatoid histotype has a worse prognosis [48].

The incidence among the three histotypes may vary among case series, but it can be stated that about 80% of MM are of epithelioid type, 10% of sarcomatoid origin, and 10%-20% of biphasic type [50]. Understanding the histotype is crucial for guiding treatment decisions and improving prognosis.

The histological classification of MM is crucial since it constitutes a prognostic indicator and allows identifying the best therapeutic strategy, avoiding patients from undergoing invasive treatments with low probability of benefit [54].

5. CLINICAL PRESENTATION

Common symptoms of MM include dyspnea, usually due to the massive pleural effusion, often associated with dry cough, chest pain, fatigue, and weight loss [52]. These may be associated with other aspecific symptoms, such as anorexia, chills, sweating, weakness, and discomfort [55].

Uncommon symptoms at the onset of neoplasia include spontaneous pneumothorax, lung collapse, and mediastinal invasion with laryngeal nerve paralysis or superior vena cava obstruction. Rarely, myalgias, aphonia, dysphagia, abdominal distension, and nausea have been reported [55].

6. DIAGNOSIS

MM is a neoplasm with a poor prognosis and 100% mortality rate [56]. This is partly due to the delay of the diagnosis and partly due to the inadequacy of traditional therapeutic approaches.

MM diagnosis is difficult. For this reason, a multidisciplinary approach, involving cytohistology, immunohistochemistry, clinical data, radiological imaging and confirmatory biopsies, is essential to identify the invasion of lung parenchyma and pleura for the determination of malignancy and to have the certainty of MM diagnosis [57, 58].

In most cases, the diagnosis can be identified or suspected directly with hematoxylin-eosin cytological samples derived from pleural effusion. However, morphological diagnosis is always complemented by immunohistochemistry (IHC) and *fluorescence in situ hybridization* (FISH) [57].

6.1 Immunohistochemistry

Immunohistochemistry (IHC) is a technique for the detection of the presence and localization of specific molecules expressed on target cells. This method is based on the use of the antigen-antibody conjugation system in combination with a detection system (enzymatic or fluorescent) that make this reaction visible with microscope [59].

Immunohistochemical staining is used to determine the mesothelial *lineage* of the neoplasm in the differential diagnosis. A panel of immuno-markers can discriminate MM from other neoplastic or reactive lesions, and discriminate different histotypes from each other as they have different prognosis. For instance, immunomarkers like pancheratin or calretinin are valuable in confirming the mesothelial origin of tumor cells. Additionally, studies have demonstrated that the absence of BAP1 expression or the homozygous deletion of the CDKN2A gene in tissue samples offers 100% specificity in distinguishing MM from benign tumor [60, 61].

Unfortunately, there is no primary antibody that is exclusively specific for the mesothelial *lineage*, the sensitivity and specificity of antibodies vary depending on the type of differential diagnosis for MM. The utility of IHC may be critical in distinguishing between epithelioid mesothelioma and pleural metastasis [60].

To date, the biomarkers with the highest specificity and sensitivity in confirming the mesothelial origin of the tissue under examination appear to be mesothelin, calretinin, WT-1, CDK5 and CDK6, D2-40 (or podoplanin), and, more recently, HEG-1 has also been introduced [62]. The generally negative markers for MM are represented by CEA (carcinoembryonic antigen), B72.3, Ber-EP4, Bg8, MOC-31, CD15, MUC4 and claudin 4 [63, 64].

In the differential diagnosis between MM and metastasis, the 2017 International Guidelines recommend the use of two or three mesothelial and two epithelial markers with sensitivity and specificity of at least 80% [65]. Typically, calretinin, WT-1 and/or D2-40, MOC-31, and claudin-4 are used [62].

In addition, depending on the type of differential diagnosis, there are IHC markers that are not expressed in MM and are specific for certain malignancies, for example: TTF-1 and napsin for lung adenocarcinoma; CD10 and PAX8 for renal carcinoma; prostate specific antigen (PSA) prostate cancer; hormone receptors and mammoglobin for breast cancer; and GATA-3 for urothelial and breast cancer. However, recent studies have shown that GATA-3, previously considered specific for non-mesothelial cancers, is actually expressed in MM as well. In this regard, its use has been proposed for the differential diagnosis between sarcomatoid MM and sarcomatoid lung carcinoma [66].

In recent years, microRNAs (miRNAs) have also been identified as potential biomarkers for the diagnosis and prognosis of MM. In particular, Micolucci et *al*. have reported a panel of circulating miRNAs (miR126-3p, miR-103a-3p, and miR-625-3p) and a panel of tissue miRNAs (miR-16-5p, miR-126-3p, miR-143-3p, miR-145-5p, miR-192 -5p, miR-193a-3p, miR-200b 3p, miR-203a-3p, and miR-652-3p) deregulated in MM, constituting a potential signature with diagnostic value [67]. miRNA signature increases accuracy of a selected clinical prognostic criteria increased compared with a model based on clinical factors alone [68].

6.2 Radiological imaging

Radiological imaging is very important not only in differential diagnosis, but also in surveillance, staging, and response to treatment of the disease [69].

Computed tomography (CT) of the chest and abdomen is the imaging modality of choice to evaluate MM. It can demonstrate the extent of the primary tumor, local invasion and intra-thoracic lymph nodes, and extra-thoracic spread [70, 71]. It is also used to identify signs of asbestos exposure (e.g., calcified plaques) [72].

Thoracic magnetic resonance imaging (MRI) is not routinely used to evaluate MM, but it can provide more accurate staging information in specific scenarios. An advantage of thoracic MRI is its high sensitivity (greater than CT and other imaging modalities) in detecting invasion of the thoracic wall, mediastinum, and diaphragm [69, 70].

6.3 TNM staging

Nowadays, the main prognostic factors for MM include the tumor-node-metastasis (TNM) staging system and histologic classification [71]. This system evaluates the extent of tumor invasion (T), lymph node involvement (N), and the presence of metastasis (M) (Table 1) [73].

TNM staging is the most important prognostic factor in many malignancies and is often used to categorize patients in clinical trials. In 1995, researchers from the Staging Project of the International Association for the Study of Lung Cancer (IASLC) and the International Mesothelioma Interest Group (IMIG) analyzed available MPM surgical databases and developed a TNM-based staging system [74].

The eighth edition of the TNM staging system updated based on IASLC recommendations was published in 2017. This project analyzed 2460 cases from 29 cancer centers spread over four continents including both surgically treated cases and patients who did not undergo surgery [71]. The current staging is shown in the table below.

Compared with the 1995 classification, the division of descriptor T1 into T1a and T1b is eliminated because there were no differences in overall survival (OS = overall survival) times [73].

Table 1. Eighth edition of the TNM classification for MM [73].

Stage	Definition
Primary tumor (T)	
TX	Primary tumor cannot be assessed
T0	No evidence of primary tumor
T1	Tumor limited to the ipsilateral parietal ± visceral ± mediastinal ± diaphragmatic pleura
T2	Tumor involving each of the ipsilateral pleural surfaces (parietal, mediastinal, diaphragmatic, and visceral pleura) with at least one of the following features: • involvement of diaphragmatic muscle • extension of tumor from visceral pleura into the underlying pulmonary parenchyma
T3	Describes locally advanced but *potentially resectable* tumor. Tumor involving all of the ipsilateral pleural surfaces (parietal, mediastinal, diaphragmatic, and visceral pleura) with at least one of the following features: • involvement of the endothoracic fascia • extension into the mediastinal fat • solitary, completely resectable focus of tumor extending into the soft tissues of the chest wall • nontransmural involvement of the pericardium
T4	Describes locally advanced *technically unresectable* tumor. Tumor involving all of the ipsilateral pleural surfaces (parietal, mediastinal, diaphragmatic, and visceral pleura) with at least one of the following features: • diffuse extension or multifocal masses of tumor in the chest wall, with or without associated rib destruction • direct transdiaphragmatic extension of tumor to the peritoneum • direct extension of tumor to the contralateral pleura • direct extension of tumor to mediastinal organs • direct extension of tumor into the spine • tumor extending through to the internal surface of the pericardium with or without a pericardial effusion, or tumor involving the myocardium
Regional lymph nodes (N)	
NX	Regional lymph nodes cannot be assessed
N0	No regional lymph node metastases
N1	Metastases in the ipsilateral bronchopulmonary, hilar, or mediastinal (including the internal mammary, peridiaphragmatic, pericardial fat pad, or intercostal lymph nodes) lymph nodes
N2	Metastases in the contralateral mediastinal, ipsilateral, or contralateral supraclavicular lymph nodes
Distant metastasis (M)	
M0	No distant metastasis
M1	Distant metastasis present

7. THERAPEUTIC APPROACHES

Although MM prognosis remains poor, in recent years there have been several important developments in the therapeutic management of MM. In particular, the development of more effective therapies as well as new discoveries that could improve the diagnosis of MM and new insights into the pathobiology of the disease [75], allowed the improvement of new diagnostic and prognostic approaches to develop new therapies such as gene therapy [76].

The most widely used approach for the treatment of MM includes surgery, chemotherapy, and radiation therapy, used singly or in combination. The choice of these therapeutic alternatives depends on the stage and the severity of the disease. To date, the *gold standard* involves a multimodal approach, applied in both curative and palliative settings, and is often preferred to increase treatment efficacy and achieve a better survival rate [77].

Surgery for pleural MM is indicated mainly in multimodal therapies. In general, two different surgical approaches are used in the management of MM for therapeutic purposes: palliative and potentially curative. Palliative surgery may include partial pleurectomy with pleurodesis or thoracoscopy with pleurodesis [77], while potentially curative is based on pleurectomy/decortication (extended) (P/D) and extrapleural pneumonectomy (EPP) with the aim of removing all macroscopically visible tumor [57]. Subsequently, adjuvant therapy is administered with the aim of eliminating possible microscopic debris [78].

However, not all patients are ideal candidates for EPP because of the high risk of post-operative complications [79]. Therefore, recently there has been a shift in surgeons' preference towards a (extended) P/D rather than EPP. This trend has been supported by numerous studies that have shown significantly lower complication rates, lower perioperative morbidity and mortality with similar (if not higher) to P/D and overall survival rates. Furthermore, post-operative quality of life (QoL) appears to be worse in patients after EPP than in P/D due to the more frequent occurrence of complications, such as pleural empyema and bronchopleural fistula [57].

No chemotherapy regimen results curative on its own; in fact, these treatments are used palliatively or in multimodal therapies [80].

The most used chemotherapy drugs are cisplatin, pemetrexed, gemcitabine, carboplatin, ranpirnase, and vinorelbine. Other treatments include methotrexate, vincristine, vinblastine, mitomycin, doxorubicin, epirubicin, cyclophosphamide, nintedanib, and ifosfamide [81].

Two chemotherapy regimens are used. The first involves the use of a combination of an antifolate agent and a platinum compound. Pemetrexed is a potent inhibitor of thymidylate synthase, an enzyme required for DNA synthesis. Platinum compounds, as cisplatin or carboplatin, are alkylating agents that work by interacting with the DNA of cancer cells, reducing tumor growth and proliferation. A multicenter phase III study evaluated pemetrexed in combination with cisplatin and cisplatin alone in 448 patients; the combination regimen showed an approximately three-month increase in overall survival

(OS) [72, 82]. To date, standard systemic therapy consists of a combination of cisplatin and pemetrexed or cisplatin and raltitrexed [58, 83].

Perioperative chemotherapy is used for pleural MM with the aim of increasing local and systemic control of the disease. Additionally, cisplatin and pemetrexed are used as pre-operative treatment to decrease tumor volume and increase the chances of more complete resection. The combination of cisplatin and pemetrexed has been used in most clinical studies and has also been combined with surgery and RT in the evaluation of trimodal therapies [57].

However, in patients who cannot tolerate cisplatin, the combination of carboplatin with pemetrexed has been shown to be a viable alternative [81].

The second protocol involves the combination of gemcitabine and cisplatin, which offers similar palliation benefits. Gemcitabine is a false nucleotide that inhibits DNA synthesis; in fact, when incorporated into DNA, it avoids its polymerization and inhibits its repair [83].

Other commonly applied combination protocols are based on epirubicin (another anthracycline) together with gemcitabine or cisplatin as first-line therapy [83].

Radiation therapy is not regarded as a standard treatment considering its unsatisfactory results in MM. The only exception is for a post-surgical use because it is important to enhance tumor control rate minimizing damage to surrounding healthy tissue [84]. Various fractionation systems have been used, and the intensity-modulated radiotherapy after EPP has shown the greatest benefit [85]. Moreover, in palliative care, radiotherapy can help to alleviate chest wall pain. However, due to the absence of large-scale clinical trials with conclusive outcomes, the role of radiation therapy remains primarily within clinical trials and palliative care [86].

However, the research for new therapeutic approaches with fewer side effects and greater therapeutic effect has led to the formulation of new methodologies (Fig.5).

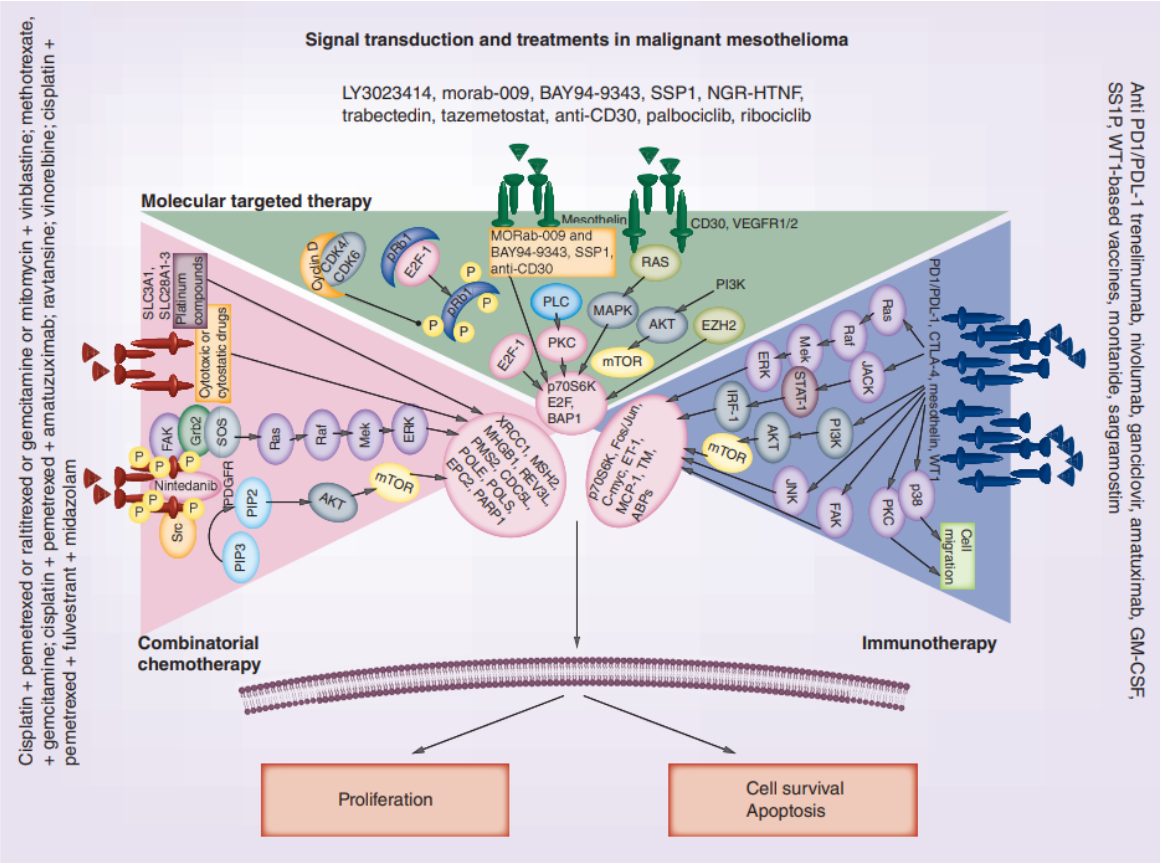

Figure 5. Signal transduction and treatments in MM. *Combination chemotherapy is the current standard treatment. This is likely to change in the future as new systemic and targeted drugs are administered based on the molecular characteristics of the tumor [81].*

The main ones are immunotherapy and *targeted therapy*, used alone or in combination with conventional therapies [47].

7.1 Immunotherapy

Immunotherapy is a treatment that aims to activate the host's immune system to fight the tumor [87].

The first cancer immunotherapy approach was developed by Coley, who demonstrated the induction of an immune response and subsequent tumor shrinkage after intratumoral injection of bacteria [88]. Currently, five different therapeutic approaches are being studied to artificially evoke an immune system response against cancer:

1. **Immune checkpoint inhibitors (ICIs)**: drugs that can block immune checkpoints. Immune checkpoints are a normal part of the immune system designed to keep immune responses from becoming too aggressive. By inhibiting these checkpoints,

these molecules enable immune cells to produce a stronger response against cancer [81].

2. ***T-cell transfer therapy***: treatment that increases the natural ability of T cells to fight tumors. For this purpose, immune cells are extracted from the tumor, and the ones most effective against it are either selected or altered in the laboratory to improve their ability to target cancer cells. These enhanced cells are then multiplied and reinfused into the patient. This type of treatment is also known as adoptive cell therapy, adoptive immunotherapy or immune cell therapy [89].

3. ***Monoclonal antibodies (mAbs):*** immune system proteins created in the laboratory and capable of binding to specific targets on cancer cells with high specificity. In particular, the antibodies currently available for therapy belong to the class of immunoglobulins G (IgG) [90].

4. ***Cancer vaccines***: aim to enhance immune system's response toward cancer cells [91].

5. ***Immune system modulators***: improve the patient's immune response against cancer. Some of these agents affect specific parts of the immune system, while others affect the immune system more generally [92].

Certain types of MM have been found to express high levels of tumor-infiltrating lymphocytes (TIL) with elevated levels of programmed death-ligand 1 (PD-L1). In light of this, the use of mAbs targeting PD-1, PD-L1, and CTLA-4 is being explored. Specifically, the antitumor effects of antibodies such as tremelimumab and ipilimumab (anti-CTLA-4), nivolumab and pembrolizumab (anti-PD-1), and durvalumab (anti-PD-L1), either alone or combined with chemotherapy, are currently under investigation for patients in advanced stages of MM [93].

7.2 *Targeted therapy*

Targeted therapy is a therapeutic approach that targets the fundamental processes of tumorigenesis (i.e., cell proliferation, differentiation, programmed cell death and invasiveness). It represents the foundation of precision medicine [94].

The U.S. Food and Drug Administration (FDA) has approved antineoplastic drugs that interact with specific molecular targets, classified into two main categories: small molecules (such as tyrosine kinase inhibitors, TKIs) and mAbs:

- ***Small molecules*** are drugs with low molecular weight (< 900 dalton) that can easily enter cells and specifically target intracellular components [94]. These molecules are mainly TKIs, which cross cell membrane to interact with the catalytic domains of tyrosine kinase receptors or other kinases involved in intracellular signaling, blocking signal transduction. The development of targeted therapies began in 1999 with the introduction of imatinib, a TKI used in the treatment of chronic myeloid leukemia (CML). Following imatinib, numerous other molecularly targeted drugs were designed and synthetized [95].

- **mAbs**, also known as therapeutic antibodies, are laboratory-produced proteins designed to bind to specific targets found on cancer cells [94]. Their use marked a significant advancement in personalized medicine. To date, about one hundred mAbs (both for hematologic and solid tumors) have been approved by FDA for cancer treatment, and are commercially available [96]. Because they retain an intact Fc region, mAbs can trigger antibody-dependent cell-mediated cytotoxicity (ADCC) by recruiting complement proteins or effector immune cells to the tumor site. Additionally, mAbs have been employed as targeting vehicles for the delivery of nanomedicines or nanoparticles loaded with cytotoxic agents. Another strategy involves conjugating mAbs directly to chemotherapeutic drugs (i.e., auristatin, maytansin, calicheamicin, or doxorubicin) [97]. However, one of the main limitations of mAbs is their large size (150 kDa), which becomes even greater when conjugated

with nanoparticles, resulting in reduced tumor penetration and slower distribution [98].

Most *target therapies* act in different ways:

- *To help the immune system destroy cancer cells*. Cancer cells grow uncontrollably because they can escape from the immune system. Some *target therapies* work by making cancer cells recognizable to the immune system; others by boosting the immune system to eradicate the cancer [99].
- *To prevent cancer cells from growing*. Cancer cells, as a result of genetic mutations, express proteins that induce cell division both in the absence and presence of proliferation signals. Some *target therapies* interfere with these proteins, preventing cell division and slowing uncontrolled tumor growth [100].
- *To block angiogenesis*. Tumors have to form new blood vessels to grow beyond a certain size through angiogenesis process. Hence, angiogenesis inhibitors are designed to interfere with these angiogenetic signals by preventing blood flow or causing death of the blood vessels themselves [101].
- *To vehicle substances that can kill cancer cells*. Some mAbs can be combined with toxins, chemotherapeutic drugs, and radiation. Once these mAbs recognize targets on the surface of cancer cells, they are absorbed causing cell death. Cells that do not have the target will not be damaged [94].
- *To cause cancer cell death*. Cancer cells have devised several strategies to evade the processes of cell death. Some *target therapies*, however, are able to induce cell death by apoptosis [102].
- *To eliminate the hormones the tumor needs to grow*. Some breast and prostate cancers require certain hormones to grow. Hormone therapies are a kind of *target therapy* that can work in two ways: some prevent the production of specific hormones; others prevent hormones from acting on target cells [94].

However, *targeted therapy* has disadvantages due to the ability of cancer cells to become resistant to this treatment. For this reason, they may work best when used in combination with other therapies, such as chemotherapy or radiotherapy. In addition, it is often difficult to design a specific drug because of the structure or function of the therapeutic target [94].

The most common side effects of targeted therapies include diarrhea and liver problems. Others might include problems with blood clotting and wound healing, hypertension, fatigue, sores in the mouth, nail changes, loss of hair color, and skin problems. Skin problems could include rashes or dry skin [103].

8. DE-REGULATED SIGNAL TRASDUCTION PATHWAYS IN MM

In MM patients, it has been observed both disruptions in the proteasome's proteolytic pathway [104] and dysregulation of various signaling pathways—such as those involving receptor tyrosine kinases (EGFR/ErbB2), Hedgehog, Axl, and Wnt—have been observed [105].

8.1 Proteasome

The levels of intracellular proteins are the result of balancing processes between their synthesis and degradation, both of which are crucial for normal cell function [106]. Protein degradation is tightly regulated and occurs via two primary pathways. The first involves lysosomes, which are vesicular organelles containing acid hydrolases that break down both endogenous proteins and those internalized from the outside through processes like endocytosis and pinocytosis [107]. The second pathway is the ubiquitin-proteasome system (UPS) which involves ubiquitin, a marker for degradation, and the proteasome 26S, a multienzymatic complex [104] (Fig. 6). Therefore, the UPS includes two distinct steps: i) the covalent binding of multiple ubiquitin molecules to the substrate protein; (ii) the degradation of the ubiquitinated protein by the proteasome [107]. This process does not require compartmentalization and the catalytic complex is ubiquitous functioning in nucleus, cytoplasm, and in association with the endoplasmic reticulum (ER). It uses ATP-

dependent mechanisms and involves numerous adjuvant molecules that collectively form what is known as the "Signalosome" [104, 106].

The UPS is responsible for the degradation of short-lived proteins involved in several cellular processes, such as:

- Cell cycle progression by proteolysis of specific regulatory proteins;
- Cell growth and proliferation through degradation of oncoproteins and signal transduction pathway proteins;
- DNA repair;
- Regulation of transcription;
- Regulation of immune and inflammatory response;
- Processing of antigens presented in association with the major histocompatibility complex class I (MHC I);
- Degradation of abnormal or misfolded proteins [106].

As the proteasome participate in several fundamental cellular processes, its inhibition leads to cell death, and its malfunctioning can underline numerous pathological events [107].

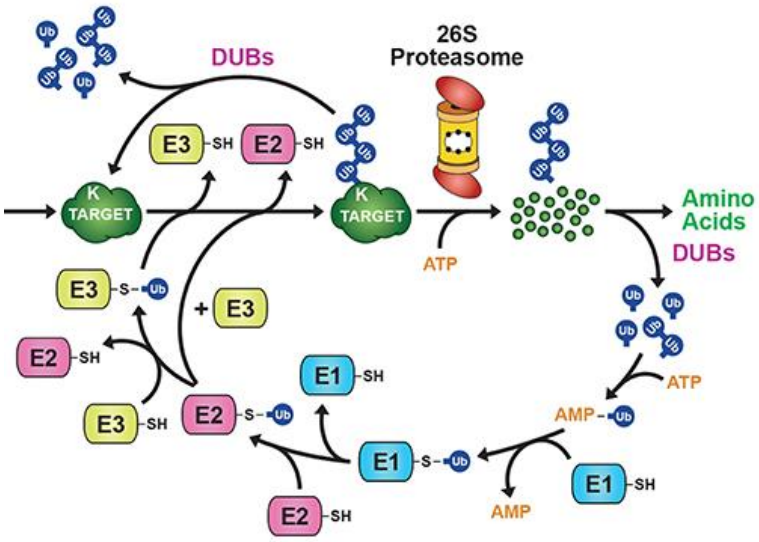

Figure 6. Representation of the Unfolded Protein System **[108]**.

8.1.1 The ubiquitination process

Hershko and colleagues identified the ubiquitin conjugation system and its role in marking proteins that are later to undergo degradation [109].

Ubiquitin is a small protein consisting of 76 amino acids, which can exist freely or be linked to other proteins either as a single unit (monoubiquitination) or in chains (polyubiquitination). This process serves various functions, including the regulation of protein degradation, controlling subcellular localization, and kinases activation [110].

The ubiquitination process involves three enzymes that act sequentially: Ubiquitin-activating enzyme (E1), ubiquitin-conjugating enzyme (E2), and ubiquitin-protein ligase (E3) [111].

Initially, ubiquitin is activated by E1 in an ATP-dependent reaction, forming a thioester bond between the C-terminal glycine (Gly) of ubiquitin and a cysteine (Cys) residue of E1. The activated ubiquitin is then transferred to the E2, which delivers it to a ligase (E3) bound to the substrate protein. E3 facilitates the formation of an isopeptide bond between ubiquitin's C-terminal Gly and a lysine (Lys) residue on the target protein. If this lacks a Lys residue, ubiquitin attaches to its N-terminus. This process repeats multiple times, forming a homopolymeric polyubiquitin chain. Each new ubiquitin molecule binds its Gly76 to the Lys48 of the previous ubiquitin in the chain. A polyubiquitin chain, consisting of at least four ubiquitin units, signals the 26S proteasome to degrade the protein and recycle the ubiquitin molecules. Recent studies show that polyubiquitination at other lysine residues (i.e. Lys63-linked polyubiquitination) and monoubiquitination are involved in other cellular processes, as DNA repair, chromatin remodelling, cellular trafficking and endocytosis [112] (Fig. 7).

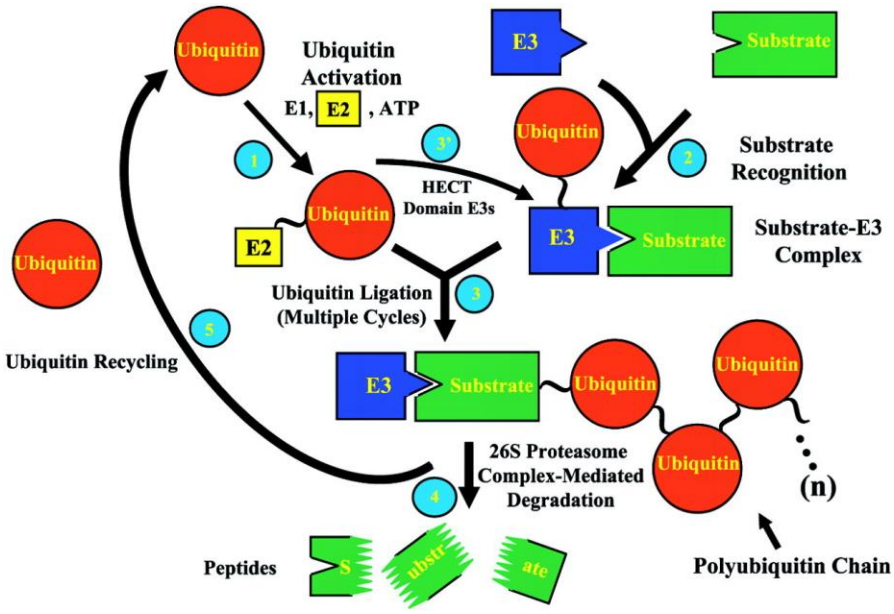

Figure 7. The ubiquitin proteolytic pathway. *1: Activation of ubiquitin; 2: Binding of the protein substrate; 3: Multiple (n) cycles of conjugation of ubiquitin to the target substrate leading to the formation of a polyubiquitin chain. 3': Similar to step 3, but the activated ubiquitin is transferred from E2 to a high-energy thiol intermediate on E3. 4: Degradation of the ubiquitin-tagged substrate by the 26S proteasome complex, resulting in the release of short peptides. 5: Recycling of ubiquitin [113].*

The ubiquitin-mediated proteolytic system operates in a hierarchical manner: a single E1 enzyme is responsible for activating ubiquitin; at least 13 different E2 enzymes have been identified, each working with one or more E3 ligases. Eukaryotic cells contain hundreds of E3 ligases, so they provide specificity in attaching ubiquitin to target proteins by recognizing distinct structural motifs [111]. E3 enzymes can belong to two main categories: (i) those containing a homologous to the E6-associated protein carboxyl terminus (HECT) domain and (ii) those with a Really Interesting New Gene (RING) domain [110, 114].

E4 enzymes, also known as assembly/elongation factors, assist the formation of ubiquitin polymer chains.

Besides ubiquitinating enzymes, deubiquitinating enzymes, belonging to the thiol-protease family, play a role in removing ubiquitin from proteins targeted for degradation and in the biosynthesis of ubiquitin itself [115]. These enzymes recognize the C-terminal end of ubiquitin and are categorized into two groups:

1. **Carboxy-terminal ubiquitin hydrolases (UCHs)**: approximately 25 kDa enzymes involved in processing pro-ubiquitin and releasing mature ubiquitin from small molecules or amine/thiol groups [115].
2. **Ubiquitin-specific proteases (UBPs)**, also known as isopeptidases: around 100 kDa enzymes, which cleave ubiquitin from either free or protein-conjugated forms. Some UBPs are free-floating, while others are associated with the 19S subunit of the proteasome, and their activity may be ATP-dependent or independent [115].

8.1.2 Proteasome 26S

The proteasome is crucial for maintaining cellular homeostasis [116]. The most common form of the proteasome is the 26S, which consists of a 20S core particle (CP) that contains the protease activity and two 19S regulatory subunits (RPs) [117, 118].

The 19S RPs, also known as PA700, flank the central CP, one at each end, and they are made up of a base and a cap. The base consists of six subunits with ATPase activity and two with structural function, and directly binds the 20S catalytic core; the lid consists in eight different subunits, all except one with no catalytic activity [118].

The 19S RP binds the ubiquitinated substrate, an entrance for that substrate opens to the 20S where it unfolds and then translocates to the 20S catalytic chamber, where degradation into peptides will occur [118].

The 20S CP is a barrel-shaped structure composed of four stacked rings, two outer **α-rings** and two inner **β-rings**.

Each ring consists of seven subunits.

- **α-rings** regulate access to the proteolytic chamber, controlling substrate entry.
- **β-rings** contain the protease active sites responsible for degrading proteins [116].

The proteolytic activity resides on specific β subunits (β1, β2, and β5) with a specific and different substrate preference. The β5 site is the chymotrypsin-like (chymotrypsin-like) site

and preferentially cleaves after binding of hydrophobic residues, the trypsin-like (trypsin-like) site (β2) preferentially cleaves after binding basic residues, and the caspase-like (caspase-like) site (β1) cleaves after binding acidic residues [117].

Consequently, the proteasome is not simply a complex of independent proteases but is a multicatalytic complex that functions only when it is fully intact [116] (Fig. 8).

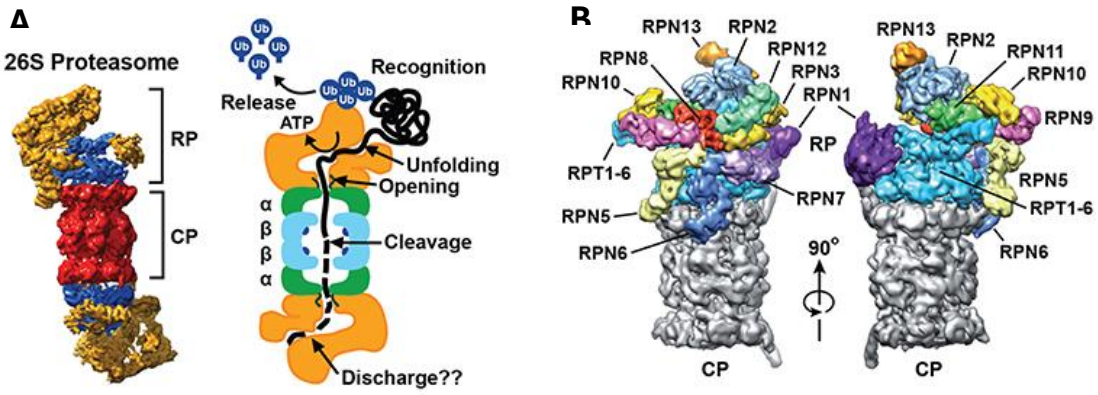

Figure 8. 3D structure of the 26S proteasome. ***(A)*** *The CP shown in red, the RP base shown in blue, and the RP lid shown in yellow (left). A cartoon representation of the 26S proteasome, highlighting specific functions of the CP and RP during substrate processing (right).* ***(B)*** *Subunit architecture of 26S proteasome RP. The CP is shown in gray, the Rpt ring is shown in light blue, and additional Rpn subunits are shown in various colors with their identity indicated [108].*

8.1.3 Effect on the cell cycle

The proteasome degrades many cell cycle regulatory proteins such as those that typically have a short half-life, such as cyclin B1, p21, p27, and oncosuppressive proteins like p53, thereby promoting cell cycle progression [119]. Many tumors rely on proteasome activity and are more sensitive to proteasome inhibition than normal cells [120, 121]. Inhibition of the proteasome leads to toxic effects, including increased reactive oxygen species (ROS) and accumulation of misfolded and damaged proteins [122, 123]. Cells respond by activating protective mechanisms as autophagy [124], but severe damage triggers programmed cell death [125, 126]. Proteasome inhibition also stabilizes tumor suppressor proteins and prevents cell cycle progression [127].

8.1.4 Activation of NF- κB

The transcription factor NF-κB regulates genes involved in innate and adaptive immunity, inflammation, stress response, B-cell development, and lymphoid organogenesis. Its activation occurs through two pathways: canonical and noncanonical, both requiring proteasome-mediated degradation of regulatory elements [128].

In canonical pathway, there is a resting state in which NF-κB is sequestered in the cytoplasm by IκB inhibitory proteins. Upon activation by pro-inflammatory cytokines, the IκB kinase (IKK) complex phosphorylates IκB, leading to its ubiquitination and degradation by the proteasome. This process releases the NF-κB/RelA complex, which translocates into the nucleus to activate gene expression [129]. In the Noncanonical Pathway, the NF-κB-p100/RelB complex remains inactive in the cytoplasm. Upon activation, kinases trigger the IKKα complex to phosphorylate NF-κB2-p100, which is then ubiquitinated and processed by the proteasome into the transcriptionally active NF-κB2-p52. The NF-κB2-p52/RelB complex translocates to the nucleus to induce target gene expression [130].

In addition, NF-κB is frequently upregulated in tumors and inflammatory diseases, promoting the expression of apoptosis inhibitory proteins (IAPs) and Bcl-2 in cancer cells [131]. In this context, the increased proteasome activity plays a pivotal role in influencing NF-κB activation by controlling the levels of its inhibitor IκB. As a results, NF-κB determines the transcription of gene involved in cell survival, but also in tumor progression, migration and angiogenesis [132, 133].

8.2 ErbB receptor family

The ErbB receptor family is a family of transmembrane receptor proteins with tyrosine kinase activity, and consists of 4 members: HER1(ErbB1, EGFR) epidermal growth factor receptor, HER2 (ErbB2), for which a specific ligand could not yet be isolated, HER3 (ErbB3) and HER4 (ErbB4), which bind neuregulins, eregulins and other growth factors of the same family [134]. Upon recognition and binding of specific ligands, these receptors form homo- and heterodimers in various combinations; this leads to trans- and auto-phosphorylation of

the receptor cytoplasmic region and subsequent activation of interconnected and overlapping signaling cascades, resulting in multiple biological responses, including proliferation, differentiation, cell motility, and inhibition of cell death (Fig. 9). Therefore, their deregulation plays a pivotal role in tumor growth, angiogenesis, invasion and metastasis processes, and drug resistance through aberrant activation of several of intracellular signaling pathways, such as those mediated by Ras/Raf/MEK/ERK and PI3K/Akt/TOR [135].

Mitogen-Activated Protein (MAP) kinases are a group of serine/threonine kinases that regulate crucial cellular processes such as proliferation, apoptosis, and survival. Disruptions in this pathway are linked to pathogenesis of various diseases. The MAP kinase family is categorized into three main groups: (i) Extracellular signal-Regulated Kinases (ERK1/2), activated by growth factors and regulates transcription factors in the nucleus; (ii) Jun N-terminal Kinase (JNK), that responds to stress signals, such as UV radiation, cytokines, and oxidative stress; and (iii) p38 MAP kinase, activated by stress signals, including cytokines and environmental stress.

The activation of the MAP kinase pathway begins when specific growth factors bind to membrane tyrosine kinase receptors, causing these receptors to dimerize and interact with G proteins. The G protein Ras, which has GTPase activity, activates Raf kinases by recruiting and phosphorylating them. Raf kinases then phosphorylate MEK kinases at two serine residues. MEK kinases further phosphorylate ERK1 and ERK2 on specific threonine and tyrosine residues. Activated ERK1/2 then move to the nucleus to activate various transcription factors that drive cell growth and prevent apoptosis.

The Ras/Raf/MEK/ERK signaling pathway is commonly altered in cancers. For instance, activating mutations in Ras are present in approximately 30% of tumors, leading to sustained activation of ERK1/2 and contributing to cancer progression [136].

The PI3K/Akt/mTOR signaling pathway is involved in various physiological functions, and its dysregulation is linked to both cancer development and resistance to therapies. The PI3K (phosphoinositide 3-kinase) family is categorized into three classes: I, II, and III. Class

I PI3Ks is the most relevant for the PI3K/Akt/mTOR pathway because it facilitates the transfer of a γ-phosphate group from ATP to phosphatidylinositol-4,5-bisphosphate (PtdIns(4,5)P2), converting it into phosphatidylinositol-3,4,5-triphosphate (PtdIns(3,4,5)P3). This conversion promotes the recruitment of Pleckstrin Homology (PH) domain-containing proteins, including Akt, to the inner membrane surface [137].

Akt, a serine/threonine kinase, exists in several isoforms, each with a similar structure: a central catalytic domain flanked by regulatory and PH domains at the N- and C-terminal region, respectively. To be fully activated Akt must first translocate to the membrane and requires a two-step phosphorylation process. Initial recruitment to the cell membrane triggers a conformational change in Akt, allowing its Thr308 residue to be phosphorylated by PDK1 (3-phosphoinositide-dependent protein kinase 1). A second phosphorylation, on Ser473, is carried out by the mTORC2 complex, completing Akt's activation [138].

Akt activity is tightly regulated by various proteins, including heat-shock protein 90 (HSP90). Cellular stress conditions—such as thermal shock, hypoxia, oxidative stress, and ultraviolet light—can lead to increased Akt activity. This hyperactivation serves as a compensatory mechanism, helping cells evade apoptosis under stressful conditions. The crosstalk between these pathways can impact processes like cell proliferation and migration [139].

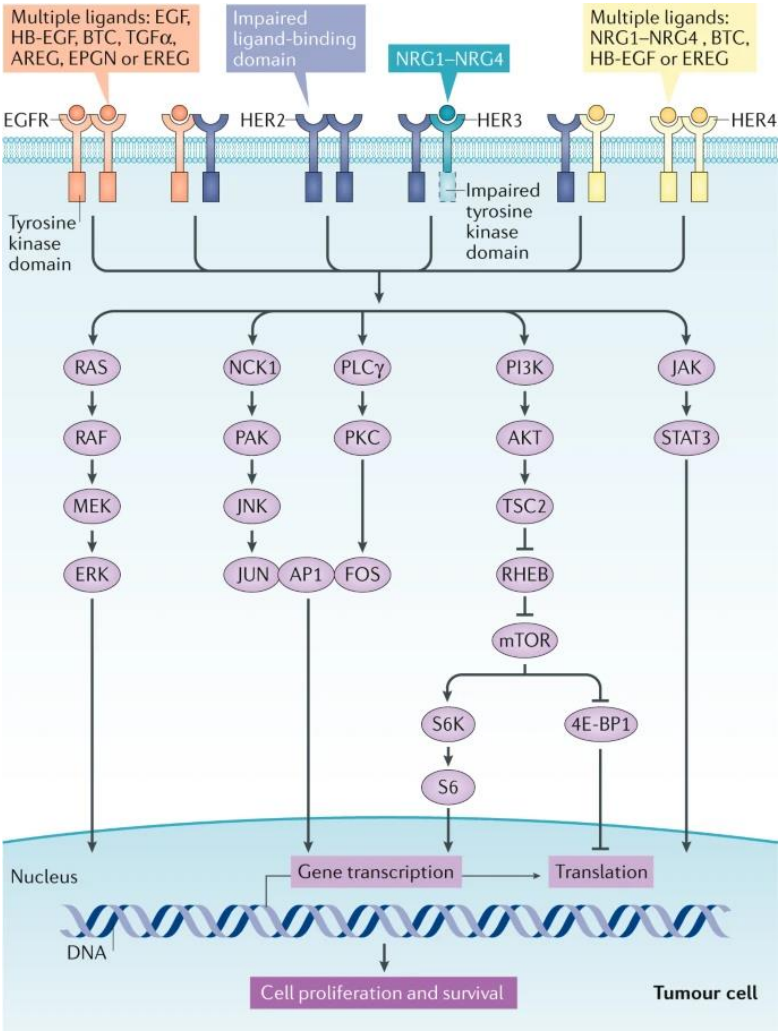

Figure 9. ErbB family receptors signaling pathways in the regulation of cell growth [140].

Aberrant expression of ErbB receptors can result from transcriptional or post-translational mechanisms, and mainly from a variety of genetic alterations, such as gene amplification, mutation, and translocation [134]. Quantitative and qualitative alterations of ErbB receptors are frequently found in about 30% of solid tumors, including MM, lung, breast, bladder, prostate, and epidermoid carcinoma of the head and neck cancers. Increased expression of one or more ErbB receptors, in fact, has been found in many patients with MM [3]. Specifically, increased EGFR signaling plays a significant role in various cancer-related processes, such as driving cell cycle progression, inhibiting apoptosis, and facilitating metastasis. The abnormal EGFR signaling leads to excessive cell proliferation, contributing to tumorigenesis and elevated EGFR levels have been observed in cancer patients, correlating with an increased risk of relapse and reduced survival rates [3].

In MPM, EGFR is overexpressed in approximately 60% of cases, whereas it is absent in normal pleural tissue [141]. Additionally, at least one member of the ErbB receptor family is expressed in 88% of these tumors. The expression of ErbB receptors varies with histological histotype, being most frequent in epithelioid MM. MM have been found to express EGFR (79.2%), HER2 (6.3%), and ErbB4 (49.0%), but do not express ErbB3 [142, 143].

Recent studies have highlighted how ErbB receptor overexpression correlates with the cellular ability to evade antitumor immunity. However, the mechanisms by which aberrant ErbB receptor signaling creates inhibitory effects on the adaptive antitumor response are not yet fully understood [135].

To date, the European Medicines Agency (EMA) in 2004 and the FDA in 2006 approve cetuximab, a chimeric mAb capable of binding the extracellular region of EGFR for MM treatment [144].

8.3 The Gas6/Axl Signaling Pathway

The Axl protein, encoded by the gene of the same name, is one of the Tyro3, Axl, MerTK (TAM) family members of RTKs [145]. TAM family members are important inflammatory mediators that inhibit certain signaling pathways activating dendritic cells, natural killer cells, and macrophages, attenuating their antitumor activity [146].

When activated by the ligand Growth Arrest Specific Gene 6 (Gas6), Axl promotes survival transduction signaling pathways, such as those mediated by PI3K/AKT and MAPK/ERK [147], increases the expression of anti-apoptotic markers (BCL-2, BCL-XL, survivin) and reduces the activity of pro-apoptotic proteins (BAD and Caspase-3) [146, 148] (Fig. 10).

In cells with low metastatic colonization potential, Axl over-expression leads to increased migratory and invasive abilities [149]. Indeed, TAM family members are able to stimulate vascular endothelial growth factor (VEGF), fibroblast growth factor (FGF), and platelet-derived growth factor (PDGF) [150].

In cancers, deregulation of the Gas6/Axl signaling pathway is associated with tumor growth, invasiveness and metastasis processes, epithelial-mesenchymal transition (EMT), angiogenesis, drug resistance, immune regulation, and stem cell maintenance [146, 151]. Several studies have shown increased expression of Axl on both cell lines and biopsies from MM patients [147, 152]. Over-expression of Axl is important for tumor progression and, often, correlates with patients' outcome and increased tumor aggressiveness [146].

Furthermore, Song W. et al. have shown that Axl protein expression levels are increased during the course of tumor progression and are associated with the presence of distant metastasis and reduced survival in patients with MM [153]. Therefore, Axl represents a promising therapeutic target in the management of this neoplasm [146]. Preclinical studies have shown that Axl inhibitors are able to stimulate apoptosis of tumor cells and suppress their ability to migrate and invade [153-155].

In addition, the *in vitro* use of target molecules that inhibit the action of Axl is able to make MM cell lines more sensitive to radio- or chemotherapy treatments, induce apoptosis in tumor cells, or reverse the EMT process [147, 153, 156].

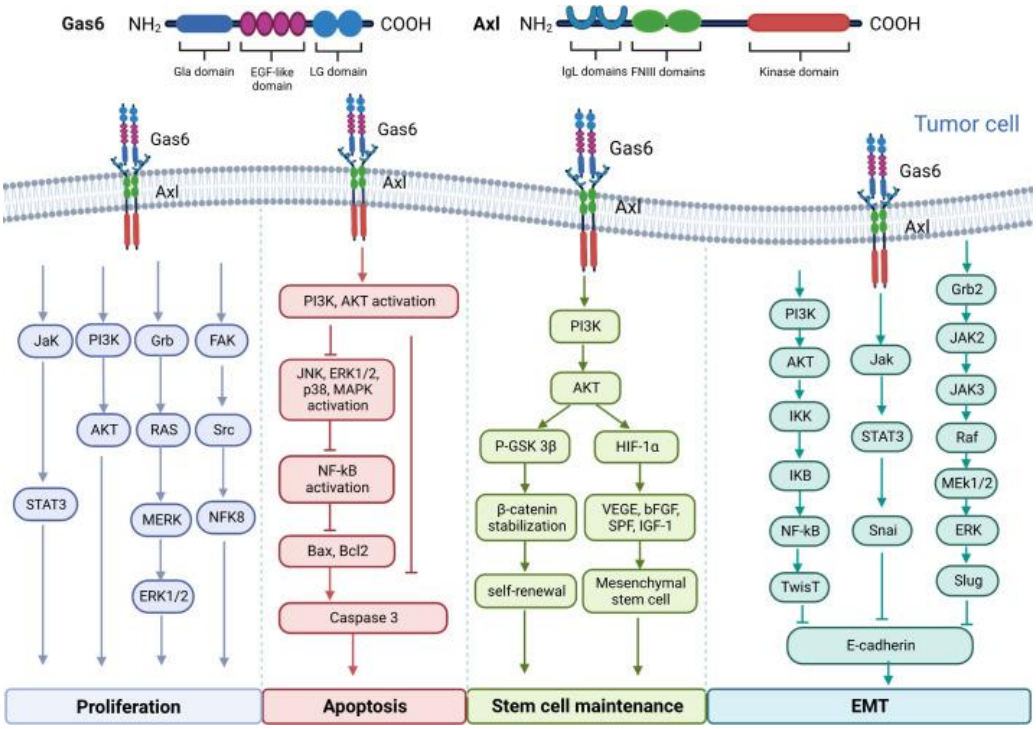

Figure 10. Gas6/AXL signaling pathways. *Diagram of the molecular structure of Gas6 and AXL and signaling pathways involved in the regulation of cancer cell proliferation, migration, apoptosis, as and the maintenance of cancer stem cells by Gas6/AXL [157].*

8.4 The FAK-Wnt Signaling Pathway

Focal adhesion kinase (FAK) is a non-receptor tyrosine kinase that plays a pivotal role as a regulator of integrin-mediated signaling, regulating important cellular processes such as migration, invasion, angiogenesis, cell survival, and EMT [158] (Fig.11). Overexpression and activation of FAK have been reported in numerous invasive and metastatic cancers [159], including thyroid [160], prostate [161], colorectal cancer [162], ovarian cancer [163], MM [164], head-neck cancer [165]. Although the molecular mechanisms responsible for FAK overexpression are not completely known, many studies associate increased levels of this protein with a worse prognosis [158].

Activation of FAK leads to the phosphorylation of downstream targets involved in cell survival signaling, such as the PI3K/AKT and MAPK/ERK pathways. These activated pathways help MM cells resist to apoptosis and continue to proliferate [166].

There is growing evidence of a functional interaction between FAK and the Wnt/β-catenin signaling pathway during tumor development and progression. The Wnt/β-catenin pathway, just like FAK, regulates multiple cellular processes [158].

Wnt proteins, in fact, by binding to Frizzled receptors induce phosphorylation of β-catenin leading to the regulation of cell proliferation, survival, differentiation and EMT [158, 167]. Finally, the Wnt/β-catenin signaling pathway also appears to be deregulated in MM tumors, leading to uncontrolled proliferation of tumor cells, promoting blockade of apoptosis and promoting cell migration [158, 168]. FAK promotes cell survival and migration, while Wnt signaling can enhance these processes through its impact on cell adhesion and proliferation [158].

Thus, these two signaling pathways could represent two important therapeutic targets for the development of new targeted therapies for MM patients.

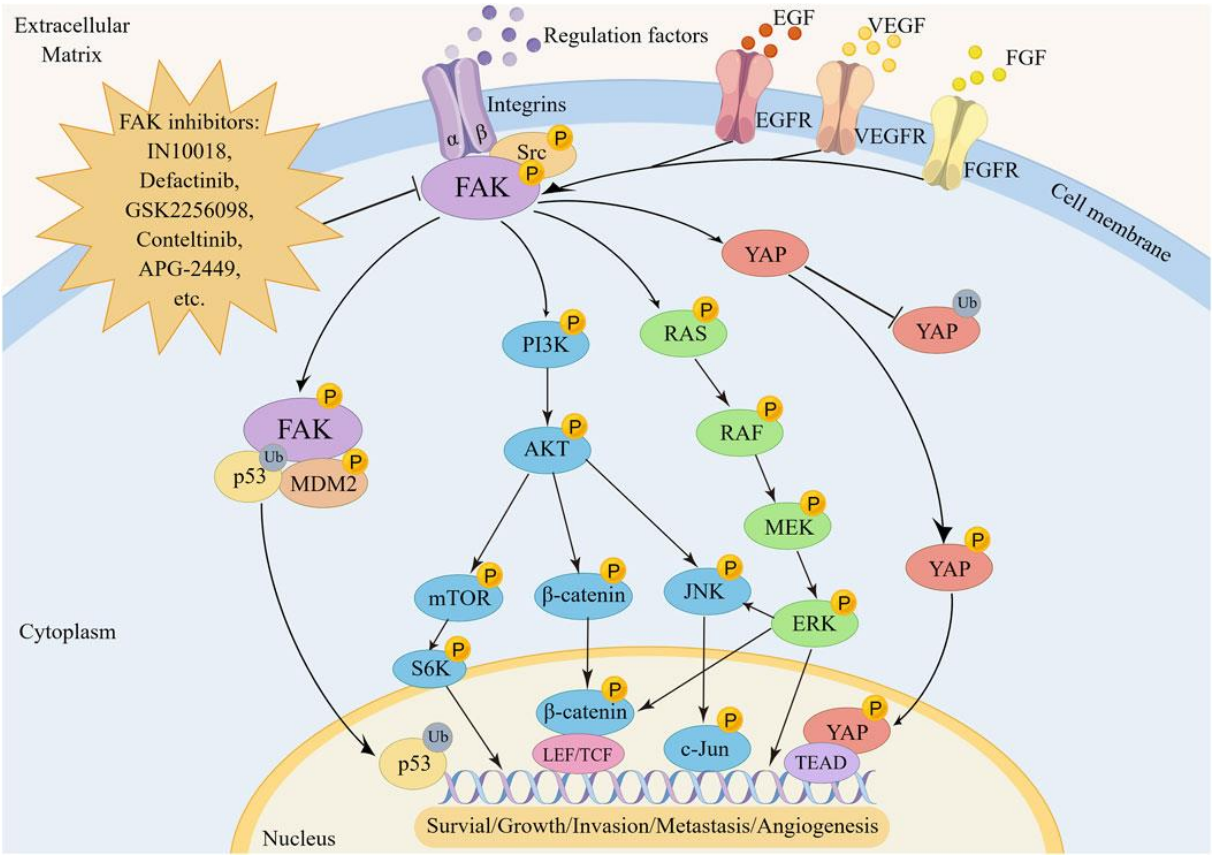

Figure 11. FAK signaling pathway in tumorigenesis, angiogenesis, and metastasis. *FAK promotes oncogenesis by activating transcription factors via p53, YAP, RAS/RAF/MEK/ERK, PI3K/AKT and downstream pathways including mTOR, β-catenin or JNK [169].*

9. INHIBITORS

9.1 Proteasome Inhibitors

Proteasome inhibitors (PIs) are one of the most important classes of therapeutic agents for the treatment of multiple myeloma [95]. Many PIs are short peptides designed to enter the substrate binding site present in the catalytic subunit. The activity of PIs depends on the C-terminal portion of the drug reacting with the nucleophilic active site of threonine to form a reversible or irreversible covalent adduct [170, 171]. Although the proteasome has three catalytic sites, inhibition of all three does not have a significant effect on protein degradation. More in detail, inhibition of β1and β2 has no significant effect on protein degradation; whereas inhibition of β5 appears to have a reducing effect on protein degradation. Therefore, many proteasome inhibitors target the β5 site even though they have less activity on β1and β2 [171, 172].

Three components of this class have been approved by the United States FDA:

1. Bortezomib (Velcade®) which is a reversible inhibitor of the proteasome 26S, with anti-proliferative and antitumor activity;

2. Carfilzomib (Kyprolys®);

3. Ixazomib (NINLARO®) which is the first compound with oral administration whose mechanism of action is proteasome inhibition [173, 174].

9.1.1 Bortezomib

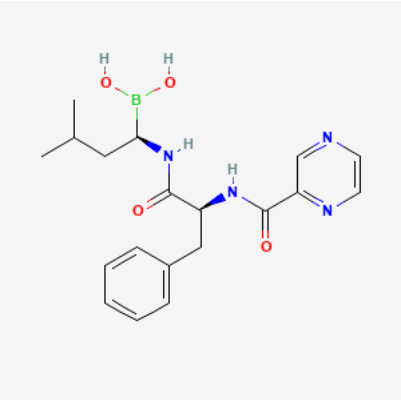

Figure 12. Bortezomib molecular structure [175].

Bortezomib (Bor) is a dipeptidyl boronic acid that selectively inhibits the ubiquitin pathway of the proteasome, which plays a role in the degradation of many intracellular proteins [176] (Fig. 12).

The full chemical name of this drug is ((1R)-3-methyl-1 - ({(2S)-3-phenyl2 - ((pyrazin-2-ylcarbonyl) amino) pro-panoyl} amino)-butyl) acid [175].

Rapidly proliferating cancer cells require high ER activity for proper protein folding, assembly, and transport, which leads to ER stress. Due to inadequate vascularization and rapid growth, cancer cells encounter unfavorable conditions, such as hypoxia and starvation [177]. Tumor hypoxia is a key factor that promotes tumor progression, reduces therapeutic response, and compromises patient survival [178]. Inhibition of the 26S proteasome contributes to ER stress, being responsible for the antitumor effects of proteasome inhibitors. Misfolded proteins are normally degraded by the proteasome, but if they are not cleared,

they can form aggregates, exacerbating ER stress. If this stress persists, the survival signal activated by the unfolded protein response (UPR) system can activate the apoptotic pathway. This highlights the importance of the 26S proteasome in the regulation of ER stress and cell survival. Therefore, inhibition of proteasome in cancer cells promotes apoptosis, exerting an antitumor effect [177, 179].

In addition, inhibition of proteasome activity by Bor leads to the accumulation and increased transcription of BH3-only proteins, such as PUMA, BIM, NOXA, and BIK [180]. These proteins can antagonize anti-apoptotic Bcl-2 family members like Bcl-xL and Mcl-1 or activate pro-apoptotic proteins like Bax and Bak, promoting apoptosis through effector caspases activation [181, 182].

Notably, NOXA induction is a critical mechanism for Bor-mediated apoptosis, driven by c-Myc and independent of p53 [183]. Bor-induced apoptosis is also associated with the activation of c-Jun N-terminal kinase (JNK), reactive oxygen species (ROS) formation, cytochrome c release, and the activation of both intrinsic (caspase 9-mediated) and extrinsic (caspase 8-mediated) apoptotic pathways. Bor has been shown to selectively induce apoptosis in some neoplastic cells, but the nature of its selectivity remains unclear [183].

Still, NF-κB is involved in suppression of apoptosis and induction of cancer cell proliferation, invasion, metastasis, carcinogenesis and angiogenesis of cancer cells [184]. Through the proteasome inhibition, Bor stabilizes the NF-κB complex in the cytoplasm, leading to reduced NF-κB-dependent gene expression [185]. Finally, it has been described that Bor can induce cell cycle arrest by affecting the expression of cell cycle regulators, such as cyclins and cyclin-dependent kinases (CDKs), thereby hampering the multiple myeloma cells proliferation [186].

In 2003, Bor received approval from the US FDA for use as a drug in the treatment of multiple myeloma relapse and in 2008 as a therapy in previously untreated multiple myeloma. It was also approved in 2006 for the treatment of refractory or relapsed mantle cell lymphoma and, in 2014 for the treatment of previously untreated mantle cell lymphoma [187, 188].

Therefore, Bor has significantly improved the treatment of multiple myeloma, but drug resistance and relapse remain common issues [189]. Resistance mechanisms include changes in proteasome subunit composition and expression, as well as mutations in the β5 binding pocket, though these mutations haven't been confirmed in patients [190]. Additionally, drug-resistant cells exhibit transcriptomic alterations, such as increased expression of anti-apoptotic proteins like Bcl-2 and heat shock proteins (HSP27, HSP70, HSP90), which help manage misfolded proteins. Extrinsic factors, including the bone marrow microenvironment and RNA dysregulation, also play a role in resistance to Bor [191]. Recent studies in our laboratory have been shown that Bor inhibited cell proliferation, triggered apoptosis, modulated the expression and activation of pro-survival signaling transduction pathways proteins activated by ErbB receptors and inhibited proteasome activity *in vitro* in head and neck carcinoma (HNCC) cell lines. Moreover, intraperitoneal administration of Bort delayed HNCC tumor growth *in vivo*, protracted survival and adjusted tumor microenvironment by increasing tumor-infiltrating immune cells (CD4+ and CD8+ T cells, B lymphocytes, macrophages, and Natural Killer cells) and by decreasing vessels density. Bort treatment modified the expression of proteasome structural subunits in transplanted HNCC cells [192].

While Bor has shown notable efficacy in hematological malignancies, it has also been tested in solid tumors like non-small cell lung cancer (NSCLC), breast cancer, and prostate cancer [193, 194]. However, Bor had demonstrated limited therapeutic success compared to hematologic cancers [195, 196].

Bor is typically administered intravenously at different doses depending on the treatment cycle, both as a monotherapy and in combination with other drugs. Combination therapies generally yield higher response rates but also greater toxicity compared to monotherapy [187].

The main obstacles to Bor therapy are its side effects, such as fatigue, peripheral neuropathy, thrombocytopenia, gastrointestinal disturbances, and cardiac abnormalities that may be the cause of decreasing the effective dose or, even, result in discontinuation of therapy [197-

199]. To improve the antitumor effects and reduce the general toxicity associated with Bor, next-generation proteasome inhibitors are being developed. Changes include irreversible inhibition of the proteasome, inhibition of all three enzyme sites, and oral rather than intravenous administration [200].

This are prompted ongoing research and the development of second-generation proteasome inhibitors to address its limitations and side effects [191].

9.2 Tyrosine Kinase Inhibitor (TKIs)

In recent years, TKIs have been developed and categorized by their binding modes [201]:

- **Type 1 inhibitors**: compete with ATP, binding to the active conformation of the kinase (DFG-in) and forming hydrogen bonds in the kinase's adenine region. They typically occupy the ATP-binding site and extend into nearby areas [202].
- **Type 2 inhibitors**: compete with ATP but target the inactive conformation (DFG-out) of the kinase, engaging an additional hydrophobic pocket (allosteric site). Imatinib is a key example [203].
- **Allosteric inhibitors**: interact with the allosteric site of the protein outside the ATP-binding region, regulating negatively or positively enzymatic activity. These inhibitors have high selectivity as they exploit binding sites characterized by high variability among the various tyrosine kinases. Cobimetinib, a MEK inhibitor, is an example [201, 204].
- **Covalent inhibitors**: form irreversible covalent bonds with the enzyme’s active site, often reacting with a nucleophilic cysteine residue [201, 205].

Each class offers different levels of specificity and effectiveness.

These drugs have been shown to possess high selectivity, high efficacy, low side effects, ease of preparation and high efficacy in the treatment of chronic myeloid leukemia (CML), non-small cell lung cancer (NSCLC), renal cell carcinoma (RCC), compared to traditional chemotherapy antineoplastic agents [206].

TKIs can be divided into EGFR and HER2 inhibitors, VEGFR inhibitors, anaplastic lymphoma kinase (ALK) inhibitors, and Bcr-Abl inhibitors [206]. First generation TKIs have been studied to bind reversibly to ATP binding sites, while second generation TKIs are irreversible inhibitors [207].

9.2.1 Afatinib

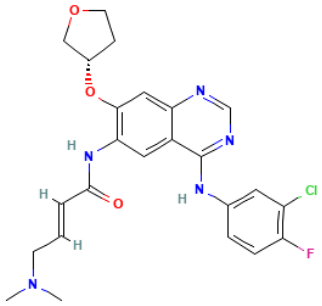

Figure 13. Afatinib molecular structure [208]

Afatinib (AFA), known by the commercial name Giotrif®, is a *small molecule* (TKIs), is an ATP-competitive molecule that irreversibly binds and inhibits the tyrosine kinase activity of members of the epidermoidal growth factor (ErbB) family including EGFR, HER2 and HER4 [209]. It binds covalently to the residue of cysteine 797 of EGFR and residue of cysteines 805 and 803 of HER2 and HER4, respectively. This binding results in a reduction of self- and trans-phosphorylation between ErbB dimers and an inhibition of the signaling pathway of all of the ErbB receptor family members (PanErbB Inhibitor) [210-212] (Fig. 13).

AFA has been demonstrated to inhibit the survival of lung cancer cells carrying the T790M mutation of the EGFR gene on xenograft (tumor cell resistance related mutation, for first generation TKIs), leading to regression of the expression of ErbB2 initially [213].

The activity of AFA has also been tested on MM cells, even in combination with other drugs. Specifically, the effect of AFA was evaluated in association with crizotinib, a drug used in NSCLC able to inhibit MET, Alk and ROS-1 kinases. It has been shown that the combined treatment determines the inhibition of MM cell proliferation than single treatments. The combination of AFA and crizotinib increases the inhibition of phospho-Akt and phospho-ERK1 / 2, involved in cell survival signaling pathway [214]. Another study on MM cells was

conducted to evaluate the synergistic effect of AFA and trastuzumab (anti-HER2 mAbs). An increase in the ADCC mechanism has been observed, with promising anticancer effects [215]. This suggests that the use of AFA in combination with inhibitors of other cellular pathways represents a good therapeutic strategy to improve the prognosis of MPM [216].

Recently, a MPM patient harboring both G719C and S768I mutations of EGFR was successfully treated with AFA [217]. These results suggest the ability of this small molecule to recognize both wild-type EGFR and mutated EGFR cancers [207, 217].

However, other clinical studies using EGFR TKIs in MM have not reported clinical efficacy [218]. Mechanisms of resistance to EGFR inhibition by TKIs could be due to a simultaneous activation of alternative pathways and rare mutation of EGFR in MM [219]. Hence, our lab has investigated the effects of AFA in combination with a multitarget polyphenol, Curcumin (CUR). Our results demonstrate that CUR enhanced AFA effects by increasing the reduction of MM cell proliferation *in vitro* and inhibiting mouse tumor growth *in vivo* [3].

9.2.2 TP-0903 (Dubermatinib®)

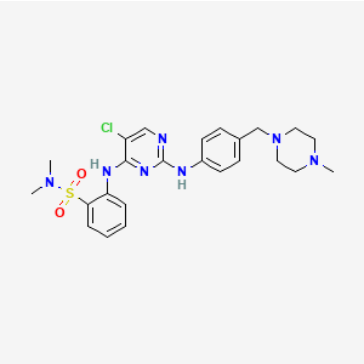

Figure 14. TP-0903 molecular structure [220]

TP-0903, whose trade name is Dubermatinib®, is a potent and selective inhibitor of the Axl receptor tyrosine kinase, the high expression of which correlates with EMT, metastatic process, and drug resistance in several cancer types, including MM [153] (Fig. 14).

TP-0903 is an orally available small molecule (Fig. 14) that follows a mechanism of competitive inhibition with ATP as it possesses a heterocyclic portion that mimics adenine resulting in binding of the inhibitor itself to the active conformation of Axl. It also targets

other kinases, including the three members of the TAM family, Aurora A, JAK2, ALK, ABL1 and VEGFR2 [221-223].

Yuqing Zhang's 2021 study showed that the use of TP-0903 in combination with chemotherapy and/or immunotherapy for the treatment of pancreatic cancer has antitumor and immunomodulatory effects. It has also been shown that treatment with TP-0903 results in a shift toward a more differentiated tumor phenotype. In conclusion, these results suggest that TP-0903 is effective in counteracting cell signaling pathways that support tumor progression *in vivo* [224].

TP-0903 is currently being evaluated in an initial phase I study in patients with advanced solid tumors, including MM [146, 154, 224, 225].

The drug is still in experimental stages but has shown promising preclinical results in targeting AXL and reducing tumor growth in cancers where AXL overexpression plays a crucial role [226, 227].

Its combination with existing chemotherapy or immunotherapy strategies is also being explored, as dual approaches may yield better outcomes in patients with resistant or advanced MM [228].

9.2.3 Y15

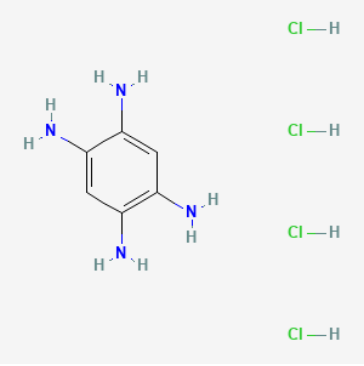

Figure 15. Y15 molecular structure [229]

Y15 is a specific inhibitor of Focal Adhesion Kinase (FAK), which inhibits its autophosphorylation, reducing the viability of tumor cells and blocking their growth (Fig. 15). FAK is expressed in all cells at basal level, but it is over-expressed in most solid tumors,

as it is involved in angiogenesis, metastatic process and invasion. Y15 specifically blocks tyrosine-397 phosphorylation of FAK and total phosphorylation of FAK in a dose- and time-dependent manner. Moreover, this inhibitor, by blocking FAK, leads to overexpression of Dkk, an inhibitor of Wnt; consequently, use of this *small molecule* results in simultaneous inhibition of two deregulated pathways in MM [158].

Y15 has been shown to have antitumor and antiproliferative effects, alone or in combination with chemotherapeutic agents, both *in vitro* and *in vivo*, in various cancer models [230].

It has been used to investigate the role of FAK in cancer and explore its potential as a therapeutic target [166]. Clinical research involving Y15 is less advanced compared to some other FAK inhibitors, but it represents an important tool for studying FAK's role in cancer and evaluating potential therapeutic strategies [169].

AIM OF THE RESEARCH

The aim of this research project is to find new targeted therapeutic strategies for the treatment of MM based on a molecular targeted approach in order to specifically inhibit the tumor growth.

To this aim, the *in vitro* and *in vivo* antitumoral effects of Bor, a 26S proteasome inhibitor, on MM tumor growth have been investigated.

For *in vitro* studies, three MM cell lines of different histotypes (MM-B1, biphasic histotype; MM-F1, fibromatous histotype; H-Meso-1, epithelial histotype) and one murine MM cell line of epithelial histotype (#40a) were used. For *in vivo* studies, C57BL/6 mice were intraperitoneally inoculated with pristane, and after a week, transplanted with syngeneic #40a cells that grow forming ascites.

It is well described that the ErbB receptor family is often overexpressed in MM patients and the use of EGFR-targeted drugs can inhibit MM cell proliferation. However, the use of unitarget drugs can induce drug-resistance leading to the activation of different deregulated signaling pathways, such as those mediated by ErbB family receptor, Hedgehog, Axl, Wnt [2, 105]. The *in vitro* effects of a specific inhibitor of ErbB family receptor, AFA, in combination with other two unitarget drug, Y15, a specific inhibitor of FAK and TP-0903, a selective inhibitor of the Axl receptor tyrosine kinase, were also investigated using three-dimensional cell culture techniques.

The results obtained could be useful for development of new therapeutic strategies for MM patients.

MATERIAL AND METHODS

Cell Lines and Treatments

Human MM cell lines (MM-F1 (fibromatous), MM-B1 (biphasic), and H-Meso-1 (epithelioid)) were kindly provided by Prof. Antonio Procopio (Università Politecnica delle Marche, Ancona, Italy) [231, 232]. The murine MM cell line #40a was kindly provided by Dr. Agnes Kane (Department of Pathology and Laboratory Medicine, Brown University, Providence, RI, USA) and previously described by Goodglick et al. (1997) [233]. The #40a cell line was derived from the 40-cell line after two passages in the peritoneal cavity of C57BL/6 mice following administration of pristane one week before cells transplantation. These passages allow the selection of cells, which reproducibly form ascites when intraperitoneally injected in mice [233].

H-Meso-1 cells have an epithelial morphology, while MM-B1 and MM-F1 cells have biphasic and sarcomatous features, respectively [233]. The murine cell line has an epithelial morphology [233].

Cells were maintained in DMEM (Dulbecco's modified Eagle's medium) containing 10% fetal bovine serum (FBS), 100 U/ml penicillin and 100 μg/ml streptomycin (complete medium). The cells were grown at 37 °C in a humidified incubator with an atmosphere of 5% CO_2.

Bor was dissolved in DMSO. For treatments, cells were incubated for the indicated times in the presence of Bor at various concentrations (dose range: 6.25–100 nM) or vehicle control (DMSO≤0.1%).

AFA (Sigma-Aldrich, Milan, Italy), Y15 and TP-0903 (Sellechem) were dissolved in DMSO. For treatments, cells were incubated for the indicated times in the presence of AFA (dose range 0.6–10 μM), Y15 (dose range 0.6–10 μM), TP-0903 (dose range 25-400 nM) or vehicle control (DMSO≤0.1%).

Sulforhodamine B Assay

Cell proliferation was investigated by Sulforhodamine B (SRB) (Sigma-Aldrich, Milan, Italy) assay, which allows the quantification of proliferating cells by measuring the cellular protein content of adherent cultures. SRB is a dye, which stoichiometric binds to basic aminoacids under mild acidic conditions and dissociates using basic conditions [192]. Cells were seeded at 5×10^3/well in 96-well plates and incubated at 37°C to allow cell attachment.

After 24 hours, the medium was changed and the cells were treated with Bor (6.25–100 nM) for 24, 48 and 72 hours.

In each experiment, cells treated with vehicle of the compounds (DMSO) have been included as negative controls.

After treatments, cells were fixed with 50 μl/well of 50% cold trichloroacetic acid (TCA) for 1 hour at 4°C. After four washes with distilled water, the plates were air-dried and stained for 30 min with 100 μl/well of 0.4% (wt/vol) SRB in 1% acetic acid. After four washes with 1% acetic acid to remove the unbound dye, the plates were air-dried, and cell-bound SRB was dissolved with 100 μl/well of 10 mM pH 10 unbuffered Trizma Base solution. The optical density (O.D.) of the samples was determined at 540 nm with a spectrophotometric plate reader. The survival percentage was calculated by normalization of their O.D. values to those of the control cultures treated with DMSO. All experiments were performed in triplicate and repeated three times [2].

Bor was dissolved in DMSO and used for cellular treatments at scalar concentrations (6.25 nM, 12.5 nM, 25 nM, 50 nM, 100 nM) for 24, 48 and 72 hours. DMSO was used as control (CTR) in the same quantities used for treatments (DMSO ≤ 0.1%).

Trypan Blue Exclusion Test

For trypan blue exclusion test, cells were seeded at 5 × 10^4/well in 24-well plates and incubated at 37°C to allow cells attachment.

After 24 hours, the medium was changed and cells were treated for 24, 48 and 72 hours with Bor (range 6.25 - 100 nM) or with DMSO.
Both adherent and suspended cells of each well were harvested and stained with trypan blue dye (Sigma-Aldrich, Milan, Italy) and counted with optic microscope [234]. The experiments were performed in triplicates and repeated three times. Percentage of cell death was determined compared to the total number of cells [235].

FACS Analysis

Asynchronized, log-phase growing cells (at 60% confluence, approximately 2.5×10^5/well in 6-well plates) were treated with Bor or DMSO in complete culture medium. Z-VAD-FMK was used at a final concentration of 40 μM for 2 hours before adding the treatments. After 48 hours adherent as well as suspended cells were collected, centrifuged at 1500 rpm for 10 min and washed twice with cold phosphate-buffered saline (PBS). The cell pellets were re-suspended in 70% ethanol and incubated for 1 hour at -20°C. The cells were then washed twice with cold PBS, centrifuged at 1500 rpm for 10 min, incubated for 1 hour in the dark with propidium iodide (25 μg/ml final concentration in 0.1% citrate and 0.1% Triton X-100) [236]. Flow cytometry analysis was performed using a FACSCalibur cytometer with CellQuest Pro 5.2 software (BD Biosciences, San Jose, CA, USA).

Preparation of Cell Lysates

About 1.5×10^6 cells were seeded in 100 mm tissue culture dishes 24 hours prior to the addition of treatments. Lately, cells were treated with Bor 12.5 nM, Bor 25 nM or DMSO and, after 14, 24 or 48 hours of treatment, were harvested by scraping and centrifuged at 1200 rpm for 5 minutes at 4°C.

The sedimented cells were washed twice with cold PBS and then lysated 25 minutes on ice using RIPA lysis buffer (Triton X-100 1%, SDS 0.1%, NaCl 200 mM, Tris HCl 50 mM pH 7.5,

PMSF 1 mM, Na_3OV_4 1 mM). The mixtures were then centrifuged at 10000 rpm for 10 min at 4°C [237]. The protein assay was performed using the colorimetric method (Bradford protein assay), based on Coomassie Brillant Blue dye binding to proteins, primarily targeting basic (arginine) and aromatic (tryptophan, tyrosine, phenylalanine) amino acids. Small amount of cell lysate (1µl) was diluted in the cuvettes with 800 µl of distilled water and stained with 200 µl of staining (Biorad); the protein concentration of the samples was determined by densitometry using a spectrophotometer with a wavelength of 595 nm. The optical density (O.D.) of each sample was compared with those obtained from a standard curve obtained using known concentrations of bovine serum albumin (BSA).

Western Blotting

Western blotting was performed using gels with different percentage of polyacrylamide (10, 12 or 15%). 80 µg of cell lysate were resolved in 10-15% sodium dodecyl sulfate–polyacrylamide gel electrophoresis (SDS-PAGE), a method that allows protein separation by mass. Then, proteins were transferred on nitrocellulose membrane by electrophoresis for 1 hour at 30 V and the transfer of proteins were verified with Ponceau red staining of the membrane. After the transfer, non-specific binding sites were blocked by incubation with a 5% solution of skimmed milk powder diluted in PBS. After blocking, the membranes were incubated with specific primary antibodies for the protein to be identified, at the concentration of 1-2 µg/ml overnight in agitation at 4°C. After washing with PBS containing 0.1% Tween 20 (PBS-T), the filters were incubated with goat anti-mouse or anti-rabbit IgG, peroxidase-conjugated secondary antibodies and, finally, developed by chemiluminescence using photographic plates [192]. Protein expression was detected using the enhanced chemiluminescence system ECL LiteAblot (Euroclone, Milan, Italy). Actin or tubulin were used as endogenous control for equal loading. ImageJ 1.53e software (National Institutes of Health, USA) was used to analyze the optical density (O.D.) of each autoradiographic band after blot scanning.

Treatment of C57BL/6 mice with Bor intraperitoneally transplanted with #40a cells

Groups of 6-to-8-weeks-old C57BL/6 mice (10 mice for each group) were intraperitoneally (i.p.) injected with 0.2 ml of suspension containing $1.5x10^6$ #40a cells in phosphate-buffered saline (PBS) 1 week following a 500 μl pristane i.p. injection. The mice were then separated into two experimental groups:

- **group I**: mice treated with Bor administered in the peritoneum (0.50 mg / kg body weight, dissolved in PBS + DMSO);

- **group II**: control mice treated with PBS + DMSO administered in the peritoneum.

The treatments were started concurrently with the inoculation of MM cells and were administered twice a week thereafter. Isolation of the murine mesothelioma #40a cell line was previously described [233]. Investigation has been conducted in accordance with the ethical standards, following the Declaration of Helsinki. A veterinary surgeon was present during the experiments. The animal care, both pre- and post-experimentation, was carried out by trained personnel. Mice were bred under pathogen-free conditions at the University of Rome "Tor Vergata" animal facility and were handled in accordance with European Union and institutional guidelines for animal research. The research project was conducted with the formal approval of the local animal care committees (institutional and national), and all animal experiments were registered according to legal requirements (Authorization from Ministry of Health no. 179_2020-PR).

Analysis of antitumor activity *in vivo*

The growth of #40a cells in the peritoneal cavity of C57BL/6 mice leads to the development of ascites. Therefore, the mice's abdominal circumference was measured prior to cell inoculation and then monitored weekly until the tumor-bearing mice were euthanized either upon showing initial signs of distress or when their abdominal circumference expanded to 12 cm.

Phenotypical analysis of immune cells from the ascitic fluid of C57BL/6 mice transplanted with #40a cells

Groups of 6-to-8-weeks-old C57BL/6 mice (5 mice per group) were i.p. inoculated with #40a cells and treated with Bor or PBS-DMSO as previously described. The treatments began simultaneously with the MM cell inoculation and continued for up to 30 days, after which mice were euthanized. To collect tumor cells and immune cells recruited to the tumor microenvironment, a peritoneal lavage was performed by injecting 5 ml of cold PBS into the peritoneal cavity, followed by gentle massage for 30 seconds to dislodge the tumor and immune cells into the PBS that was then recovered. These cell suspensions were then using density gradient centrifugation with Pancoll separating solution (PAN-Biotech Cat #P04-69600) to isolate mononuclear immune cells from tumor ones and erythrocytes present in the ascitic fluid. Spleens were also harvested, and spleen cells were obtained by passing spleen tissue through a cell strainer. Red blood cells lysis was performed to remove contaminating erythrocytes (Roche Cat #11814389001). Multicolor flow cytometry was then performed to characterize the phenotype of immune cells contained in the ascitic fluid compared to those from the spleen. Dead cells were excluded using fixable Viability Dye eFluor780 (eBioscience, San Diego, California, Cat #65-0865-14) for 30 minutes at room temperature. Surface staining was carried out by incubating cells with antibodies for 20 minutes at 4°C in PBS containing 2% FBS. Intracellular staining was achieved using True-Nuclear™ Transcription Factor Buffer Set (Sony Biotechnology, Cat #2722005) following the manufacturer's instructions. Before IFN-γ staining, cells were stimulated for 4 h at 37 °C with Cell Stimulation Cocktail plus protein transport inhibitors (eBioscience Cat #00-4975-03). Data were acquired and analyzed using CytoExpert Acquisition and Analysis Software Version 2.5 on a Cytoflex instrument (Beckman Coulter). For the gating strategy, lymphocytes were selected based on SSC-A and FSC-A and dead cells were excluded from the analysis.

Tumor spheroid growth and drug-treatment

Tumor spheroids were generated by plating 2 x 10^3 cells/well of MM-B1 and MM-F1 cell lines in 96-well round-bottom ULA plates (Corning B.V. Life Sciences, Amsterdam, The Netherlands). Plates were incubated at 37°C, 5% CO^2 and 95% humidity for 4 days and then treated with:

- Scalar concentrations of Y15 (1.25 μM, 2.5 μM, 5 μM, 10 μM and 20 μM);
- Scalar concentrations of AFA (1.25 μM, 2.5 μM, 5 μM, 10 μM and 20 μM);
- Scalar concentrations of TP-0903 (0.05 μM, 0.1 μM, 0.2 μM, 0.4 μM, 0.8 μM).
- Double combination with Y15 (5-10 μM) + AFA (5 μM);
- Double combination with Y15 (5-10 μM) + TP-0903 (0.1 μM);
- Double combination with AFA (5 μM) + TP-0903 (0.1 μM);
- Triple combination with Y15 (5-10 μM) + AFA (5 μM) + TP-0903 (0.1 μM).

DMSO was used as control vehicle (CTR) in the same quantities used for treatments (DMSO ≤ 0.1%). Responses to drug treatment were assessed by measuring the diameter of the spheroids at regular intervals of 24, 48 and 72 hours from images captured with an inverted microscope equipped with a CCD camera and ImageJ software analysis (http://imagej.nih.gov/ij). The experiments were performed in duplicates and repeated three times.

3D viability assay

Viability of MM-B1 and MM-F1 spheroids was measured using the Real Time Glo MT assay (Promega). Specifically, spheroids were seeded as triplicate into 96-well plates and treated with the following doses of inhibitors, used alone or in double or triple combination:

- Y15 5 μM for MM-F1 cell line and 10 μM for MM-B1 cell line;
- AFA 5 μM for both MM-F1 and MM-B1 cell lines;
- TP-0903 0.1 μM for both MM-F1 and MM-B1 cell lines.

DMSO was used as control (CTR) in the same quantities used for treatments (DMSO ≤ 0.1%). Blank cell-free control was also included. Then, plates were incubated at 37 °C overnight. MT Cell Viability Substrate and NanoLuc® Enzyme were added to the spheroids at the concentration of 2X. Luminescence was monitored for up to 72 hours using Glomax reader (Promega).

Statistical analysis

Statistical analysis was performed using the GraphPad Prism software, version 8.0 (La Jolla, California). Data distribution for cell survival, different phases of the cell cycle and cell death were preliminarily verified using the Kolmogorov–Smirnov test, and the data sets were analyzed by one-way analysis of variance (ANOVA), followed by the Newman-Keuls test. Differences in the intensity of immunoreactive bands were determined using a two-tailed Student's t-test. Values with $p \leq 0.05$ were considered statistically significant. Survival curves and differences in tumor volumes in mice abdomen were assessed using the Kaplan–Meier method and compared with a log-rank test (Mantel-Cox) [238]. Flow cytometry results, specifically differences in the frequency of stained cells, were also evaluated using a two-tailed Student's t-test.

Additionally, data from 3D *in vitro* experiments were analyzed by one-way analysis of variance (ANOVA) followed by the Newman-Keuls test (GraphPad Prism 8.0 software). In all studies, the significance threshold was set at $p \leq 0.05$.

RESULTS

Effect of Bor on the inhibition on human and mouse MM cell survival and death.

In order to determine the effect of the proteasome inhibitor, Bor, on cell survival and death, SRB and Trypan blue exclusion assays, respectively, were performed on human (H-Meso-1, MM-F1, MM-B1) and murine (#40a) MM cell lines after exposure to increasing doses of Bor (6.25 nM, 12.5 nM, 25 nM, 50 nM and 100 nM) or DMSO (used as control) for 24, 48 and 72 hours.

SRB assay demonstrated that Bor inhibited cell growth in a dose- and time-dependent manner in all cell lines treated. Notably, Bor's effect became statistically significant after 48 hours of treatment at all tested concentrations in MM-F1 and MM-B1 cell lines, and at concentrations of 12.5 nM or higher in H-Meso-1 and #40a cell lines (Fig. 16).

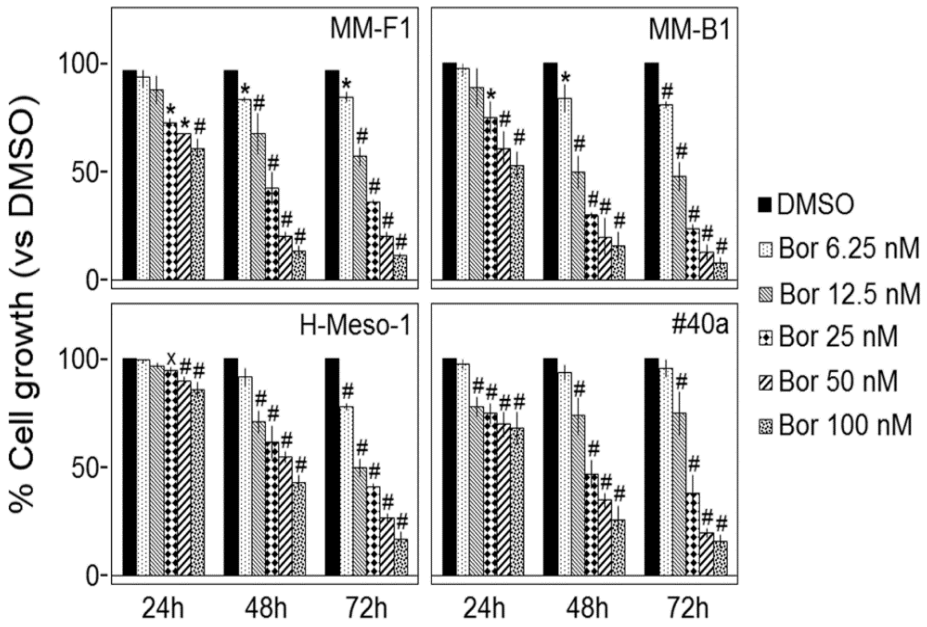

Figure 16. Effect of Bor on MM cells survival. *The survival of human (MM-B1, MM-F1, H-Meso-1) and murine (#40a) cell lines was evaluated by the SRB assay after 24, 48, and 72 hours of treatment with Bor or DMSO. The percentage of surviving cells treated with the compound was calculated by normalizing the O.D. value to that of the control cultures (DMSO). The results are expressed as mean ± standard deviation (SD) of three independent experiments performed in triplicate (ˣp≤0.05; *p≤0.01; #p≤0.001 vs. DMSO).*

Bor concentration that causes the inhibition of 50% (IC50) of the cell growth was also determined for each cell line (Table 2) Our results show that MM-B1 was the most sensitive, whereas H-Meso-1 was the less sensitive cell line, after 48 h of treatment.

Table 2. Bor concentrations at 50% of cell growth inhibition (IC50) on human and murine MM cell lines.

	Hours of Bor treatment	**IC_{50} ± SD (nM)**
MM-F1	48	21.7 ± 2.7
	72	18.2 ± 1.2
MM-B1	48	15.0 ± 1.0
	72	13.3 ± 0.8
H-Meso-1	48	62.3 ± 13.9
	72	16.9 ± 1.5
#40a	48	30.0 ± 3.9
	72	21.9 ± 3.8

In addition, Trypan blue exclusion assay allowed to distinguish viable cells from necrotic ones. As shown in Figure 17, Bor was able to significantly increase the percentage of dead cells in a dose- and time-dependent manner after 24, 48 and 72 hours, in all MM cell lines tested compared to control.

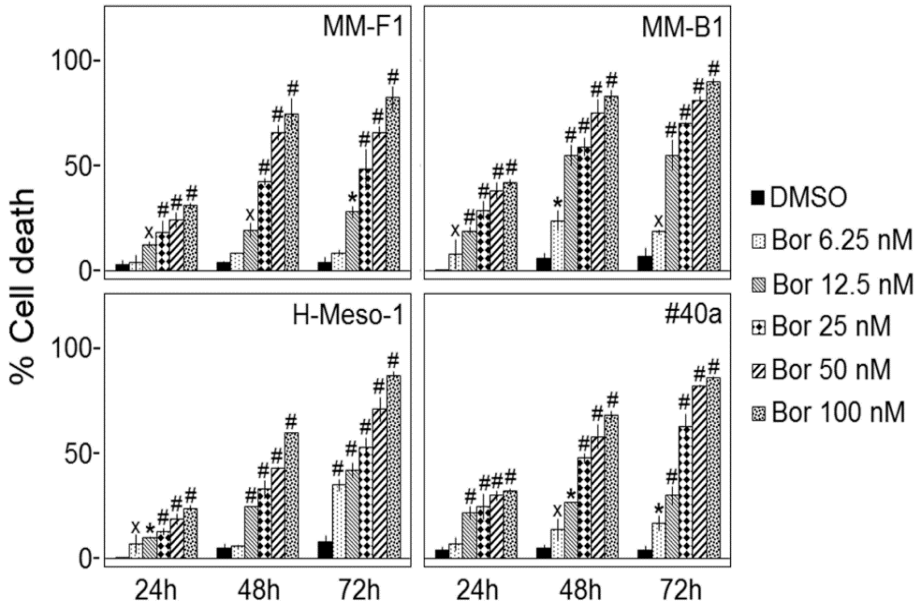

Figure 17. Effect of Bor on MM cell lines death. *The death of human (MM-B1, MM-F1, H-Meso-1) and murine (#40a) cell lines was demonstrated by the Trypan blue assay after 24, 48, and 72 hours of treatment with Bor or DMSO. The results are expressed as mean ± SD of three independent experiments performed in triplicate (ˣp≤0.05; *p≤0.01; #p≤0.001 vs. DMSO).*

Effect of Bor on apoptosis and cell cycle distribution on human and murine MM cell lines.

To determine the effect of Bor on apoptosis and on the modulation of cell cycle, flow cytometric analysis (FACS) of cellular DNA content was carried out. Human (MM-B1, MM-F1, H-Meso-1) and murine (#40a) MM cell lines were treated for 48 hours with increasing doses of Bor (6.25 nM – 50 nM) or DMSO as control.

As shown in Fig. 18, Bor treatment significantly increases the percentage of cells in the subG1 phase, compared to DMSO, in all cell lines treated. Specifically, in MM-B1 and #40a cell lines, the percentage of sub-G1 cells increased at Bor concentrations of 6.25 nM or higher, while in MM-F1 and H-Meso-1 cell lines, a significant increase in the sub-G1 fraction was observed at concentrations of 12.5 nM and 25 nM, respectively (Fig. 18).

Overall, the increase in sub-G1 cells was accompanied by a reduction in the G0/G1 phase in all cell lines, on the contrary the S and G2/M phases decreased in a cell-dependent manner

and only at selected Bor concentrations. Cells in the sub-G1 phase are characterized by hypodiploid DNA content, which is typically, though not exclusively, associated with apoptosis.

To corroborate Bor's role in inducing apoptosis, MM cells were treated with Bor at the highest concentration (50 nM) in the presence of a universal caspase inhibitor, Z-VAD-FMK. In all MM cell lines, the percentage of sub-G1 fraction was significantly reduced when Bor was combined with Z-VAD-FMK, confirming that Bor is able to induces apoptotic cell death (Fig. 18).

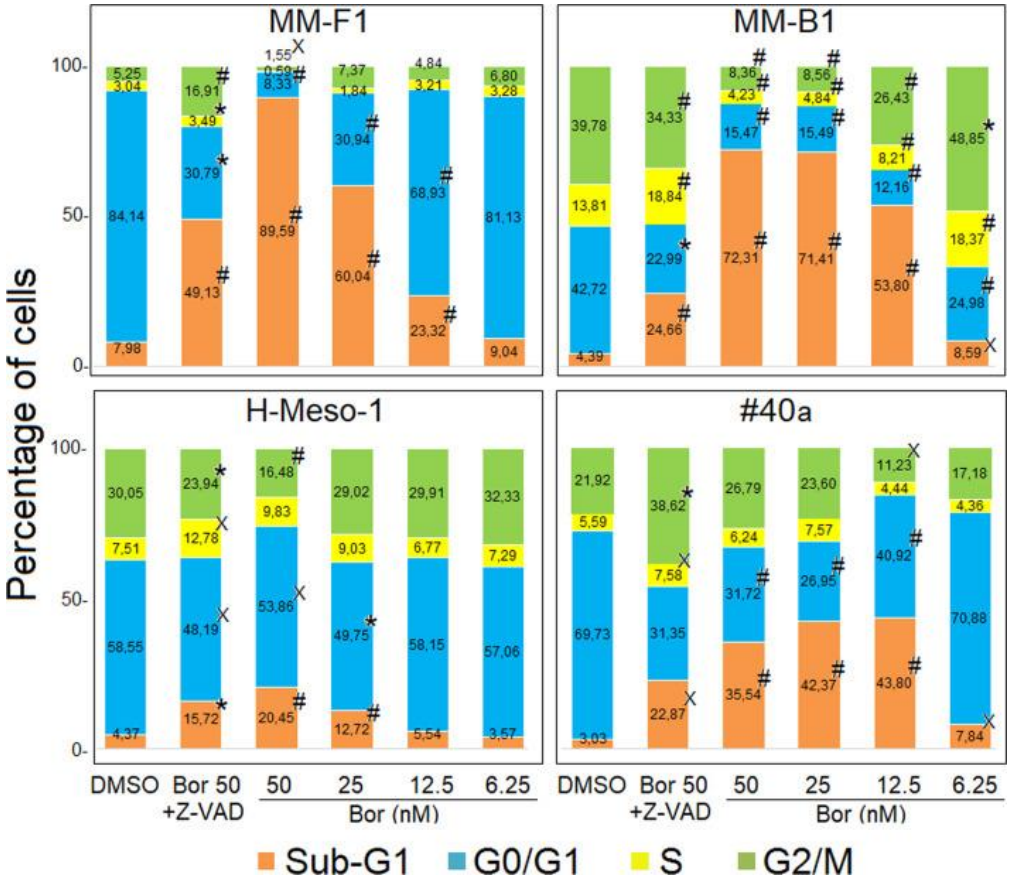

Figure 18. Effect of Bor on cell cycle distribution and apoptotic process. *Cells were treated with Bor at the concentrations range of 6.25 nM – 50 nM, for 48 hours and then analyzed by FACS analysis. Stacked bar graphs showing the percentage of cells in subG1, G0/G1, S, and G2/M phases of the cell cycle. Percentage of cells in different phases was obtained from two independent experiments and calculated with CellQuest Pro 5.2 software. Results represent mean values from two independent experiments. Statistical significance of the effect of Bor vs DMSO and Bor 50nM + Z-VAD-FMK vs Bor 50 nM were calculated with one-way ANOVA (x p≤0.05; *p≤0.01, # p≤0.001).*

Effect of Bor on the expression of molecules involved in apoptosis in human and murine MM cell lines.

To confirm Bor's effect on inducing apoptosis in MM cells, the levels of Bax, Bcl-2, cleaved-caspase 3, cleaved poly (ADP-ribose) polymerase-1 (PARP-1), and γH2AX were examined through Western blotting (Fig. 19). Bor increased the levels of the pro-apoptotic Bax protein in all cell lines, and a decreasing in the levels of the anti-apoptotic Bcl-2 protein was evidenced in MM-B1, H-Meso-1, and #40a cells (Fig. 19a). Consequently, Bor treatment significantly increased the Bax/Bcl-2 ratio in MM-F1 ($p<0.05$), MM-B1 ($p<0.01$), H-Meso-1 ($p<0.01$), and #40a ($p<0.05$) cell lines compared to DMSO-treated cells (Fig. 19b).

The proteasome inhibitor is able to determine the cleavage of Caspase 3 and its activation in all cell lines tested, as indicated by the presence of the specific band corresponding to the cleaved form of the protein in the Western blotting analysis (Fig. 19a). Activated-Caspase 3 promotes the proteolytic inactivation of PARP-1, which leads to impaired DNA repair and prevents DNA repair-associated cell survival [239, 240]. In line with this, Bor treatment increased the levels of the 89 kDa cleaved PARP fragment in MM-F1, MM-B1, and H-Meso-1 cells (Fig. 19a). Additionally, DNA fragmentation during apoptosis is known to trigger the phosphorylation of histone H2AX at Ser139, creating the γH2AX form [241, 242]. A significant increase in γH2AX levels was observed in all cell lines after Bor treatment compared to DMSO-treated controls (Fig. 19a, c). Notably, H-Meso-1 showed the smallest increase in γH2AX levels, which correlated with its lower percentage of cells with hypodiploid DNA content, as revealed by FACS analysis. In conclusion, these results confirm the induction of apoptosis in Bor-treated MM cells.

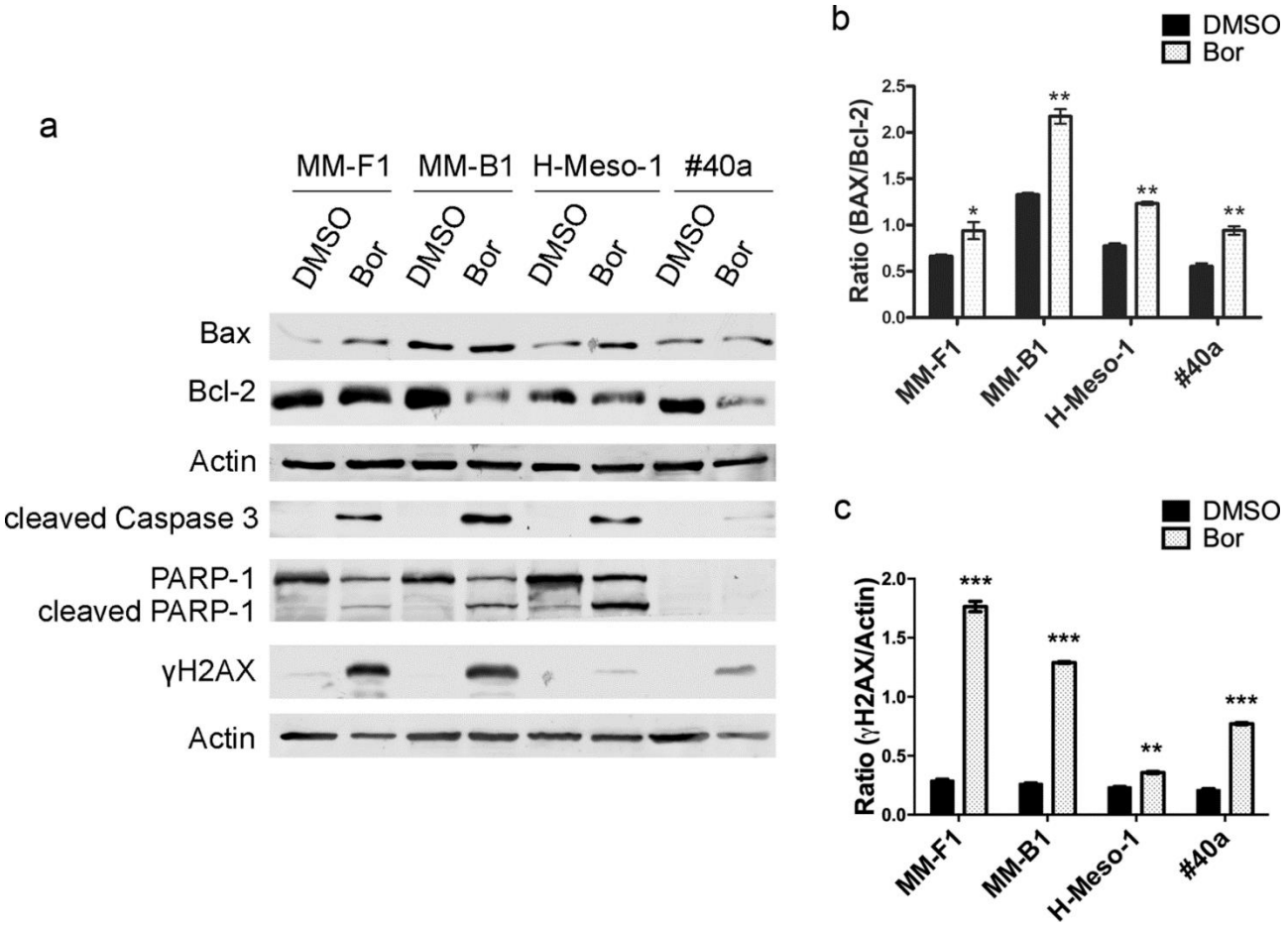

***Figure 19. Effects of Bor on molecules involved in apoptotic process in human and murine MM cell lines**. **a.** The expression of Bax, Bcl-2, cleaved caspases 3, PARP-1, cleaved PARP-1 and γH2AX was evaluated by Western blotting analysis following treatment for 48 hours of MM cells with Bor 25nM or DMSO as reported in Materials and Methods. Actin was used as internal control. **b, c.** Densitometric ratios between Bax and Bcl-2 **(b)**, and between γH2AX and Actin **(c)**. The densitometric analysis of the bands was calculated using the ImageJ 1.53e software after blot scanning of two independent experiments and expressed as mean ± SD values (*p≤0.05; **p≤0.01; ***p≤0.001).*

Furthermore, to verify Bor's effect on the proteasome inhibition, Bor-treated MM cell lysates were analyzed through Western blot using an anti-ubiquitin antibody. Elevated levels of ubiquitinated proteins were detected in all cell lines following Bor treatment (Fig. 20), supporting Bor-induced proteasome inhibition [192].

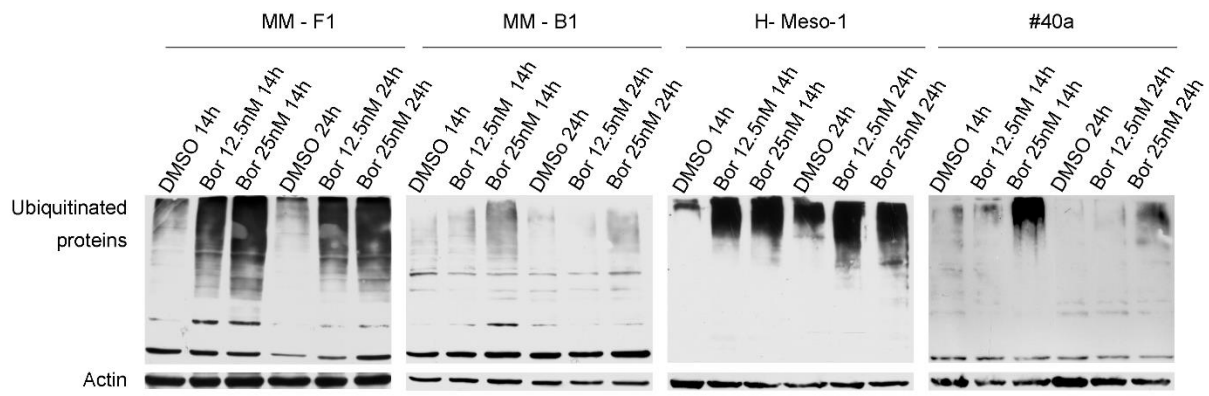

Figure 20. Effect of Bor on protein ubiquitination. *Western blotting analysis was performed on lysates from human and murine MM cell lines treated with Bor (12.5 and 25 nM) or DMSO for 14 or 24 hours. Blots were probed with an anti-ubiquitin antibody. Actin was used as internal control.*

Effect of Bor on autophagy and ER stress in human and murine MM cell lines.

Autophagy is one of the mechanism of cells to respond to stressors. It has been demonstrated that Bor can influence autophagy and the resistance to Bor treatment is potentially being linked to the activation of autophagic process [243, 244]. In order to demonstrate whether Bor was able to induce autophagy in MM cell lines, the expression of proteins involved in the autophagic flux including the selective autophagy substrate Beclin-1, p62/SQSTM-1, and the levels of the autophagosome marker Microtubule-Associated Protein Light Chain 3-II (LC3-II) was analyzed by Western blotting in Bor-treated cells and compared to DMSO-treated cells used as control (Fig. 21). Modulation in the expression of LC3-II and SQSTM-1/p62 are interconnected since an increase in LC3-II could indicate either higher autophagosome formation or reduced autophagosome clearance. Therefore, concomitant changes in LC3-II and SQSTM-1/p62 levels help distinguish between autophagy induction and impaired autophagic flux [245].

In the murine #40a MM cell line, Bor treatment increased both LC3-II and SQSTM-1/p62 levels, suggesting that Bor inhibits autophagic flux (Fig. 21a, c, d). In the three human MM cell lines (MM-F1, MM-B1 and H-Meso-1), Bor increased LC3-II levels but did not significantly affect SQSTM-1/p62 expression levels (Fig. 21a, c, d). Additionally, Beclin-1, a

protein involved in various autophagic processes and known for its anti-apoptotic functions [246], was reduced by Bor in two human MM cell lines (MM-F1 and H-Meso-1) and the murine #40a MM cell line (Fig. 21a, e). While Bor's effects on these autophagy markers were cell line-specific, the overall data imply that Bor may interfere with autophagic flux in human MM cell lines and decrease it in murine MM cell line.

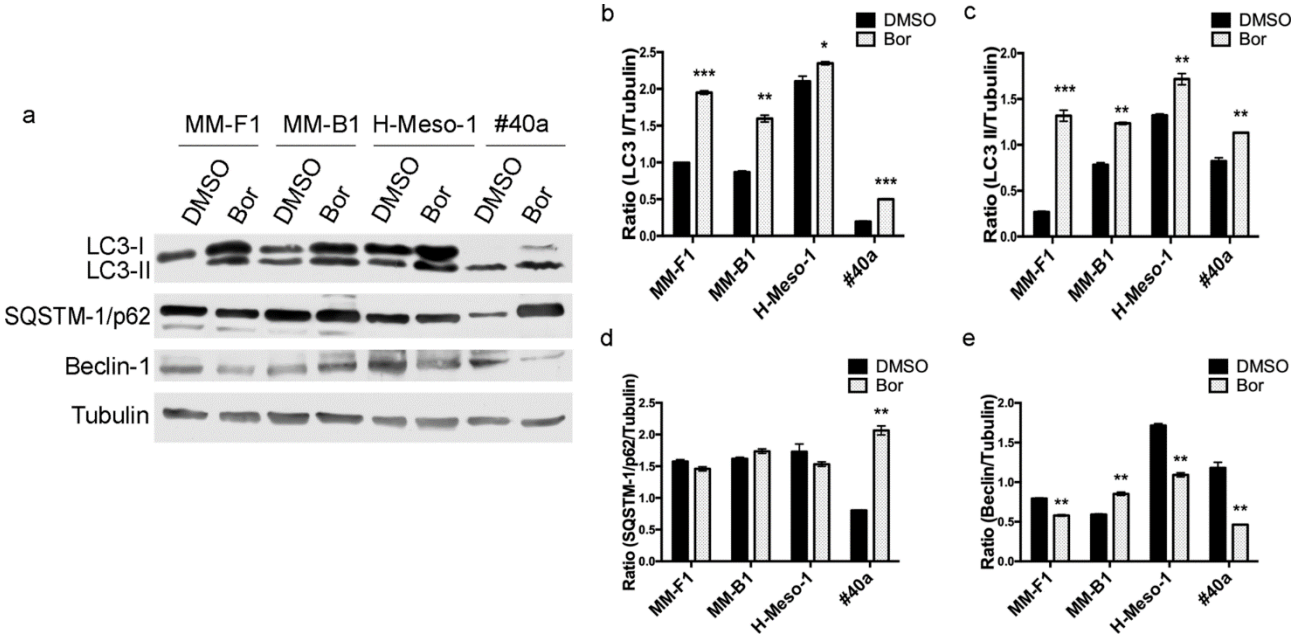

Figure 21. Effect of Bor on autophagy in MM cell lines. *Western blotting analysis was performed on human and murine MM cells treated with Bor 25nM or DMSO as reported in Materials and Methods. Tubulin was used as an internal control.*
b–e. *Densitometric ratios between LC3-I and Tubulin* ***(b)****; LC3-II and Tubulin* ***(c)****; SQSTM-1/ p62 and Tubulin* ***(d)****; Beclin-1 and Tubulin* ***(e)****. The densitometric analysis of the bands was calculated using the ImageJ 1.53e software after blot scanning of two independent experiments and expressed as mean ± SD values (*p≤0.05; **p≤0.01; ***p≤0.001).*

Proteasome inhibitors, like Bor, trigger ER stress by preventing the degradation of misfolded and unfolded proteins. Since cancer cells are often already under ER stress due to their high rates of protein, proteasome's inhibition further worsens ER stress. This activates the Unfolded Protein Response (UPR), a cellular mechanism designed to restore normal ER function by reducing protein synthesis, increasing the capacity to fold proteins or leading to apoptosis [247, 248]. To evaluate Bor's effect on ER stress and UPR in human and murine MM cells, the expression of Glucose-Regulated Protein 78/ Binding immunoglobulin Protein (GRP78/BiP), an ER chaperone with anti-apoptotic functions, and CCAAT-enhancer-binding protein homologous protein (CHOP), a key protein in ER stress-induced apoptosis, were examined through Western blotting analysis [249, 250].

GRP78/BiP levels were significantly elevated in all human and murine Bor-treated MM cell lines (Fig. 22a, b), suggesting that Bor induces ER stress and activates the UPR [247]. However, Bor treatment reduced significantly CHOP expression in the three human MM cell lines, but had no significant effect on CHOP levels in the murine #40a MM cell line (Fig. 22a, c). These findings suggest that, in MM cell lines treated with Bor, UPR activation does not contribute to apoptosis but may instead reduce sensitivity to Bor's cytotoxic effects.

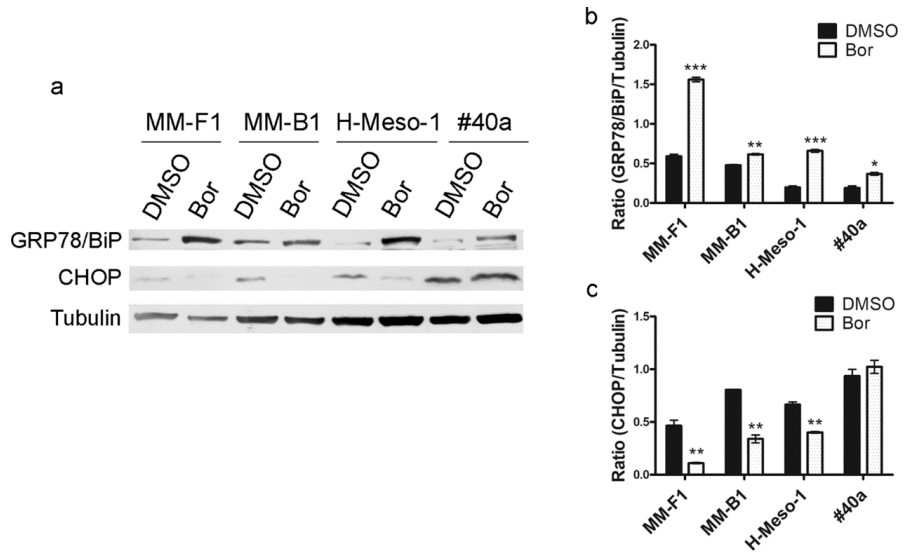

Figure 22. Effect of Bor on ER stress in MM cell lines. a. *Western blotting analysis was performed on human and murine MM cell lines treated with Bor 25 nM or DMSO for 48 hours as reported in Materials and Methods. Tubulin was used as internal control.* ***b, c.*** *Densitometric ratios between GRP78 and Tubulin* ***(b)****, and between CHOP and Tubulin* ***(c)****. The densitometric analysis of the bands was calculated using the ImageJ 1.53e software after blot scanning of two independent experiments and expressed as mean ± SD values (*p≤0.05; **p≤0.01; ***p≤0.001).*

Effect of Bor on the expression and activation of ErbB receptors (EGFR and ErbB2) and pro-survival signaling transduction pathway molecules (ERK, p38, AKT) in human and murine MM cell lines.

In MM, overexpression and deregulation of ErbB receptors family can activate the MAP kinase and phosphoinositide 3-kinase/AKT signaling pathways, which contribute to cancer cell proliferation, survival, and drug resistance [2, 251].

In order to elucidate the effects of Bor treatment on signaling pathways deregulated in MM, the expression of EGFR and ErbB2, along with the activation of key downstream pro-survival signaling proteins such as ERK1/2, AKT and p38, was analyzed by Western blotting analysis (Fig. 23)

Although Bor modestly increased of EGFR levels in H-Meso-1 cell line and decreased it in #40a cell line, no significant changes in its expression were observed in MM-F1 and MM-B1 cell lines treated with Bor compared to control ones (Fig. 23a, b). Bor reduced ErbB2 expression levels in MM-B1, H-Meso-1, and #40a cell lines, but no change was observed in MM-F1 cell line (Fig. 23a, c). Thus, Bor reduced the expression of at least one of the two ErbB family receptors (EGFR and ErbB2) in all MM cell lines examined, excluded MM-F1.

The activation of the MAPKs, ERK1 and ERK2 is also reduced by Bor treatment in all MM cell lines analyzed. Specifically, it lowered the phosphorylated levels of both ERK1 and ERK2 in MM-F1 and MM-B1 cell lines, while a reduction in the phosphorylation of at least one of the two kinases was determined in H-Meso-1 and #40a cell lines (Fig. 23a, d, e). Conversely, Bor increased AKT phosphorylation in all treated human MM cell lines (Fig. 23a, f), but had no significant effect on p38 activation/phosphorylation (Fig. 23a, g).

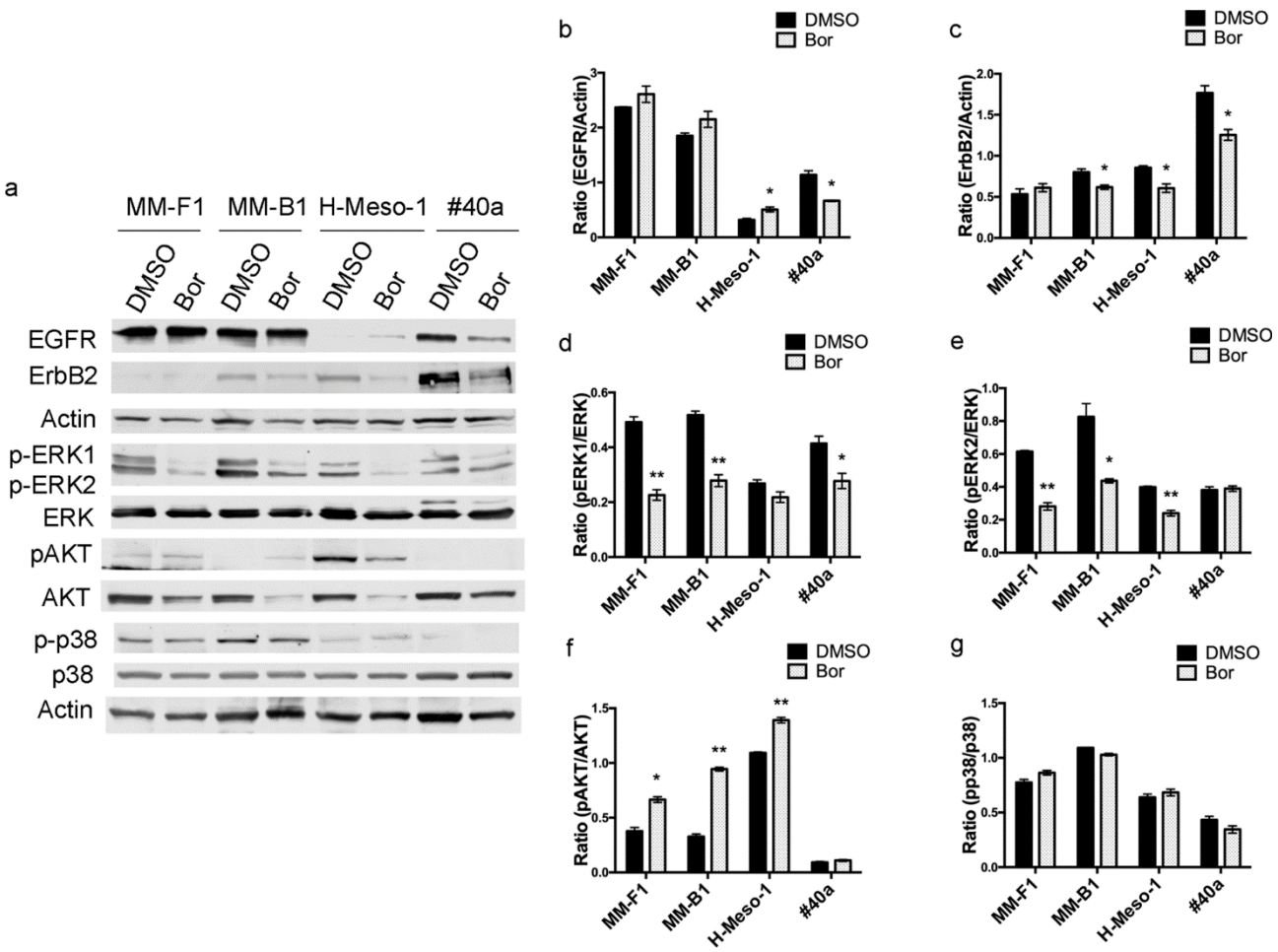

Figure 23. Effect of Bor on the expression and activation of signaling pathway molecules in MM cell lines. *Expression of EGFR, ErbB2, expression and activation of ERK1/2, Akt and p38, in MM-F1, MM-B1, H-Meso-1 and #40a cell lines were evaluated by Western blotting analysis following treatment with Bor or DMSO for 48 hours as described in Materials and Methods. Actin was used as internal control.* ***b–h****. Densitometric ratios between EGFR and Actin* ***(b)****, ErbB2 and Actin* ***(c)****, phospho-ERK1 and ERK* ***(d)****, phospho-ERK2 and ERK* ***(e)****, phospho-AKT and AKT* ***(f)****, phospho-p38 and p38* ***(g)****. The densitometric analysis of the bands was calculated using the ImageJ 1.53e software after blot scanning of two independent experiments and expressed as mean ± SD values (*p≤0.05; **p≤0.01; ***p≤0.001).*

In vivo effects of treatment with Bor on the growth of MM #40a cells in C57BL / 6 mice.

C57BL/6 mice (10 per group) were intraperitoneally (i.p.) inoculated with 1.5×10^6 MM #40a cells and simultaneously treated via i.p. injection with 0.5 mg/kg of Bor dissolved in PBS-DMSO, while the control group (CTR) received only the vehicle (PBS-DMSO). The treatments were administered twice a week. Tumor growth, which induces ascites, was monitored by measuring the mice's abdominal circumference prior to cell inoculation and weekly afterward.

After four weeks of treatment, Bor-treated mice exhibited a significant reduction in abdominal circumference compared to CTR mice (*p=0.015*, mean value 7.1±0.6 vs. 7.9±0.7 cm) (Fig. 24a). By week five, the difference was more pronounced compared to control mice (*p=0.0003*, mean value 7.4±0.8 vs. 9.1±0.8 cm). After seven weeks, all CTR mice had been euthanized due to excessive abdominal circumference (≥12 cm), whereas 50% of the Bor-treated mice were still alive (Fig. 24b).

Consequently, the median survival of the Bor-treated mice was significantly longer than that of the CTR group (*p=0.02*, 7.2 vs. 5.7 weeks) (Fig. 24b). Survival analysis using the log-rank test (Mantel–Cox) revealed a Hazard Ratio (HR) of 4.1 for CTR mice compared to Bor-treated mice (Table 3).

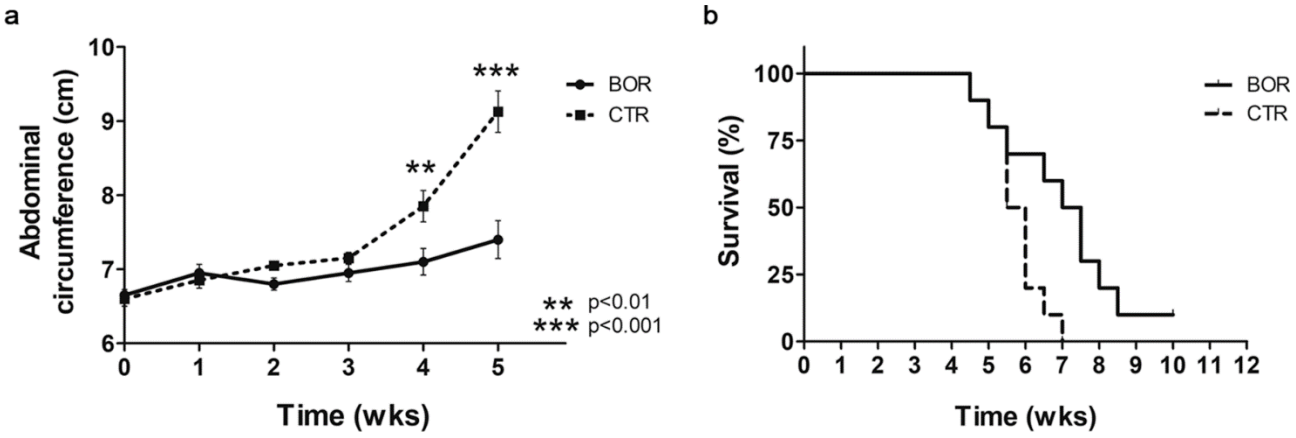

Figure 24. Bor reduced tumor growth and increased survival of C57BL/6 mice i.p. injected with syngeneic MM #40a cells. ***a)*** *Difference in mean abdominal circumferences among C57BL/6 mice treated with Bor and control ones (CTR).* ***b)*** *Differences in mean survival duration of C57BL/6 mice treated with Bor or PBS + DMSO (CTR). The numbers of treated mice are reported in the section "Materials and Methods".*

Table 3. Analysis of the survival in C57BL/6 mice after treatment with Bor or vehicle (CTR) by the log-rank test (Mantel–Cox).

Variable	Contrast	Hazard Ratio (HR)	95% HR confidence limits		*p* value	Median Survival (weeks)
			Lower	Upper		
Treatment	CTR vs Bor	4.1	1.28	13.11	0.0172	5.75 vs 7.25

In vivo effect of Bor on the frequency of immune cells infiltration in the tumor microenvironment of C57BL/6 mice transplanted with syngeneic #40a MM cells.

To assess the impact of Bor on the phenotype and frequency of immune cells recruited to the tumor microenvironment, two groups of five mice were injected i.p. with MM #40a cells, treated with Bor or PBS-DMSO (CTR), and sacrificed after 30 days. Immune cells from the ascitic fluid were collected through peritoneal lavage and analyzed by flow cytometry, with spleen cells from the same mice serving as controls. The gating strategy for identifying leukocyte subpopulations is shown in Figure 25.

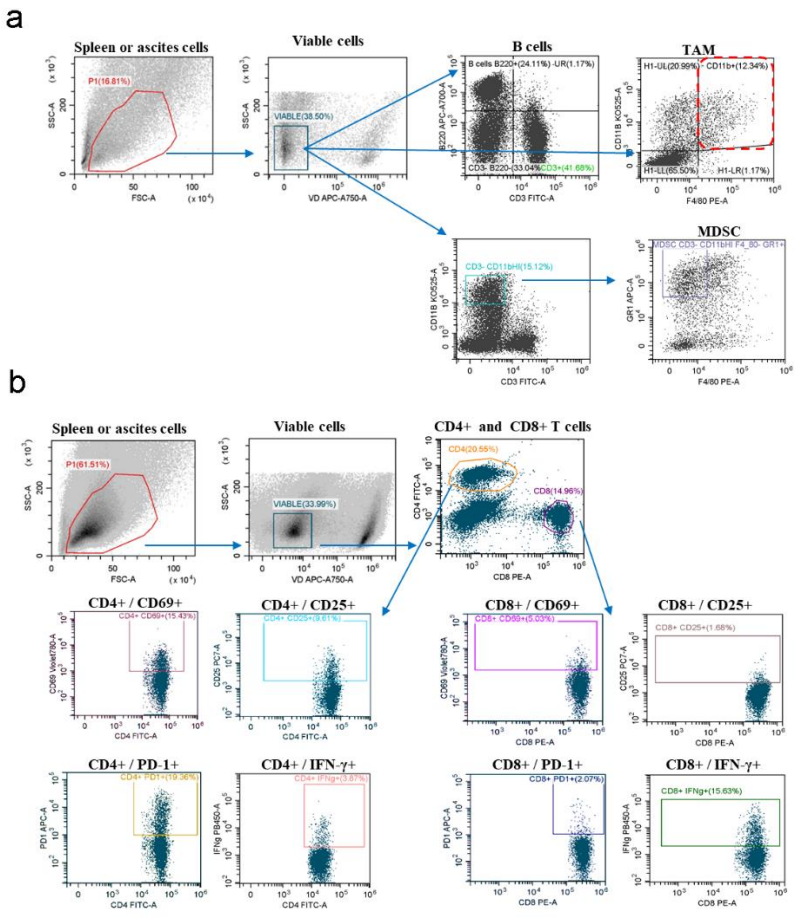

Figure 25. Gating strategies for leukocyte subpopulations identification. a) *Flow cytometry gating strategy used to characterize B cells (CD3$^-$B220$^+$), MDSCs (CD3$^-$CD11b^{HI}F4/80$^-$Gr-1$^+$) and TAMs (F4/80$^+$CD11b$^+$) in the spleens or ascitic fluids of C57BL/6 mice i.p. transplanted with MM #40a cells.* ***b)*** *Flow cytometry gating strategy used to characterize CD4 and CD8 T cells (CD4+ or CD8+), activated T cells (CD4$^+$CD69$^+$ or CD4$^+$CD25$^+$or CD8$^+$CD69$^+$ or CD8$^+$CD25$^+$), and expression of PD-1 and IFN-γ on CD4 and CD8 T cells in the spleens or ascitic fluids of C57BL/6 mice i.p. transplanted with MM #40a cells. Leukocytes were gated based on SSC-A versus FSC-A, and dead cells were excluded with Fixable Viability Dye.*

In Bor-treated mice the frequency of CD4+ and CD8+ T lymphocytes in the spleen resembled that of the CTR mice (Table 4). However, in the ascitic fluid, CD4+ T lymphocyte frequency was significantly reduced in Bor-treated mice compared to CTR mice (Bor 5.1±2.4 vs. CTR 13.8±2.7, $p<0.001$), while CD8+ T lymphocyte levels remained comparable (Table 4, Fig. 26a). The frequency of B lymphocytes (CD3−/B220+ cells) significantly decreased in the spleen of Bor-treated mice (Bor 23.9±3.0 vs. CTR 30.4±5.0, $p<0.05$), with a non-significant trend toward a decrease in ascitic fluid (Table 4, Fig. 26a).

Table 4. Frequency of immune infiltrate in spleen and peritoneal ascitic fluid of C57BL/6 mice transplanted with syngeneic #40a murine MM cells.

Cells	Spleen			Ascites		
	CTR	**Bor**	***p* value**	**CTR**	**Bor**	***p* value**
$CD4^+$	18.8±3.7	19.6±3.8	ns	13.8±2.87	5.1±2.4	$p \leq 0.001$
$CD8^+$	18.0±3.2	18.6±2.1	ns	14.4±1.1	12.8±6.1	ns
B cells	30.4±5.0	23.9±3.0	$p \leq 0.05$	22.2±5.5	17.7±2.1	ns
MDSC	56.6±18.0	70.2±5.2	ns	26.6±8.8	22.1±9.6	ns
TAM	3.6±3.7	1.2±0.3	ns	13.0±2.9	11.8±2.1	ns

MDSC = myeloid-derived suppressor cells; TAM = tumor-associated macrophages; *ns* = not significant

Myeloid-derived suppressor cells (MDSCs), an immune population characterized by their ability to suppress T cell responses and regulate innate immunity by modulating macrophages cytokines production, were identified as CD3+/$CD11b^{HIGH}$/F4/80−/Gr1+ cells. Their frequency in the spleen was similar between Bor-treated and CTR mice, and although lower in ascitic fluid than in the spleen, the MDSC frequency was comparable between Bor-treated and CTR mice (Table 4 Fig. 26a). Tumor-associated macrophages (TAMs), identified as F4/80+/CD11b+ cells, were more abundant in ascitic fluid than in the spleen, but showed no significant difference between Bor-treated and CTR mice (Table 4 Fig. 26a).

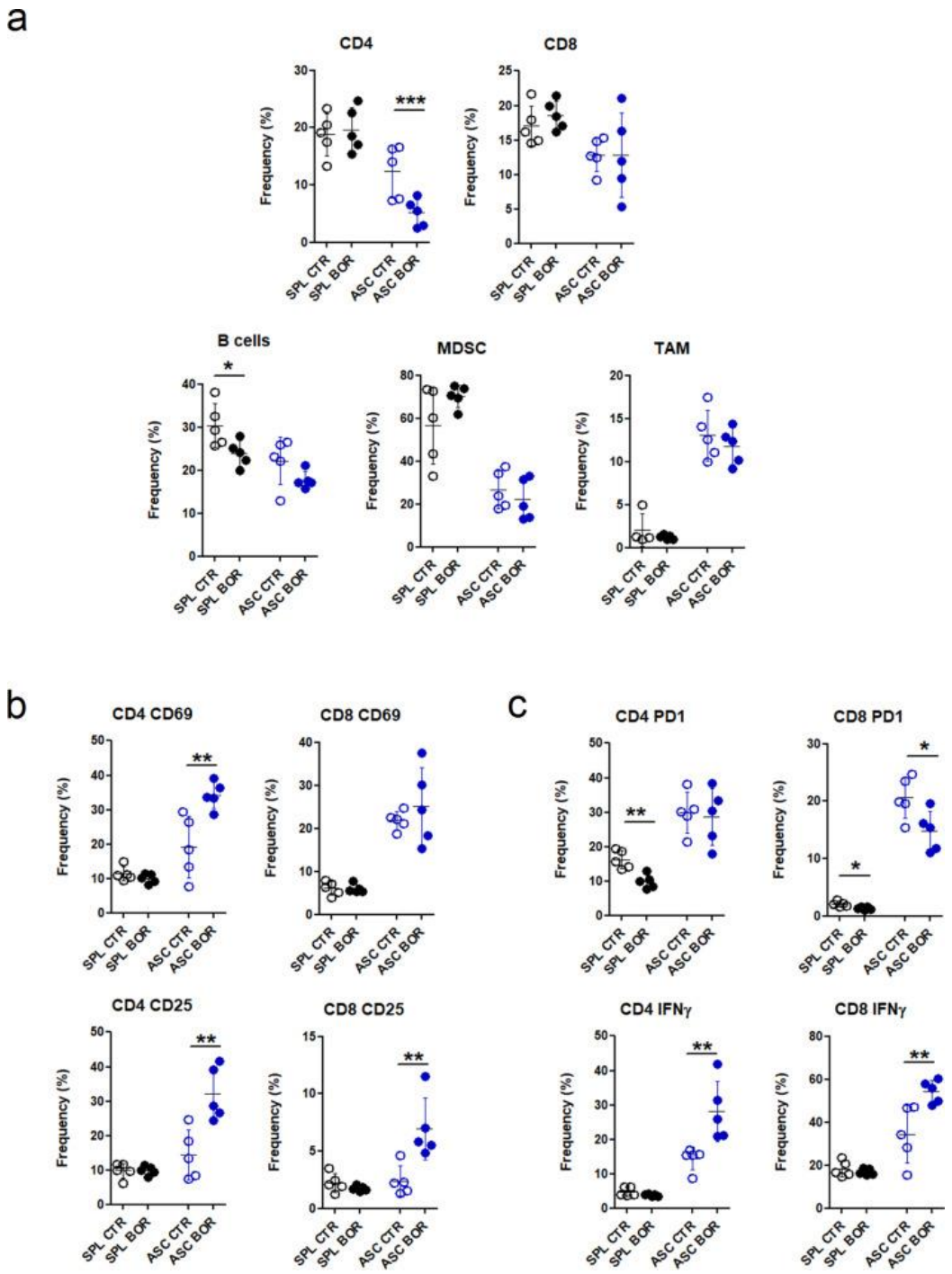

Figure 26. Effect of Bor on the immune cells frequency and on the T cells functional status in the tumor microenvironment. ***a)*** *Frequency of CD4+ and CD8+ T lymphocytes, B lymphocytes, Myeloid-derived suppressor cells (MDSCs) and Tumor associated macrophages (TAMs) in the spleen (SPL) and peritoneal ascitic fluid (ASC) of tumor-bearing mice (day 30) treated with Bor (n=5) or CTR (n=5), as assessed by flow cytometry.* ***b)*** *Frequency of CD4+/CD69+, CD8+/CD69+ and of CD4+/CD25+, CD8+/CD25+ T lymphocytes in the spleen (SPL) or in the peritoneal ascitic fluid (ASC) of tumor-bearing mice (day 30) treated with Bor (n=5) or with CTR (n=5), as assessed by flow cytometry.* ***c*** *Frequency of CD4+/PD-1+, CD8+/PD-1+ and of CD4+/IFN-γ+, CD8+/IFN-γ+ T lymphocytes in the spleen (SPL) or in the peritoneal ascitic fluid (ASC) of tumor-bearing mice (day 30) treated with Bor (n=5) or with CTR (n=5), as assessed by flow cytometry. Reported are mean ± SD values. Statistical significance of the differences observed between Bor- and CTR-treated mice was evaluated by Student t-test (*p≤0.05; **p≤0.01; ***p≤0.001).*

In vivo effect of Bor on the functional status of T cells recruited to the tumor microenvironment in C57BL/6 mice transplanted with syngeneic #40a MM cells.

The functional status of CD4+ and CD8+ T lymphocytes infiltrating the ascitic fluid of mice i.p. injected with MM #40a cells was assessed by flow cytometry, focusing on activation markers, cytokine production, and expression of the immune checkpoint inhibitor Programmed Cell Death 1 (PD-1).

T cell activation markers, CD69 and CD25, were first examined. In the spleen, similar frequencies of CD25+ and CD69+ T lymphocytes were observed between Bor-treated and CTR mice (Table 5, Fig. 26b). However, Bor-treated mice showed more than twice the frequency of CD4+/CD69+ cells in ascitic fluid compared to CTR mice (Bor 34.2±3.9 vs. CTR 13.1±9.0), while no significant differences were seen in CD8+/CD69+ cells between the groups (Table 5, Fig. 26b). Regarding the CD25 activation marker, Bor led to a significant increase in both CD4+/CD25+ (Bor 32.1±7.8 vs. CTR 14.5±7.2) and CD8+/CD25+ T cells (Bor 6.9±2.7 vs. CTR 2.4±1.3) in the ascitic fluid (Table 5, Fig. 26b).

Table 5. Frequency of T lymphocytes expressing CD69 and CD25 activation markers in spleen and peritoneal ascitic fuid of C57BL/6 mice injected with murine #40a MM cells.

Cells	Spleen			Ascites		
	CTR	**Bor**	***p* value**	**CTR**	**Bor**	***p* value**
$CD4^+CD69^+$	11.4±2.1	10.0±1.3	ns	13.1±9.0	34.2±3.9	$p \leq 0.01$
$CD8^+CD69^+$	6.1±1.6	5.9±1.0	ns	21.8±2.2	25.1±8.9	ns
$CD4^+CD25^+$	9.8±2.2	9.8±1.4	ns	14.5±7.2	32.1±7.8	$p \leq 0.01$
$CD8^+CD25^+$	2.3±0.8	1.7±0.2	ns	2.4±1.3	6.9±2.7	$p \leq 0.01$

ns = not significant

PD-1, a key inhibitory receptor that allows cancer cells to evade T cell-mediated immune responses, was also analyzed. Bor -treated mice had reduced frequencies of both CD4+/PD-1+ and CD8+/PD-1+ cells in the spleen compared to CTR mice (CD4+/PD-1+: Bor 9.9±2.1 vs. CTR 16.2±2.7; CD8+/PD-1+: Bor 1.3±0.3 vs. CTR 2.1±0.5). Similarly, the number of CD8+/PD-1+ cells in the ascitic fluid was lower in Bor-treated mice compared to controls (Bor 14.8±3.4

vs. CTR 20.6±3.6) (Table 6, Fig. 26c). Additionally, Bor treatment significantly increased the proportion of T cells producing IFN-γ in the ascitic fluid, both in CD4+ (Bor 28.2±8.7 vs. CTR 14.3±3.3) and CD8+ (Bor 54.2±5.3 vs. CTR 34.4±13.3) cells (Table 6, Fig. 26c).

Table 6. Frequency of T lymphocytes expressing PD-1 and IFN-γ in spleen and peritoneal ascitic fluid of C57BL/6 mice injected with #40a murine MM cells.

Cells	Spleen			Ascites		
	CTR	**Bor**	***p* value**	**CTR**	**Bor**	***p* value**
$CD4^+PD\text{-}1^+$	16.2±2.7	9.9±2.1	$p \leq 0.01$	29.9±0.6	28.6±8.2	ns
$CD4^+IFN\text{-}\gamma^+$	4.8±1.3	3.8±0.4	ns	14.3±3.3	28.2±8.7	$p \leq 0.01$
$CD8^+$ $PD\text{-}1^+$	2.1±0.5	1.3±0.3	$p \leq 0.05$	20.6±3.6	14.8±3.4	$p \leq 0.05$
$CD8^+IFN\text{-}\gamma^+$	18.2±3.6	16.9±1.4	ns	34.4±13.3	54.2±5.3	$p \leq 0.01$

ns = not significant

These results suggest that Bor promotes T cell activation in MM-bearing mice by reducing PD-1 expression and enhancing IFN-γ production. Together with findings from *in vitro* experiments, the data indicate that Bor delays MM progression by both directly inhibiting tumor growth and stimulating T cell-mediated immune responses.

The ErbB receptor family is often overexpressed in MM patients and the use of EGFR-targeted drugs can inhibit MM cell proliferation. It is described that the use of a specific unitarget drugs can induce drug-resistance leading to the activation of different deregulated signaling pathways, such as those mediated by ErbB family receptor, Hedgehog, Axl, Wnt [2]. Recent studies in our laboratory, investigated the *in vitro* and *in vivo* effects of a specific inhibitor of ErbB family receptor, AFA, in combination with a multitarget molecule, CUR. CUR was able to enhance AFA effects increasing the AFA-induced reduction of the proliferation rate and pro-apoptotic effects *in vitro*. Indeed, i*n vivo* AFA-antitumor activity was enhanced by its combination with CUR significantly increasing mice overall survival [3].

In another study from our laboratory the effects of inhibitors of Hh- (GANT-61) and ErbB receptors (AFA)-mediated signaling pathways, when used alone or in combination has been evaluated, demonstrating that combined treatment with two inhibitors counteracting the activation of two different signaling pathways involved in neoplastic transformation and progression, such as those activated by ErbB and Hh signaling, is more effective than the single treatments in reducing MM growth *in vitro* and *in vivo*, overcame the occurrence of drug resistance [2].

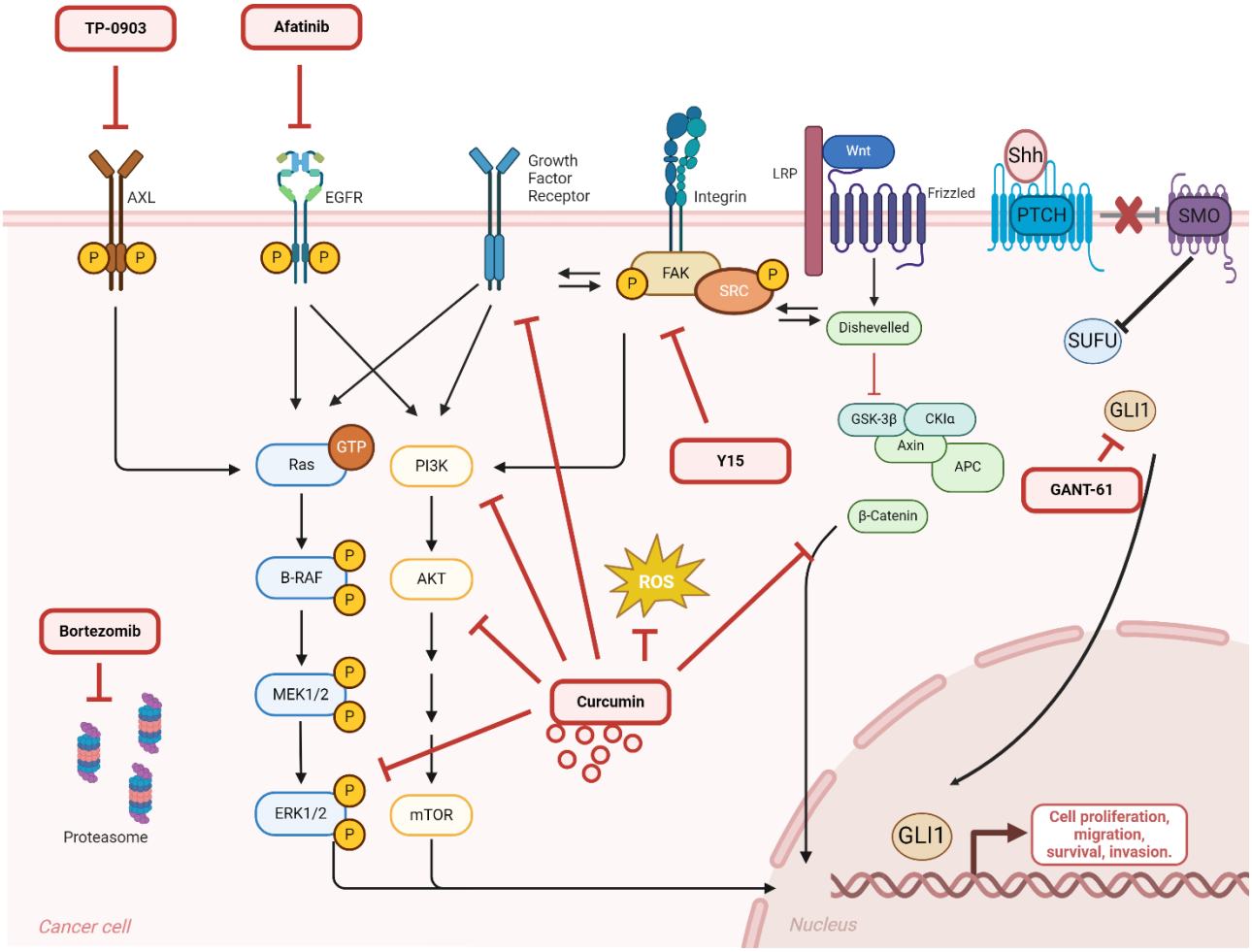

Figure 27. Graphical representation of de-regulated signaling pathways and their inhibitors in MM [1-3]. Created in BioRender.com

Based on these results, we are currently studying whether combined treatment using three different molecular targeted drugs, used at low doses, is more effective than single and dual treatments in inhibiting tumor growth in MM.

Effect of Y15, AFA and TP-0903 on MM spheroids growth.

The aim of this project is to evaluate the effects of three specific inhibitors, AFA, an EGFR family inhibitor, Y15, a FAK inhibitor, and TP-0903, an Axl inhibitor used alone or in combination, on MM tumor growth *in vitro*, using a 3D cellular model. For this purpose, we first evaluated the capability of human (MM-F1, MM-B1 and H-Meso-1) and murine #40a MM cell lines to form spheroids, three-dimensional systems that are more complex and more representative of *in vivo* tumor models. Although MM-B1 and MM-F1 were able to

generate good tumor spheroids when plated under specific conditions described in the Materials and Methods, H-Meso-1 and #40a cells, the human and murine epithelioid histotype of MM were not able to form stable spheroids (Fig. 28).

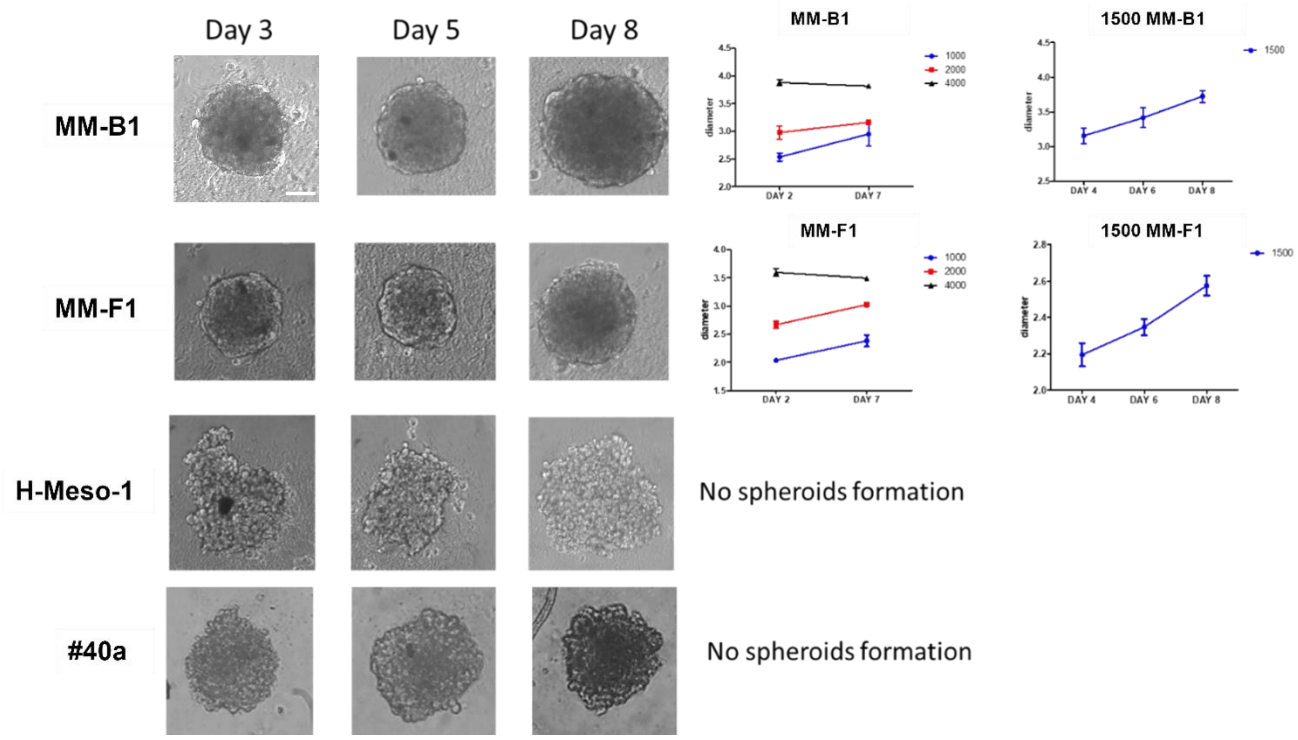

Figure 28. MM 3D spheroids formation*. Human (MM-B1, MM-F1, H-Meso-1) and murine (#40a) MM cell lines were plated at different concentration to form tumor spheroids and monitored for 8 days. Scale bar = 50μm.*

In order to evaluate the antitumoral effects of AFA, Y15 and TP-0903, four-day-old 3D tumor spheroids derived from MM-B1 (Fig. 29) and MM-F1 (Fig. 30) were treated with increasing concentrations of the single inhibitors, in particular Y15 (dose range 1.25 - 20 μM), AFA (dose range 1.25 – 10 μM) and TP-0903 (dose range 0.05 – 0.8 μM) for 24, 48 and 72 hours. MM tumor spheroids diameter was monitored daily. As shown in the figures 29-30, all compounds tested were able of inducing dose- and time-dependent inhibition of MM spheroid growth. Notably, MM-F1 spheroids are more sensitive to the Y15 inhibitor, in fact drug efficacy can be observed already at the concentration of 5 μM, while MM-B1 spheroids are most resistant. In contrast, sensitivity to AFA is similar in both MM-F1 and MM-B1 spheroids, already at (5 μM concentration the spheroids diameter results reduced significantly. Lower concentrations of TP-0903 are sufficient to reduce spheroid growth, in fact significant effects can be seen already at the contraction of 0.1μM.

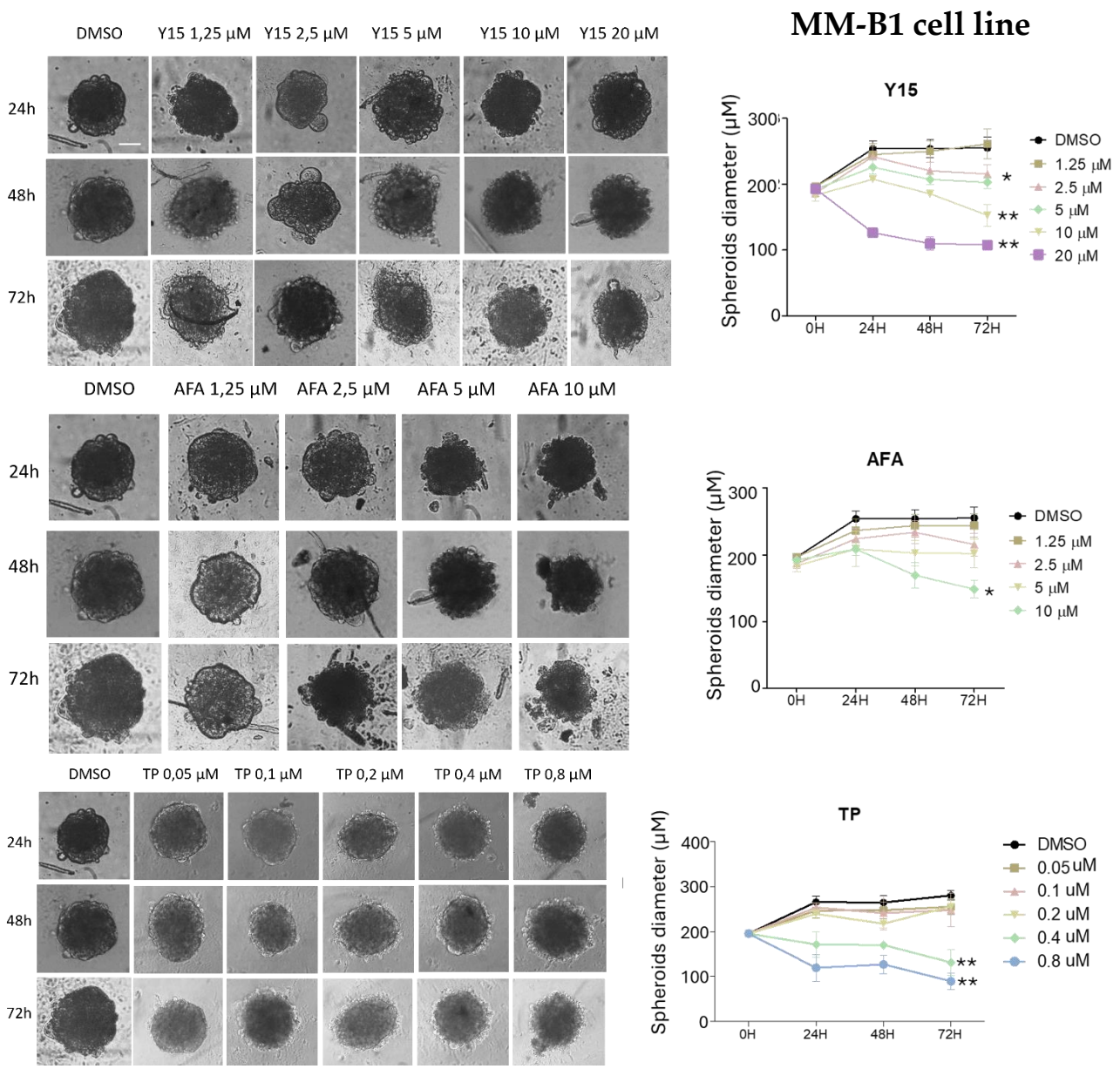

Figure 29. Effect of Y15, AFA and TP-0903, used alone, at different concentrations on MM-B1 tumor spheroids. *MM tumor diameter measurement at 24, 48 and 72 hours after treatments. Statistical significance was calculated with one-way ANOVA. (*p<0.05, **p<0.01). Scale bar = 50µm.*

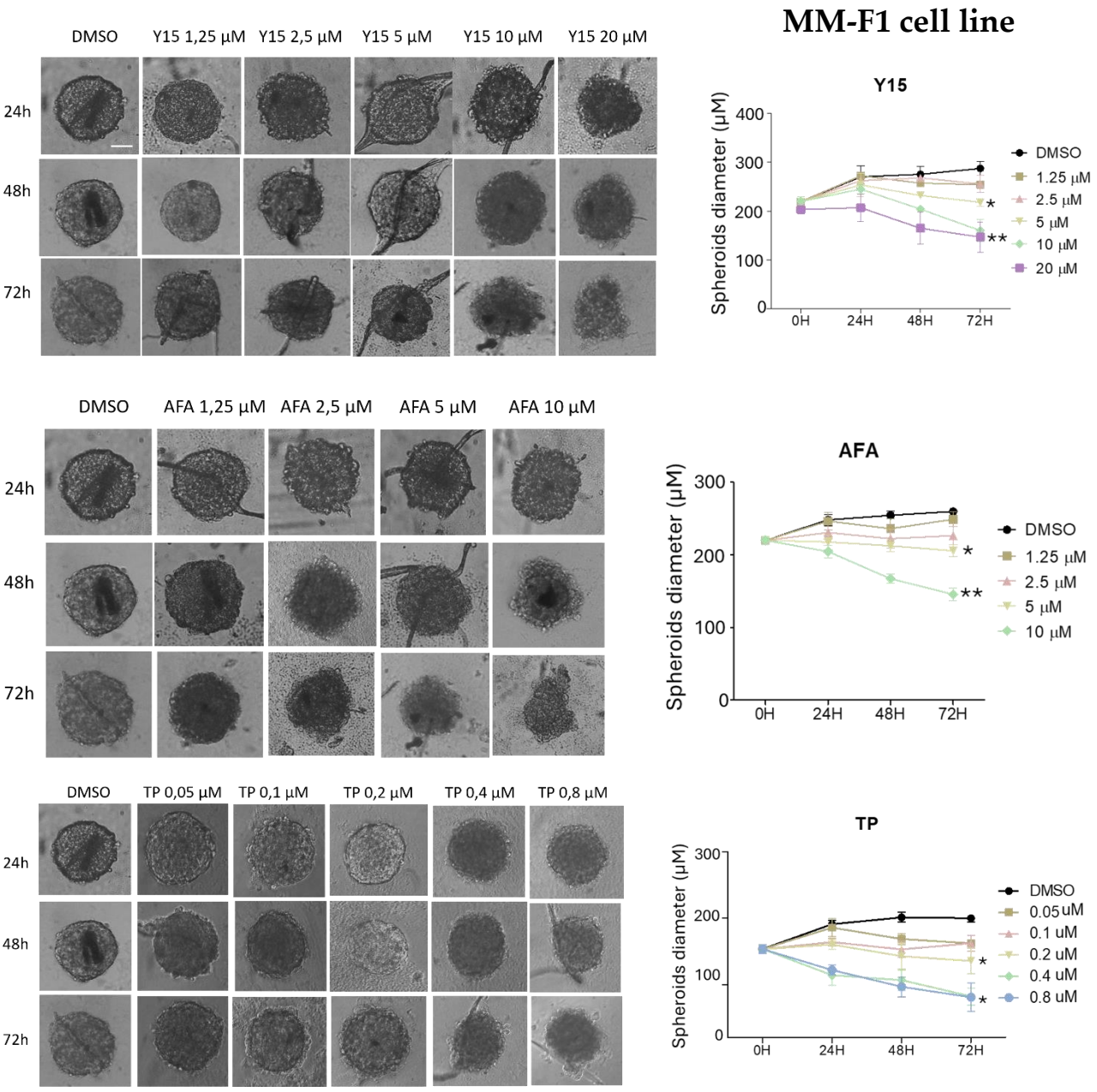

Figure 30. Effect of Y15, AFA and TP-0903, used alone, at different concentrations on MM-F1 tumor spheroids. *MM tumor diameter measurement at 24, 48 and 72 hours after treatments. Statistical significance was calculated with one-way ANOVA. (*p<0.05, **p<0.01). Scale bar = 50µm.*

The lowest concentrations of Y15, AFA and TP-0903 that demonstrated an effect on the growth of MM tumor spheroids were used to test the antitumoral effects of the different combinations of the inhibitors on MM spheroids growth.

MM spheroids were treated with the following inhibitors concentrations, used alone or in double or triple combination:

- Y15 5 μM for MM-F1 cell line and 10 μM for MM-B1 cell line;
- AFA 5 μM for both MM-F1 and MM-B1 cell lines;
- TP-0903 0.1 μM for both MM-F1 and MM-B1 cell lines.

The growth of the MM spheroids was assessed by measuring their diameter after 24 and 48 hours of treatment. As illustrated in Figure 31, the MM-B1 spheroids did not exhibit a significant reduction in growth when treated with single inhibitors or in double combinations.

Hence, the use of the single treatments with Y15 10 μM and AFA 5 μM do not affect the inhibition of cell growth compared to control (DMSO). This is probably due to the use of its low concentrations. An appreciable antiproliferative effect is observed in MM-B1 spheroids treated with AFA 5 μM at 48 hours. The double combination with AFA 5 μM + TP-0903 0.1 μM and the triple combination (Y15 10 μM + AFA 5 μM + TP-0903 0.1 μM) appears to be effective already 24 hours compared to treatments with Y15 10 μM, AFA 5 μM, Y15 10 μM + AFA 5 μM, Y15 10 μM +TP-0903 0.1 μM and the control (DMSO). However, a further significant inhibition in MM-B1 cell growth is observed at 48 hours after administration of triple treatment (Y15 10 μM + AFA 5 μM + TP-0903 0.1 μM).

Therefore, the triple combination still led to a significant reduction in MM tumor spheroids diameter compared to the control, single, and double treatments at 48 hours after its administration.

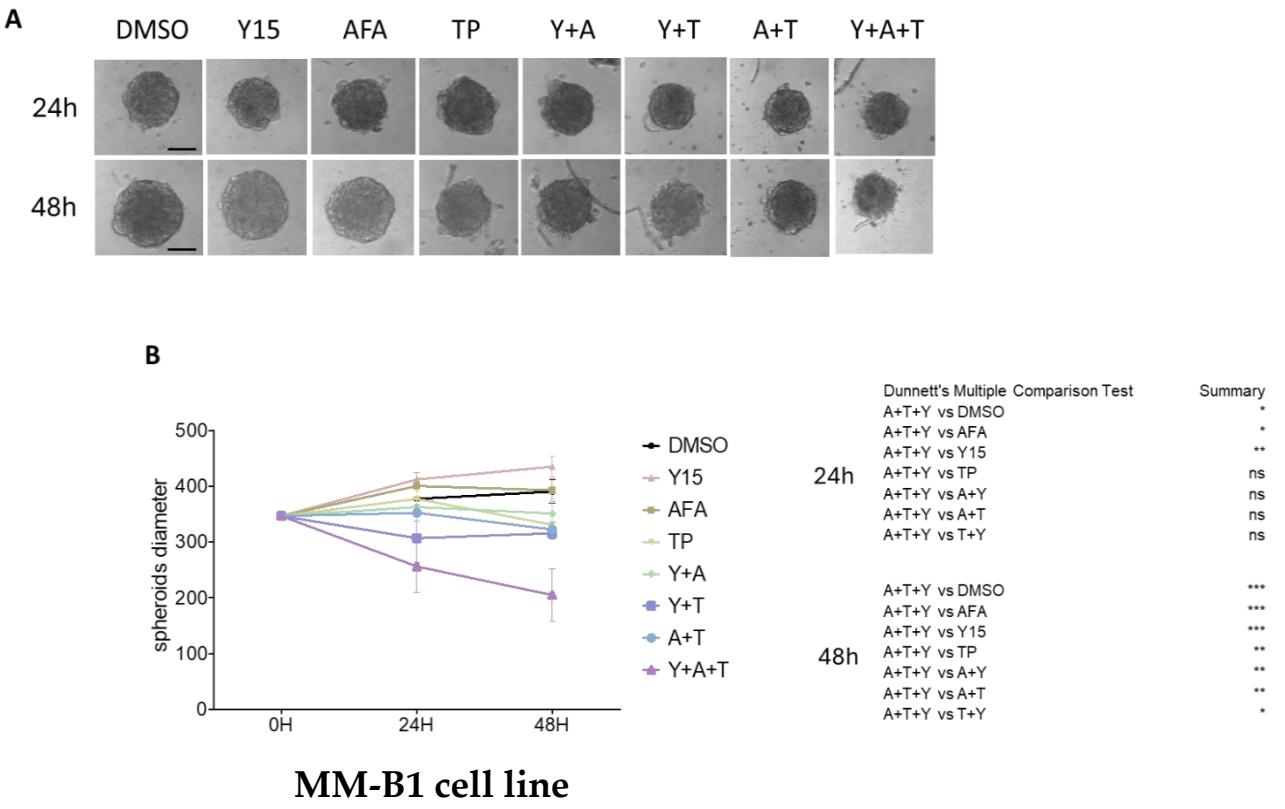

Figure 31. Effect of Y15, AFA and TP-0903 used alone or in combination on MM-B1 tumor spheroids. A) *Photos of tumor spheroids at 24 and 48 hours of treatment. Scale bar=50μm.* ***B)*** *Measure of tumor diameter after 24 and 48 hours of treatment. Statistical significance was calculated with Dunnet multiple comparison test. (*p<0.05, **p<0.01, ***p<0.001). Scale bar = 50μm.*

In contrast, the MM-F1 spheroids treated with single inhibitors or in double combinations showed a reduced diameter compared to the control group. The triple combination with Y15, AFA, and TP-0903 was able to significantly inhibits MM spheroids growth compared to the control, to single treatments, and double combinations at 48 hours after their administration.

As shown in Figure 32, the diameter of MM-F1 spheroids treated with the single combination of Y15 5 μM, AFA 5 μM and the double combination (AFA 5 μM + TP-0903 0.1 μM) had no difference compared to the control spheroids at 24 hours, on the other hand MM-F1 spheroids treated with TP-0903 0.1 μM showed a reduced diameter already at 24 hours after its administration. In addition, double treatments with Y15 5 μM + AFA 5 μM and AFA 5 μM + TP-0903 0.1 μM determine a relevant reduction in MM-F1 spheroids

diameter at 48 hours compared to single treatments with Y15 5 μM and AFA 5 μM and to control (DMSO). Indeed, double treatments with Y15 5 μM + TP-0903 0.1 μM significantly inhibit cell growth in MM-F1 spheroids both at 24 and 48 hours compared to control (DMSO). Finally, tumor spheroids treated triple combination with Y15 5 μM + AFA 5 μM + TP-0903 0.1 μM visibly reduce their diameter already at 24 hours, and after 48 hours further spheroid's impairment results, leading to reduction in spheroid diameter in a time-dependent manner.

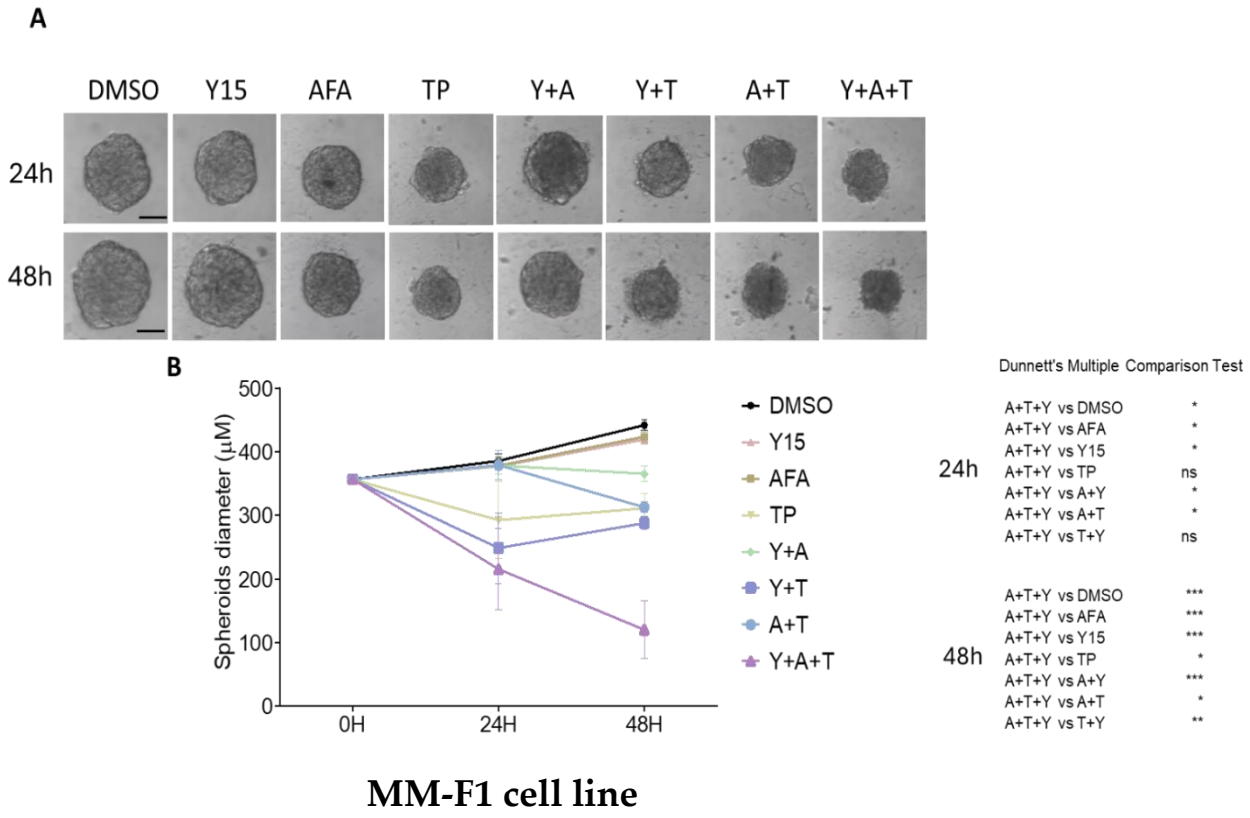

Figure 32. Effect of Y15, AFA and TP-0903 used alone or in combination on MM-F1 tumor spheroids. A) *Photos of MM tumor spheroids after 24 and 48 hours of treatment. Scale bar=50μm.* ***B)*** *Tumor diameter measurement at 24 and 48h after treatments. Statistical significance was calculated with Dunnet multiple comparison test. (*p<0.05, **p<0.01, ***p<0.001). Scale bar = 50μm.*

Effect of low-dose combination of Y15, AFA and TP-0903 on the cell viability of tumor spheroids.

The cell viability of MM-F1 and MM-B1 tumor spheroids treated with the inhibitors Y15, AFA and TP-0903, used at low doses in single, double and triple combination of the specific inhibitors or with the vehicle control (DMSO) has been evaluating using the Real Time Glo MT assay (Promega), which quantify ATP using a luminescence endpoint measurement, which serves as a surrogate indicator of cell viability.

As shown in the Figure 33, cell viability of MM-B1 spheroids treated with the inhibitors in double combination (Y15 10 μM + AFA 5 μM; Y15 10 μM + TP-0903 0.1 μM; AFA 5 μM + TP-0903 0.1 μM) appears to be reduced 72 hours after treatment. Furthermore, a significant reduction in cell viability of the triple-treated (Y15 10 μM + AFA 5 μM +TP-0903 0.1 μM) tumor spheroids occurs compared with single, double treatments and the control (DMSO).

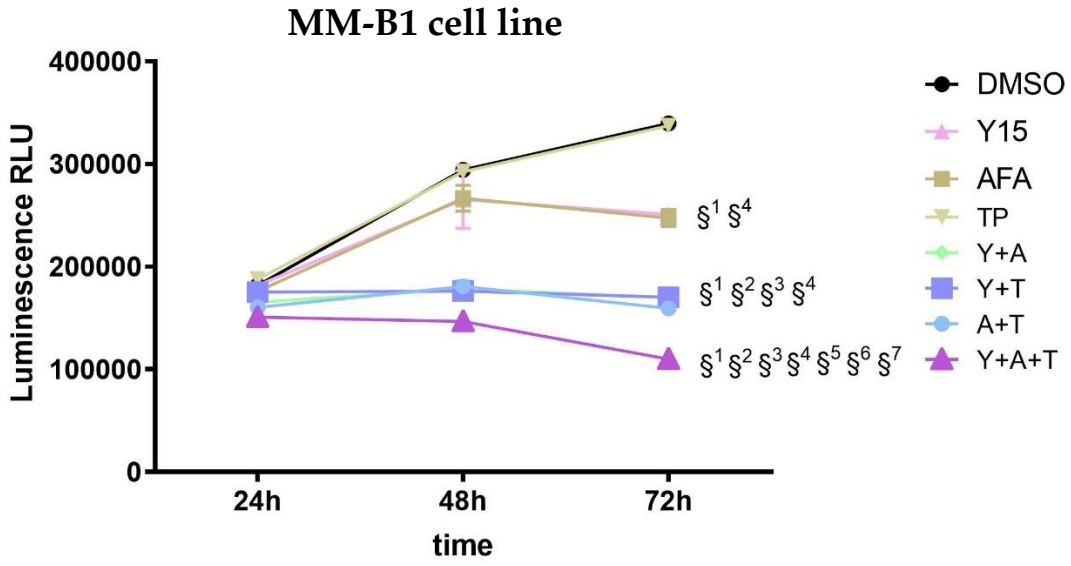

Figure 33. Cell viability assay on MM-B1 tumor spheroids after treatment with Y15, AFA and TP-0903, used alone or in combination*. The cell viability was assessed by Real-time Glo MT-assay (Promega) measuring the luminescence after 24, 48 and 72 hours of treatment. Statistical significance was calculated with one-way ANOVA at 72h. (˟p≤0.05; *p≤0.01; #p≤0.001; § p≤0.0001 vs. DMSO). *RLU= Relative Light Unit*

On the other side, in MM-F1 tumor spheroids result more sensitive to the double treatment with AFA 5 μM + TP-0903 0.1 μM at 72 hours compared with single, double treatments and DMSO. Even in this MM tumor spheroids, the triple combination with Y15 5 μM + AFA 5μM + TP-0903 0.1μM significantly inhibits cell viability in a time-dependent-manner (Figure 34).

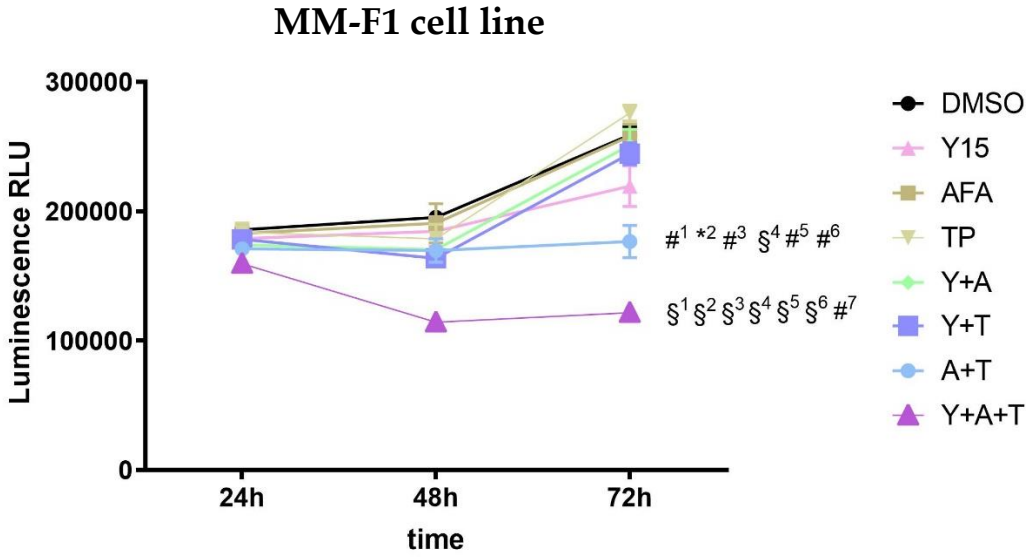

Figure 34. Cell viability assay on MM-F1 tumor spheroids after treatment with Y15, AFA and TP-0903, used alone or in combination*. The cell viability was assessed by Real-time Glo MT-assay (Promega) measuring the luminescence at 24, 48 and 72 hours of treatment. Statistical significance was calculated with one-way ANOVA at 72h. (×p≤0.05; *p≤0.01; #p≤0.001; § p≤0.0001 vs. DMSO). *RLU= Relative Light Unit*

These preliminary data show that the low dose combination of three different inhibitors targeting three different signal transduction pathways deregulated in MM is more effective in inhibiting MM growth in a 3D cellular model, corroborating that the contemporary inhibition of different pathways could avoid the overcome of drug resistance and could be helpful in decreasing the doses of the pharmacological molecules employed in the anticancer therapy.

DISCUSSION

Malignant mesothelioma (MM) is a rare and aggressive neoplasm that originates from the mesothelial cells lining the serous cavity, such as the pleura, peritoneum, pericardium, and tunica vaginalis. It mainly affects people between 50 and 70 years old, with a male to female mortality ratio of 4:1 [1].

MM is considered a professional disease because its onset is correlated in 80% of cases with asbestos exposure [252]. However, there are other etiological causes related to it, such as SV-40 infection, genetic predisposition, exposure to ionizing radiation and other biological factors [253].

In particular, several studies have shown that asbestos-induced tumorigenesis is associated with the onset of chronic inflammation caused by the infiltration of asbestos fibers in the intrapleural space, which promotes production of ROS and pro-inflammatory cytokines leading to DNA damage and triggering the progression of neoplastic transformation [254]. In addition, asbestos activates membrane receptors with tyrosine kinase activity such as EGFR or TNFR, promoting cell proliferation [255].

Diagnosis is difficult mainly due to the high cytological and histological polymorphism of the lesion itself. Notably, according to the 2021 WHO classification, MM can be classified into three different histotype depending on the presence of globular or spindle cells in the tumor tissue: (i) epithelioid; (ii) sarcomatoid; and (iii) biphasic or mixed [256]. The incidence of the three histotypes differs among case studies; however, the epithelioid one is the most common accounting for 80% of all diagnosed MM [257].

Nowadays, the gold standard for MM treatment is surgery, chemotherapy, and radiotherapy, used alone or in combination, depending on the disease's stage and severity. Despite a multimodal approach, combining these therapies, is preferred to increase efficacy and survival rates, MM prognosis remains poor [49]. This partly due to the delay of the diagnosis (reached at 6-8 months) and partly due to the inadequacy of available therapeutic approaches. Effectively, untreated MM patients have a mean survival of about 6 months,

with most deceasing within 24 months of diagnosis [72]. The average overall survival of MM patients treated with single-agent chemotherapy is around 7–8 months, and only a small number of drugs exhibit a response rate of 15–20% [258].

The MM treatment involves a combination of cisplatin and pemetrexed. However, this approach is largely palliative, with limited efficacy in extending survival (response rate of approximately 40%) [72, 82]. Studies have demonstrated that adding anti-angiogenic therapy to first-line treatment can improve overall survival [259, 260].

In addition, combination of surgery with chemotherapy and/or radiotherapy continues to be explored as a means of improving outcomes, particularly with the use of hyperthermic intraperitoneal chemotherapy (HIPEC) in order to extend survival rate [72, 261]. Despite these advances, therapeutic strategies for MM are generally considered "life-extending treatments" [262].

In recent years, significant advances have been made in the therapeutic management of this neoplasm. These include the development of more effective treatments, new diagnostic tools, and deeper insights into the disease's pathobiology, all of which have led to improved diagnostic and prognostic approaches and potential new therapies, such as *targeted therapy* [263].

These novel strategies include inhibitors targeting molecules involved in deregulated pathways, involving mTOR, angiogenesis, folate, receptor tyrosine kinases, and cyclooxygenase, as well as synthetic lethal treatments, miRNA-based treatments, oncolytic viral therapies, and immunotherapy, used either alone or in combination with chemotherapy [72, 262, 264-266].

Alternative approaches are based on inhibitors of the ubiquitin-proteasome pathway and other deregulated signaling transduction pathways, such as those mediated by ErbB family receptor, Hedgehog, Axl, Wnt [2, 267]. Thus, molecules involved in these signaling pathways could be used to develop novel therapeutic targeted therapy protocol.

Bor is a 26S proteasome inhibitor that is used primarily in the treatment of certain types of cancer, especially multiple myeloma [186]. By inhibiting the proteasome 26S, Bor disrupts the degradation of ubiquitinated proteins involved in various cellular process, including cell cycle and apoptosis. This drug is often administered intravenously or subcutaneously and is typically used in combination with other drugs to enhance its effectiveness. Like many cancer treatments, it can have side effects, including neuropathy, fatigue, and gastrointestinal problems. Its use and dosage are usually carefully managed to balance efficacy with minimizing adverse effects [268].

AFA is a TKI that irreversibly binds to EGFR, HER2, and HER4, inhibiting their signaling pathways. This molecule targets both mutated and wild-type EGFR [269]. However, acquired resistance to TKIs treatment inevitably develops in cancer patients, remaining a significant biological challenge. Phenomena of drug-resistance to TKIs may result from the concurrent activation of alternative signaling pathways [219, 270].

TP-0903 is a potent and selective inhibitor of the Axl receptor tyrosine kinase, high expression of which correlates with EMT, metastatic process, and drug resistance in several cancer, including lung cancer, pancreatic cancer, colorectal cancer, neuroblastoma and MM [224, 225, 271]. TP-0903 is an orally available small molecule that follows a mechanism of competitive inhibition with ATP binding to Axl's active conformation. It also targets other kinases, including the three members of the TAM family, JAK2, ABL1 and VEGFR2.

Y15 is a specific inhibitor of FAK, which blocks its autophosphorylation in a dose e time dependent manner, reducing the viability and growth of tumor cells. FAK is over-expressed in most solid tumors, such as MM, head and neck cancer, colorectal cancer, glioblastoma and thyroid cancer. It is involved in angiogenesis, metastatic process and invasion. Y15 has been shown to have antitumor and antiproliferative effects, alone or in combination with chemotherapeutic agents, both *in vitro* and *in vivo*. While clinical research on Y15 is less advanced compared to other FAK inhibitors, it remains a valuable tool for understanding FAK's role in cancer and exploring its therapeutic potential [272].

The aim of this study is to find new targeted therapeutic strategies for the treatment of MM based on a molecular targeted approach in order to specifically inhibit the tumor growth.

In this study, we investigated the effects of Bor on cell survival, cell cycle distribution and modulation of apoptotic and pro-survival pathways in human MM cell lines of different histotypes cultured *in vitro* [1]. Further, using a mouse MM cell line that reproducibly forms ascites when intraperitoneally injected in syngeneic C57BL/6 mice, we investigated the effects of intraperitoneal Bor administration *in vivo on* both tumor growth and the modulation of the tumor immune microenvironment. Firstly, based on the *in vitro* results conducted on all four MM cell lines (MM-F1, MM-B1, H-Meso-1 and #40a), Bor can inhibit MM cell proliferation with IC50 values in the range of $10 < IC_{50} < 100$ nM and $10 < IC_{50} < 25$ nM after 48 and 72 hours of treatment, respectively. These values align with those previously reported in studies on MM cells [252, 273] and are lower than the peak plasma levels observed in patients with solid tumors after i.v. administration of Bor [274]. Trypan blue staining showed that the inhibition of MM cell growth was accompanied by an increase in cell death, primarily occurred through apoptosis, as indicated by the increase in cells with a hypodiploid, sub-G1 DNA content. Supporting the induction of apoptotic cell death, Bor treatment increased Bax/Bcl-2 ratio, the levels of cleaved caspase 3 and γH2AX in all MM cell lines analyzed [275].

Different mechanisms can contribute to determining the sensitivity to cell death following Bor treatment. Previous studies have highlighted high proteasome activity and expression [104, 276], along with dysregulation of the NOXA-dependent mitochondrial apoptotic pathway [277], as factors that may reduce Bor's cytotoxic efficacy in MM cells. In this context, we here focused on two cellular responses that can be triggered by proteasome inhibition: autophagy and the ER stress-induced UPR [1].

Discordant findings have been reported regarding the effect of Bor on autophagy in cancer cells. Some studies suggest that Bor induces autophagy as an alternative protein degradation mechanism, helping cancer cells survive from the toxic effects of proteasome inhibition. Conversely, other studies have shown different outcomes [192, 243, 278]. The

autophagic response to Bor treatment has not been previously investigated in MM cells to our knowledge. Although the effects of Bor on the autophagy markers appeared to be cell line-dependent, the concurrent changes of LC3-II, SQSTM-1/p62 and beclin-1 levels we observed in Bor-treated cells indicate that Bor disrupts with the autophagic activity of human MM cell lines and decreases autophagy in the mouse MM cell line. Therefore, autophagy induction does not appear to play a role as a rescue mechanism that may decrease Bor efficacy on MM [1].

Regarding ER stress and UPR markers, Bor treatment activates a pro-survival mechanism in MM cells by increasing the anti-apoptotic GRP78/BiP protein and reducing the pro-apoptotic CHOP protein. GRP78/BiP, an ER-resident chaperone, plays a crucial role in regulating ER stress by binding and inhibiting UPR upstream activators, PKR-like ER kinase (PERK), inositol-requiring enzyme 1 (IRE1) and activating transcription factor 6 (ATF6), based on the level of unfolded proteins in the ER lumen. In ER stress conditions, unfolded proteins accumulate and are bound by GRP78/BiP, which in turn dissociates from PERK, IRE1 and ATF6, leading to UPR activation. While the different UPR pathways are primarily aimed at restoring cellular homeostasis, in case of severe or unresolved ER stress some UPR signaling branches will commit cells to death by apoptosis [279, 280]. CHOP, a transcription factor induced via PERK/ATF4 pathway, plays a pivotal role in the pro-apoptotic branch of UPR by downregulating the expression of Bcl-2 family proteins, promoting ROS production, and exacerbating proteotoxic stress [279, 280]. In line with our results, Bor treatment increased GRP78/BiP levels in all MM cell lines analyzed, consistent with ER stress and UPR activation [249]. However, the concurrent reduction of CHOP levels observed in three human MM cell lines and the unchanged CHOP levels observed in the murine cell line suggest that Bor-induced UPR activation has a pro-survival effect, potentially reducing MM cell sensitivity to Bor's cytotoxicity [1, 281].

That evasion from UPR-mediated apoptosis can be involved in mediating resistance to Bor cytotoxicity in MM cells has been previously reported in a study performed using a MM cell line adapted to grow in the presence of increasing Bor concentrations (up to 40 nM) over a

period of more than six months [282]. Our data, obtained using four different MM cell lines, suggest that primary resistance to UPR-mediated apoptosis may as well be an intrinsic common feature of MM cells. Remarkably, these results have therapeutic implications, since they highlight that the combination with modulators of the UPR, some of which are already clinically available [279, 283], may represent a possible strategy to overcome Bor resistance in MM. In this respect, ER stress signaling is emerging as a key pharmacological target for MM treatment [284].

Considering the involvement of aberrant ErbB signaling in MM [2, 285] and the evidence of the regulation of the levels of ErbB receptors, such as EGFR and ErbB2, by proteasomal degradation [286, 287], we also investigated whether Bor treatment could affect the expression of EGFR and ErbB2 and the activation of downstream pro-survival signaling effectors [1]. The treatment resulted in reduced levels of at least one among EGFR and ErbB2 receptors in all cell lines except MM-F1. We recently reported a similar downregulation of EGFR and ErbB2 levels in Bor-treated head and neck carcinoma cells [192]. However, in the present study, Bor appeared to modulate EGFR levels in a cell line-dependent manner in MM, whereas more consistent effects were observed regarding ErbB2, whose levels were lowered by the proteasomal inhibitor in three out of the four MM cell lines investigated. The reduction of ErbB2 levels following treatment with proteasome inhibitors has also recently been observed in breast cancer cell lines, where it has been ascribed to both transcriptional downregulation and the induction of lysosomal degradation mechanisms [288]. As for the activation of the pro-survival pathways mediated by ERK1/2, AKT, and p38, Bor treatment was found to reduce the phospho-activation of ERK1 and/or ERK2 in all cell lines, had no significant effects on p38 phosphorylation levels, but increased the phosphorylation of AKT in the three human MM cell lines [1]. In fact, Bor has been reported to either activate or inhibit AKT in a cell type-dependent manner, and the downregulation of phospho-AKT is regarded as an important determinant of Bor-induced apoptosis in cancer cells [192, 289, 290]. Notably, in addition to its activation in response to growth factor receptors stimulation, AKT can also be activated by GRP78/BiP in ER stress conditions [291]. Moreover, the downregulation of AKT activity appears to play a crucial role in the induction of CHOP

expression during ER stress [292]. Taken together, these considerations suggest that the type of ER stress induced by Bor in human MM cells may lead to the activation of AKT via the upregulation of GRP78/BiP; in turn, AKT may concur to reduce CHOP levels and impair the pro-apoptotic branch of the UPR. This latter hypothesis is indirectly supported by the observation that following Bor treatment CHOP expression was reduced in the three human MM cell lines showing increased phospho-AKT levels. While further studies are required to define the actual mechanisms responsible for Bor-induced AKT activation in MM cells, the reported findings point to the use AKT inhibitors as a therapeutic strategy aimed at increasing the apoptotic response of MM cells to Bor [290, 293]. The efficacy of Bor in mediating MM growth inhibition *in vivo* has been previously demonstrated in a study performed on immunodeficient (nude *xid*) mice carrying i.p. xenografts of human (REN) MM cells [273]. In the present study, we used a different model established in immunocompetent C57BL/6 mice, in which the growth of i.p. transplanted syngeneic #40a MM cells reproducibly leads to ascites formation [2, 235, 294, 295]. The results obtained using this model confirm the ability of Bor to suppress MM growth *in vivo* and extend mice survival [1]. In particular, while vehicle-treated mice had a median survival of 5.7 weeks, that of Bor-treated mice was of 7.2 weeks, with a Hazard Ratio for control vs. Bor-treated mice equal to 4.1.

Thanks to this model, we also evaluated the frequency and phenotype of immune cell populations recruited to the tumor site in mice transplanted with #40a MM cells and treated with Bor or vehicle for 30 days [1]. In fact, although MM has been traditionally regarded as a non-immunogenic tumor, further studies have clarified that it is infiltrated by a non-negligible number of immune cells that, however, are functionally impaired via multiple factors operating in its immunosuppressive microenvironment [33, 296-298]. In particular, the infiltration of MM tissues by hypofunctional lymphocytes has been reported by several authors and lately, due to the great clinical interest in ICIs, many studies have been focused on the involvement of lymphocyte inhibitory receptors such as PD-1 in MM immune escape [298-300].

When comparing the frequencies of CD4+, CD8+, B lymphocytes, MDSCs and TAMs in mice spleens with those in the ascitic fluids, we found significantly different values for MDSCs and TAMs only. At the tumor site MDSCs had a reduced frequency, while TAMs had an increased frequency as compared to the spleen. Still, the frequencies of both immune types were similar in the Bor-treated and CTR groups [1].

When comparing the frequency of the immune populations in the spleens of Bor-treated and CTR mice, the only significant change was a reduction in the frequency of B lymphocytes in the Bor-treated group, which however was not paralleled by a decreased frequency at the tumor site. Indeed, when comparing the frequency of the immune populations in the ascitic fluids of Bor- and vehicle-treated mice, the only significant change was a reduction in the frequency of CD4+ lymphocytes in the Bor-treated group.

More widespread differences were instead observed as regards the functional status of T lymphocytes from Bor-treated as compared to CTR mice. First, the ascitic fluids of Bor-treated mice had an increased frequency of both CD4+ and CD8+ T lymphocytes expressing the activation marker CD25, and an increased frequency of CD4+ T lymphocytes expressing the early activation marker CD69. Remarkably, this effect of Bor appeared specific for CD4+ and CD8+ cells recruited at the tumor site, since the same T populations collected from mice spleens showed no significant changes in the proportion of cells expressing the two markers. Next, consistent with the previous finding, Bor treatment resulted in a significant increase in the proportion of tumor-recruited CD4+ and CD8+ T cells expressing IFN-γ, a main cytokine marker for the activity of tumor-infiltrating lymphocytes [298], while it had no significant effects on the amount of IFN-γ+ T cells in the spleen. Finally, Bor treatment resulted in negative regulation of PD-1 expression in T cells. In contrast with the previous findings, the effect of Bor on the expression of the PD-1 immune checkpoint receptor was not limited to the lymphocytes recruited to the tumor site, since the proportion of CD8+/PD-1+ cells was reduced both in the spleen and ascitic fluid, and that of CD4+/PD-1+ cells in the spleen of the drug-treated mice [1]. Overall, these findings indicate that Bor can sustain the activation of CD4+ and CD8+ T cells. Thus, besides its direct growth inhibitory and pro-

apoptotic effects on tumor cells, Bor could delay MM progression by promoting the activation of T cell-mediated immune responses. Furthermore, by overcoming the exhaustion of T cells recruited in the tumor microenvironment, Bor could improve the outcomes of immunotherapy approaches in MM patients, as reported in preclinical studies performed on different cancer types [301, 302].

According to two phase II clinical trials where the therapeutic efficacy of Bor on MM was investigated alone (NCT00513877) or in combination with cisplatin (NCT00458913), the proteasomal inhibitor failed to significantly improve clinical outcomes [303, 304]. However, in both studies, Bor was administered i.v., whereas the therapeutic potential of intracavitary-administered Bor has not yet been investigated in patients with MM to our knowledge. Nonetheless, clinical results obtained in patients with recurrent ovarian cancer and myelomatous pleural effusions indicate that the intrapleural/intraperitoneal administration of Bor is feasible and has promising antitumor activity [305, 306]. In fact, that the anticancer properties of Bor are currently underexploited for the treatment of solid tumors is evidenced by the many efforts which have recently been devoted to the development of Bor-based drug delivery systems that may improve its accumulation at the targeted tumor site [307]. Furthermore, a definitive assessment of Bor clinical utility for the treatment of MM would require the definition of criteria for the selection of patients to enroll in clinical trials [303]. An interesting avenue to explore in this regard may be to evaluate the possible impact of the mutational status of the de-ubiquitinating enzyme BRCA-1-associated protein BAP1 on the therapeutic outcome of Bor treatment. Indeed, BAP1 is a tumor suppressor frequently inactivated in several cancers including MM and its depletion has been reported to decrease tumor cells sensitivity to Bor, raising the hypothesis that this proteasomal inhibitor may have an increased efficacy in MM patients whose tumors express the wild type BAP1 protein [308, 309].

Furthermore, the frequent overexpression of ErbB family receptors in MM has justified testing EGFR-TKIs in MM patients [310]. However, it is described that the use of unitarget

drugs can induce drug-resistance leading to the activation of alternative signaling pathways already mentioned [285, 311].

Previous studies in our laboratory have shown that the use of inhibitors that simultaneously inhibit two different signaling pathways may have greater efficacy in inhibiting tumor growth. Bei et al. had demonstrated that a combined treatment using AFA, an EGFR-TKI, in combination with GANT-61, a specific GLI1/2 inhibitor, that target two different pathways involved in cancer development and progression, was more effective than single-pathway inhibition in reducing tumor growth both *in vitro* and *in vivo* in MM [2]. The study by Benvenuto et al. had pointed out that CUR, a natural polyphenolic compound able to target several molecules involved in cell proliferation, cell death, autophagy, angiogenesis, invasion, migration, metastasis and chemoresistance, can potentiate AFA antitumor activity in MM both *in vitro* and *in vivo* [3].

Based on this evidence, we focused on the use of a combined treatment using AFA in combination with other two unitarget drugs, Y15, a FAK inhibitor, and TP-0903, an Axl inhibitor, used at low doses, in order to simultaneously inhibit three distinct aberrantly activated signaling transduction pathways in MM. For this purpose, we employed 3D tumor spheroids obtained from two human MM cell lines (MM-F1 and MM-B1).

Several studies have highlighted that, unlike traditional 2D cell cultures, which grow as flat monolayers, 3D spheroids provide a more realistic and complex environment resembling the *in vivo* counterparts in morphology, interactions with other cells and extracellular matrix, gene and protein expression levels, sensitivity to external factors, proliferation and differentiation status [312]. Hence, three-dimensional cell culture models closely mimic the architecture of solid tumors, making them useful in experimental cancer research for studying tumor biology, drug response, and resistance. The integration of 3D assay models is becoming increasingly popular for the purpose of furthering translational biology [313].

Preliminary data showed that MM tumor spheroids treated with AFA, Y15 and TP-0903, used singly or in a double combination, showed less growth than control spheroids. A significantly greater decrease in spheroid growth was obtained after treating tumor

spheroids with the triple combination of the inhibitors. These results are also consistent with the cell viability assay confirming that triple treatment (AFA + Y15 + TP-0903) decreases the number of viable cells of tumor spheroids compared to control, single and double treatments in a time-dependent manner.

The combined treatment with three inhibitors (AFA + Y15 + TP-0903) could affect not only cell cycle and survival of MM cancer cells, but also other biological events, such as invasion and EMT, inhibiting migreation, angiogenesis and metastasis formation [314, 315]. Therefore, further experiments should be conducted to evaluate cell migration, cell death and the modulation of the implicated molecular transduction pathways. At last, *in vivo* experiments have just been approved, to study the effects of the three inhibitors on C57BL6 mouse models, analyzing the immune infiltrate recalled in the tumor microenvironment.

In conclusion, these studies may have new clinical implications for the development of new targeted therapy approaches for MM as molecularly targeted therapy offers significant promise in achieving better treatment outcomes with fewer adverse effects than conventional therapies. Nevertheless, given the peculiar characteristics of MM, which is marked by high local invasiveness and low metastatic efficiency [1], clinically effective concentrations of the compound can be directly delivered to the tumor site in MM patients through intracavitary approach [316, 317]. These factors, along with the findings presented here, justify the need for future studies to further investigate the therapeutic potential of combination regimens for treating MM patients.

However, challenges such as resistance development and patient heterogeneity remain substantial obstacles.

References

1. Benvenuto, M., V. Angiolini, C. Focaccetti, D. Nardozi, C. Palumbo, R. Carrano, A. Rufini, R. Bei, M.T. Miele, P. Mancini, G. Barillari, M. Cirone, E. Ferretti, G.R. Tundo, L. Mutti, L. Masuelli, and R. Bei, Antitumoral effects of Bortezomib in malignant mesothelioma: evidence of mild endoplasmic reticulum stress in vitro and activation of T cell response in vivo. *Biol Direct*, 2023. 18(1): p. 17.DOI: 10.1186/s13062-023-00374-w.
2. Bei, R., M. Benvenuto, C. Focaccetti, S. Fazi, M. Moretti, D. Nardozi, V. Angiolini, S. Ciuffa, L. Cifaldi, R. Carrano, C. Palumbo, M.T. Miele, R. Bei, G. Barillari, V. Manzari, E. De Smaele, A. Modesti, and L. Masuelli, Combined treatment with inhibitors of ErbB Receptors and Hh signaling pathways is more effective than single treatment in reducing the growth of malignant mesothelioma both in vitro and in vivo. *J Transl Med*, 2022. 20(1): p. 286.DOI: 10.1186/s12967-022-03490-9.
3. Benvenuto, M., D. Nardozi, C. Palumbo, C. Focaccetti, R. Carrano, V. Angiolini, L. Cifaldi, V. Lucarini, P. Mancini, B. Kerpi, W. Currenti, R. Bei, and L. Masuelli, Curcumin potentiates the ErbB receptors inhibitor Afatinib for enhanced antitumor activity in malignant mesothelioma. *Int J Food Sci Nutr*, 2023. 74(7): p. 746-759.DOI: 10.1080/09637486.2023.2251723.
4. Jain, S.V. and J.M. Wallen, *Malignant Mesothelioma*, in *StatPearls*. 2024: Treasure Island (FL).
5. Hiriart, E., R. Deepe, and A. Wessels, Mesothelium and Malignant Mesothelioma. *J Dev Biol*, 2019. 7(2).DOI: 10.3390/jdb7020007.
6. Travis, W.D., E. Brambilla, A.G. Nicholson, Y. Yatabe, J.H.M. Austin, M.B. Beasley, L.R. Chirieac, S. Dacic, E. Duhig, D.B. Flieder, K. Geisinger, F.R. Hirsch, Y. Ishikawa, K.M. Kerr, M. Noguchi, G. Pelosi, C.A. Powell, M.S. Tsao, I. Wistuba, and W.H.O. Panel, The 2015 World Health Organization Classification of Lung Tumors: Impact of Genetic, Clinical and Radiologic Advances Since the 2004 Classification. *J Thorac Oncol*, 2015. 10(9): p. 1243-1260.DOI: 10.1097/JTO.0000000000000630.
7. Mezei, G., E.T. Chang, F.S. Mowat, and S.H. Moolgavkar, Epidemiology of mesothelioma of the pericardium and tunica vaginalis testis. *Ann Epidemiol*, 2017. 27(5): p. 348-359 e11.DOI: 10.1016/j.annepidem.2017.04.001.
8. Benvenuto, M., R. Mattera, G. Taffera, M.G. Giganti, P. Lido, L. Masuelli, A. Modesti, and R. Bei, The Potential Protective Effects of Polyphenols in Asbestos-Mediated Inflammation and Carcinogenesis of Mesothelium. *Nutrients*, 2016. 8(5).DOI: 10.3390/nu8050275.
9. Trassl, L. and G.T. Stathopoulos, KRAS Pathway Alterations in Malignant Pleural Mesothelioma: An Underestimated Player. *Cancers (Basel)*, 2022. 14(17).DOI: 10.3390/cancers14174303.
10. Iliopoulou, M., C. Bostantzoglou, R. Nenna, and V.S. Skouras, Asbestos and the lung: highlights of a detrimental relationship. *Breathe (Sheff)*, 2017. 13(3): p. 235-237.DOI: 10.1183/20734735.010017.

11. Fenton, S., E. Rydz, P.A. Demers, and C.E. Peters, Prevalence and Level of Occupational Exposure to Asbestos in Canada in 2016. *Ann Work Expo Health*, 2023. 67(4): p. 536-545.DOI: 10.1093/annweh/wxac077.
12. Attanoos, R.L., A. Churg, F. Galateau-Salle, A.R. Gibbs, and V.L. Roggli, Malignant Mesothelioma and Its Non-Asbestos Causes. *Arch Pathol Lab Med*, 2018. 142(6): p. 753-760.DOI: 10.5858/arpa.2017-0365-RA.
13. Robinson, B.W., A.W. Musk, and R.A. Lake, Malignant mesothelioma. *Lancet*, 2005. 366(9483): p. 397-408.DOI: 10.1016/S0140-6736(05)67025-0.
14. INAIL. Available from: https://www.inail.it/portale/it/inail-comunica/pubblicazioni/catalogo-generale/catalogo-generale-dettaglio.2022.01.il-registro-nazionale-dei-mesoteliomi-settimo-rapporto-.html.
15. Carbone, M., P.S. Adusumilli, H.R. Alexander, Jr., P. Baas, F. Bardelli, A. Bononi, R. Bueno, E. Felley-Bosco, F. Galateau-Salle, D. Jablons, A.S. Mansfield, M. Minaai, M. de Perrot, P. Pesavento, V. Rusch, D.T. Severson, E. Taioli, A. Tsao, G. Woodard, H. Yang, M.G. Zauderer, and H.I. Pass, Mesothelioma: Scientific clues for prevention, diagnosis, and therapy. *CA Cancer J Clin*, 2019. 69(5): p. 402-429.DOI: 10.3322/caac.21572.
16. Paajanen, J., S. Laaksonen, I. Ilonen, T. Vehmas, M.I. Mayranpaa, E. Sutinen, E. Kettunen, J.A. Salo, J. Rasanen, H. Wolff, and M. Myllarniemi, Clinical Features in Patients With Malignant Pleural Mesothelioma With 5-Year Survival and Evaluation of Original Diagnoses. *Clin Lung Cancer*, 2020. 21(6): p. e633-e639.DOI: 10.1016/j.cllc.2020.05.020.
17. Marinaccio, A., D. Consonni, C. Mensi, D. Mirabelli, E. Migliore, C. Magnani, D. Di Marzio, V. Gennaro, G. Mazzoleni, P. Girardi, C. Negro, A. Romanelli, E. Chellini, I. Grappasonni, G. Madeo, E. Romeo, V. Ascoli, F. Carrozza, I.F. Angelillo, D. Cavone, R. Tumino, M. Melis, S. Curti, G. Brandi, S. Mattioli, S. Iavicoli, and M.W.G. ReNa, Association between asbestos exposure and pericardial and tunica vaginalis testis malignant mesothelioma: a case-control study and epidemiological remarks. *Scand J Work Environ Health*, 2020. 46(6): p. 609-617.DOI: 10.5271/sjweh.3895.
18. Mensi, C., S. Giacomini, C. Sieno, D. Consonni, and L. Riboldi, Pericardial mesothelioma and asbestos exposure. *Int J Hyg Environ Health*, 2011. 214(3): p. 276-9.DOI: 10.1016/j.ijheh.2010.11.005.
19. Carbone, M., B.H. Ly, R.F. Dodson, I. Pagano, P.T. Morris, U.A. Dogan, A.F. Gazdar, H.I. Pass, and H. Yang, Malignant mesothelioma: facts, myths, and hypotheses. *J Cell Physiol*, 2012. 227(1): p. 44-58.DOI: 10.1002/jcp.22724.
20. Gualtieri, A.F., G. Lusvardi, A. Pedone, D. Di Giuseppe, A. Zoboli, A. Mucci, A. Zambon, M. Filaferro, G. Vitale, M. Benassi, R. Avallone, L. Pasquali, and M. Lassinantti Gualtieri, Structure Model and Toxicity of the Product of Biodissolution of Chrysotile Asbestos in the Lungs. *Chem Res Toxicol*, 2019. 32(10): p. 2063-2077.DOI: 10.1021/acs.chemrestox.9b00220.
21. Gilham, C., C. Rake, G. Burdett, A.G. Nicholson, L. Davison, A. Franchini, J. Carpenter, J. Hodgson, A. Darnton, and J. Peto, Pleural mesothelioma and lung

cancer risks in relation to occupational history and asbestos lung burden. *Occup Environ Med*, 2016. 73(5): p. 290-9.DOI: 10.1136/oemed-2015-103074.
22. Linton, A., J. Vardy, S. Clarke, and N. van Zandwijk, The ticking time-bomb of asbestos: its insidious role in the development of malignant mesothelioma. *Crit Rev Oncol Hematol*, 2012. 84(2): p. 200-12.DOI: 10.1016/j.critrevonc.2012.03.001.
23. Marinaccio, A., A. Binazzi, M. Bonafede, D. Di Marzio, A. Scarselli, and C. Regional Operating, Epidemiology of malignant mesothelioma in Italy: surveillance systems, territorial clusters and occupations involved. *J Thorac Dis*, 2018. 10(Suppl 2): p. S221-S227.DOI: 10.21037/jtd.2017.12.146.
24. (IARC), I.A.f.R.o.C., IARC monographs on the evaluation of the carcinogenic risk of chemicals to man: asbestos. *IARC Monogr Eval Carcinog Risk Chem Man*, 1977. 14: p. 1-106.
25. Sage, A.P., V.D. Martinez, B.C. Minatel, M.E. Pewarchuk, E.A. Marshall, G.M. MacAulay, R. Hubaux, D.D. Pearson, A.A. Goodarzi, G. Dellaire, and W.L. Lam, Genomics and Epigenetics of Malignant Mesothelioma. *High Throughput*, 2018. 7(3).DOI: 10.3390/ht7030020.
26. Marinaccio, A., A. Binazzi, G. Cauzillo, D. Cavone, R.D. Zotti, P. Ferrante, V. Gennaro, G. Gorini, M. Menegozzo, C. Mensi, E. Merler, D. Mirabelli, F. Montanaro, M. Musti, F. Pannelli, A. Romanelli, A. Scarselli, R. Tumino, and G. Italian Mesothelioma Register Working, Analysis of latency time and its determinants in asbestos related malignant mesothelioma cases of the Italian register. *Eur J Cancer*, 2007. 43(18): p. 2722-8.DOI: 10.1016/j.ejca.2007.09.018.
27. D'Agostin, F., P. De MIchieli, and C. Negro, Mesothelioma From Household Asbestos Exposure. *J Lung Healt Dis*, 2018. 1(1): p. 27-30.DOI: https://doi.org/10.29245/2689-999X/2017/1.1110.
28. Marinaccio, A., A. Binazzi, M. Bonafede, M. Corfiati, D. Di Marzio, A. Scarselli, M. Verardo, D. Mirabelli, V. Gennaro, C. Mensi, G. Schallemberg, E. Merler, C. Negro, A. Romanelli, E. Chellini, S. Silvestri, M. Cocchioni, C. Pascucci, F. Stracci, V. Ascoli, L. Trafficante, I. Angelillo, M. Musti, D. Cavone, G. Cauzillo, F. Tallarigo, R. Tumino, M. Melis, and M.W.G. ReNa, Malignant mesothelioma due to non-occupational asbestos exposure from the Italian national surveillance system (ReNaM): epidemiology and public health issues. *Occup Environ Med*, 2015. 72(9): p. 648-55.DOI: 10.1136/oemed-2014-102297.
29. Mirabelli, D., R. Calisti, F. Barone-Adesi, E. Fornero, F. Merletti, and C. Magnani, Excess of mesotheliomas after exposure to chrysotile in Balangero, Italy. *Occup Environ Med*, 2008. 65(12): p. 815-9.DOI: 10.1136/oem.2007.037689.
30. Salute.gov. *Norme relative alla cessazione dell'impiego dell'amianto.* 1992. Available from: https://www.salute.gov.it/resources/static/primopiano/amianto/normativa/Legge_27_marzo_1992.pdf.
31. INAIL. 2021. Available from: https://www.inail.it/portale/it/inail-comunica/pubblicazioni/catalogo-generale/catalogo-generale-dettaglio.2022.01.il-registro-nazionale-dei-mesoteliomi-settimo-rapporto-.html.

32. Cox, L.A.T., Jr., Biological mechanisms of non-linear dose-response for respirable mineral fibers. *Toxicol Appl Pharmacol*, 2018. 361: p. 137-144.DOI: 10.1016/j.taap.2018.06.016.
33. Izzi, V., L. Masuelli, I. Tresoldi, C. Foti, A. Modesti, and R. Bei, Immunity and malignant mesothelioma: from mesothelial cell damage to tumor development and immune response-based therapies. *Cancer Lett*, 2012. 322(1): p. 18-34.DOI: 10.1016/j.canlet.2012.02.034.
34. Sekido, Y., Genomic abnormalities and signal transduction dysregulation in malignant mesothelioma cells. *Cancer Sci*, 2010. 101(1): p. 1-6.DOI: 10.1111/j.1349-7006.2009.01336.x.
35. Manning, C.B., V. Vallyathan, and B.T. Mossman, Diseases caused by asbestos: mechanisms of injury and disease development. *Int Immunopharmacol*, 2002. 2(2-3): p. 191-200.DOI: 10.1016/s1567-5769(01)00172-2.
36. Robledo, R. and B. Mossman, Cellular and molecular mechanisms of asbestos-induced fibrosis. *J Cell Physiol*, 1999. 180(2): p. 158-66.DOI: 10.1002/(SICI)1097-4652(199908)180:2<158::AID-JCP3>3.0.CO;2-R.
37. Upadhyay, D. and D.W. Kamp, Asbestos-induced pulmonary toxicity: role of DNA damage and apoptosis. *Exp Biol Med (Maywood)*, 2003. 228(6): p. 650-9.DOI: 10.1177/153537020322800602.
38. Liu, G., P. Cheresh, and D.W. Kamp, Molecular basis of asbestos-induced lung disease. *Annu Rev Pathol*, 2013. 8: p. 161-87.DOI: 10.1146/annurev-pathol-020712-163942.
39. Yang, H., Z. Rivera, S. Jube, M. Nasu, P. Bertino, C. Goparaju, G. Franzoso, M.T. Lotze, T. Krausz, H.I. Pass, M.E. Bianchi, and M. Carbone, Programmed necrosis induced by asbestos in human mesothelial cells causes high-mobility group box 1 protein release and resultant inflammation. *Proc Natl Acad Sci U S A*, 2010. 107(28): p. 12611-6.DOI: 10.1073/pnas.1006542107.
40. Zanella, C.L., C.R. Timblin, A. Cummins, M. Jung, J. Goldberg, R. Raabe, T.R. Tritton, and B.T. Mossman, Asbestos-induced phosphorylation of epidermal growth factor receptor is linked to c-fos and apoptosis. *Am J Physiol*, 1999. 277(4): p. L684-93.DOI: 10.1152/ajplung.1999.277.4.L684.
41. Ospina, D., V.E. Villegas, G. Rodriguez-Leguizamon, and M. Rondon-Lagos, Analyzing biological and molecular characteristics and genomic damage induced by exposure to asbestos. *Cancer Manag Res*, 2019. 11: p. 4997-5012.DOI: 10.2147/CMAR.S205723.
42. Ault, J.G., R.W. Cole, C.G. Jensen, L.C. Jensen, L.A. Bachert, and C.L. Rieder, Behavior of crocidolite asbestos during mitosis in living vertebrate lung epithelial cells. *Cancer Res*, 1995. 55(4): p. 792-8.
43. Galani, V., A. Varouktsi, S.S. Papadatos, A. Mitselou, I. Sainis, S. Constantopoulos, and Y. Dalavanga, The role of apoptosis defects in malignant mesothelioma pathogenesis with an impact on prognosis and treatment. *Cancer Chemother Pharmacol*, 2019. 84(2): p. 241-253.DOI: 10.1007/s00280-019-03878-3.

44. Carbone, M., A. Gazdar, and J.S. Butel, SV40 and human mesothelioma. *Transl Lung Cancer Res*, 2020. 9(Suppl 1): p. S47-S59.DOI: 10.21037/tlcr.2020.02.03.
45. Vera, M. and P. Fortes, Simian virus-40 as a gene therapy vector. *DNA Cell Biol*, 2004. 23(5): p. 271-82.DOI: 10.1089/104454904323090903.
46. Pass, H.I., M. Bocchetta, and M. Carbone, Evidence of an important role for SV40 in mesothelioma. *Thorac Surg Clin*, 2004. 14(4): p. 489-95.DOI: 10.1016/j.thorsurg.2004.06.003.
47. Wadowski, B., A. De Rienzo, and R. Bueno, The Molecular Basis of Malignant Pleural Mesothelioma. *Thorac Surg Clin*, 2020. 30(4): p. 383-393.DOI: 10.1016/j.thorsurg.2020.08.005.
48. Sauter, J.L., S. Dacic, F. Galateau-Salle, R.L. Attanoos, K.J. Butnor, A. Churg, A.N. Husain, K. Kadota, A. Khoor, A.G. Nicholson, V. Roggli, F. Schmitt, M.S. Tsao, and W.D. Travis, The 2021 WHO Classification of Tumors of the Pleura: Advances Since the 2015 Classification. *J Thorac Oncol*, 2022. 17(5): p. 608-622.DOI: 10.1016/j.jtho.2021.12.014.
49. Dacic, S., Pleural mesothelioma classification-update and challenges. *Mod Pathol*, 2022. 35(Suppl 1): p. 51-56.DOI: 10.1038/s41379-021-00895-7.
50. Brcic, L. and I. Kern, Clinical significance of histologic subtyping of malignant pleural mesothelioma. *Transl Lung Cancer Res*, 2020. 9(3): p. 924-933.DOI: 10.21037/tlcr.2020.03.38.
51. A.I.O.M. 2018. Available from: https://www.aiom.it/wp-content/uploads/2018/11/2018_LG_AIOM_Mesotelioma.pdf.
52. Musso, V., C. Diotti, A. Palleschi, D. Tosi, A. Aiolfi, and P. Mendogni, Management of Pleural Effusion Secondary to Malignant Mesothelioma. *J Clin Med*, 2021. 10(18).DOI: 10.3390/jcm10184247.
53. WebPathology. Available from: https://www.webpathology.com/case.asp?case=595.
54. Loomis, D., D.B. Richardson, and L. Elliott, Quantitative relationships of exposure to chrysotile asbestos and mesothelioma mortality. *Am J Ind Med*, 2019. 62(6): p. 471-477.DOI: 10.1002/ajim.22985.
55. Bibby, A.C., S. Tsim, N. Kanellakis, H. Ball, D.C. Talbot, K.G. Blyth, N.A. Maskell, and I. Psallidas, Malignant pleural mesothelioma: an update on investigation, diagnosis and treatment. *Eur Respir Rev*, 2016. 25(142): p. 472-486.DOI: 10.1183/16000617.0063-2016.
56. Robinson, B.W. and R.A. Lake, Advances in malignant mesothelioma. *N Engl J Med*, 2005. 353(15): p. 1591-603.DOI: 10.1056/NEJMra050152.
57. Baas, P., D. Fennell, K.M. Kerr, P.E. Van Schil, R.L. Haas, S. Peters, and E.G. Committee, Malignant pleural mesothelioma: ESMO Clinical Practice Guidelines for diagnosis, treatment and follow-up. *Ann Oncol*, 2015. 26 Suppl 5: p. v31-9.DOI: 10.1093/annonc/mdv199.
58. Abdel-Rahman, O., Z. Elsayed, H. Mohamed, and M. Eltobgy, Radical multimodality therapy for malignant pleural mesothelioma. *Cochrane Database Syst Rev*, 2018. 1(1): p. CD012605.DOI: 10.1002/14651858.CD012605.pub2.

59. Hussaini, H.M., B. Seo, and A.M. Rich, Immunohistochemistry and Immunofluorescence. *Methods Mol Biol*, 2023. 2588: p. 439-450.DOI: 10.1007/978-1-0716-2780-8_26.
60. Klebe, S., A. Swalling, L. Jonavicius, and D.W. Henderson, An immunohistochemical comparison of two TTF-1 monoclonal antibodies in atypical squamous lesions and sarcomatoid carcinoma of the lung, and pleural malignant mesothelioma. *J Clin Pathol*, 2016. 69(2): p. 136-41.DOI: 10.1136/jclinpath-2015-203184.
61. Matsumoto, S., K. Nabeshima, T. Kamei, K. Hiroshima, K. Kawahara, S. Hata, K. Marukawa, Y. Matsuno, K. Taguchi, and T. Tsujimura, Morphology of 9p21 homozygous deletion-positive pleural mesothelioma cells analyzed using fluorescence in situ hybridization and virtual microscope system in effusion cytology. *Cancer Cytopathol*, 2013. 121(8): p. 415-22.DOI: 10.1002/cncy.21269.
62. Raafat, N., S.D. Blacksell, and R.J. Maude, A review of dengue diagnostics and implications for surveillance and control. *Trans R Soc Trop Med Hyg*, 2019. 113(11): p. 653-660.DOI: 10.1093/trstmh/trz068.
63. Henderson, D.W., G. Reid, S.C. Kao, N. van Zandwijk, and S. Klebe, Challenges and controversies in the diagnosis of malignant mesothelioma: Part 2. Malignant mesothelioma subtypes, pleural synovial sarcoma, molecular and prognostic aspects of mesothelioma, BAP1, aquaporin-1 and microRNA. *J Clin Pathol*, 2013. 66(10): p. 854-61.DOI: 10.1136/jclinpath-2013-201609.
64. Amatya, V.J., K. Kushitani, A.S. Mawas, Y. Miyata, M. Okada, T. Kishimoto, K. Inai, and Y. Takeshima, MUC4, a novel immunohistochemical marker identified by gene expression profiling, differentiates pleural sarcomatoid mesothelioma from lung sarcomatoid carcinoma. *Mod Pathol*, 2017. 30(5): p. 672-681.DOI: 10.1038/modpathol.2016.181.
65. Husain, A.N., T.V. Colby, N.G. Ordonez, T.C. Allen, R.L. Attanoos, M.B. Beasley, K.J. Butnor, L.R. Chirieac, A.M. Churg, S. Dacic, F. Galateau-Salle, A. Gibbs, A.M. Gown, T. Krausz, L.A. Litzky, A. Marchevsky, A.G. Nicholson, V.L. Roggli, A.K. Sharma, W.D. Travis, A.E. Walts, and M.R. Wick, Guidelines for Pathologic Diagnosis of Malignant Mesothelioma 2017 Update of the Consensus Statement From the International Mesothelioma Interest Group. *Arch Pathol Lab Med*, 2018. 142(1): p. 89-108.DOI: 10.5858/arpa.2017-0124-RA.
66. Henderson, D.W., G. Reid, S.C. Kao, N. van Zandwijk, and S. Klebe, Challenges and controversies in the diagnosis of mesothelioma: Part 1. Cytology-only diagnosis, biopsies, immunohistochemistry, discrimination between mesothelioma and reactive mesothelial hyperplasia, and biomarkers. *J Clin Pathol*, 2013. 66(10): p. 847-53.DOI: 10.1136/jclinpath-2012-201303.
67. Eccher, A., I. Girolami, E. Lucenteforte, G. Troncone, A. Scarpa, and L. Pantanowitz, Diagnostic mesothelioma biomarkers in effusion cytology. *Cancer Cytopathol*, 2021. 129(7): p. 506-516.DOI: 10.1002/cncy.22398.
68. Kirschner, M.B., Y.Y. Cheng, N.J. Armstrong, R.C. Lin, S.C. Kao, A. Linton, S. Klebe, B.C. McCaughan, N. van Zandwijk, and G. Reid, MiR-score: a novel 6-microRNA

signature that predicts survival outcomes in patients with malignant pleural mesothelioma. *Mol Oncol*, 2015. 9(3): p. 715-26.DOI: 10.1016/j.molonc.2014.11.007.
69. Sinha, S., A.J. Swift, M.A. Kamil, S. Matthews, M.J. Bull, P. Fisher, D. De Fonseka, S. Saha, J.G. Edwards, and C.S. Johns, The role of imaging in malignant pleural mesothelioma: an update after the 2018 BTS guidelines. *Clin Radiol*, 2020. 75(6): p. 423-432.DOI: 10.1016/j.crad.2019.12.001.
70. Fels Elliott, D.R. and K.D. Jones, Diagnosis of Mesothelioma. *Surg Pathol Clin*, 2020. 13(1): p. 73-89.DOI: 10.1016/j.path.2019.10.001.
71. Bonomi, M., C. De Filippis, E. Lopci, L. Gianoncelli, G. Rizzardi, E. Cerchiaro, L. Bortolotti, A. Zanello, and G.L. Ceresoli, Clinical staging of malignant pleural mesothelioma: current perspectives. *Lung Cancer (Auckl)*, 2017. 8: p. 127-139.DOI: 10.2147/LCTT.S102113.
72. Tsao, A.S., H.I. Pass, A. Rimner, and A.S. Mansfield, New Era for Malignant Pleural Mesothelioma: Updates on Therapeutic Options. *J Clin Oncol*, 2022. 40(6): p. 681-692.DOI: 10.1200/JCO.21.01567.
73. Rusch, V.W., K. Chansky, H.L. Kindler, A.K. Nowak, H.I. Pass, D.C. Rice, L. Shemanski, F. Galateau-Salle, B.C. McCaughan, T. Nakano, E. Ruffini, J.P. van Meerbeeck, M. Yoshimura, I. Staging, a.b. Prognostic Factors Committee, and i. participating, The IASLC Mesothelioma Staging Project: Proposals for the M Descriptors and for Revision of the TNM Stage Groupings in the Forthcoming (Eighth) Edition of the TNM Classification for Mesothelioma. *J Thorac Oncol*, 2016. 11(12): p. 2112-2119.DOI: 10.1016/j.jtho.2016.09.124.
74. Gill, R.R., A.K. Nowak, D.J. Giroux, M. Eisele, A. Rosenthal, H. Kindler, A. Wolf, R.T. Ripley, A. Bille, D. Rice, I. Opitz, A. Rimner, M. de Perrot, H.I. Pass, V.W. Rusch, S. members of the International Association for the Study of Lung Cancer, A.B. Prognostic Factors Committee, and I. Participating, The International Association for the Study of Lung Cancer Mesothelioma Staging Project: Proposals for Revisions of the "T" Descriptors in the Forthcoming Ninth Edition of the TNM Classification for Pleural Mesothelioma. *J Thorac Oncol*, 2024. 19(9): p. 1310-1325.DOI: 10.1016/j.jtho.2024.03.007.
75. Treasure, T. and A. Sedrakyan, Pleural mesothelioma: little evidence, still time to do trials. *Lancet*, 2004. 364(9440): p. 1183-5.DOI: 10.1016/S0140-6736(04)17108-0.
76. Meyerhoff, R.R., C.F. Yang, P.J. Speicher, B.C. Gulack, M.G. Hartwig, T.A. D'Amico, D.H. Harpole, and M.F. Berry, Impact of mesothelioma histologic subtype on outcomes in the Surveillance, Epidemiology, and End Results database. *J Surg Res*, 2015. 196(1): p. 23-32.DOI: 10.1016/j.jss.2015.01.043.
77. Sugarbaker, D.J., M.T. Jaklitsch, R. Bueno, W. Richards, J. Lukanich, S.J. Mentzer, Y. Colson, P. Linden, M. Chang, L. Capalbo, E. Oldread, S. Neragi-Miandoab, S.J. Swanson, and L.S. Zellos, Prevention, early detection, and management of complications after 328 consecutive extrapleural pneumonectomies. *J Thorac Cardiovasc Surg*, 2004. 128(1): p. 138-46.DOI: 10.1016/j.jtcvs.2004.02.021.
78. Weder, W., P. Kestenholz, C. Taverna, S. Bodis, D. Lardinois, M. Jerman, and R.A. Stahel, Neoadjuvant chemotherapy followed by extrapleural pneumonectomy in

malignant pleural mesothelioma. *J Clin Oncol*, 2004. 22(17): p. 3451-7.DOI: 10.1200/JCO.2004.10.071.
79. Duranti, L., A. Pardolesi, L. Bertolaccini, L. Tavecchio, P. Scanagatta, L. Rolli, and U. Pastorino, Extra-pleural pneumonectomy. *J Thorac Dis*, 2019. 11(3): p. 1022-1030.DOI: 10.21037/jtd.2019.02.61.
80. Sinn, K., B. Mosleh, and M.A. Hoda, Malignant pleural mesothelioma: recent developments. *Curr Opin Oncol*, 2021. 33(1): p. 80-86.DOI: 10.1097/CCO.0000000000000697.
81. Sobhani, N., S.P. Corona, D. Bonazza, A. Ianza, T. Pivetta, G. Roviello, M. Cortale, A. Guglielmi, F. Zanconati, and D. Generali, Advances in systemic therapy for malignant mesothelioma: future perspectives. *Future Oncol*, 2017. 13(23): p. 2083-2101.DOI: 10.2217/fon-2017-0224.
82. Vogelzang, N.J., J.J. Rusthoven, J. Symanowski, C. Denham, E. Kaukel, P. Ruffie, U. Gatzemeier, M. Boyer, S. Emri, C. Manegold, C. Niyikiza, and P. Paoletti, Phase III Study of Pemetrexed in Combination With Cisplatin Versus Cisplatin Alone in Patients With Malignant Pleural Mesothelioma. *J Clin Oncol*, 2023. 41(12): p. 2125-2133.DOI: 10.1200/JCO.22.02542.
83. Cedres, S., J.D. Assaf, P. Iranzo, A. Callejo, N. Pardo, A. Navarro, A. Martinez-Marti, D. Marmolejo, A. Rezqallah, C. Carbonell, J. Frigola, R. Amat, A. Pedrola, R. Dienstmann, and E. Felip, Efficacy of chemotherapy for malignant pleural mesothelioma according to histology in a real-world cohort. *Sci Rep*, 2021. 11(1): p. 21357.DOI: 10.1038/s41598-021-00831-4.
84. Baldini, E.H., External beam radiation therapy for the treatment of pleural mesothelioma. *Thorac Surg Clin*, 2004. 14(4): p. 543-8.DOI: 10.1016/S1547-4127(04)00108-2.
85. Ahamad, A., C.W. Stevens, W.R. Smythe, A.A. Vaporciyan, R. Komaki, J.F. Kelly, Z. Liao, G. Starkschall, and K.M. Forster, Intensity-modulated radiation therapy: a novel approach to the management of malignant pleural mesothelioma. *Int J Radiat Oncol Biol Phys*, 2003. 55(3): p. 768-75.DOI: 10.1016/s0360-3016(02)04151-2.
86. Abdel-Rahman, O., Role of postoperative radiotherapy in the management of malignant pleural mesothelioma : A propensity score matching of the SEER database. *Strahlenther Onkol*, 2017. 193(4): p. 276-284.DOI: 10.1007/s00066-016-1092-7.
87. Riley, R.S., C.H. June, R. Langer, and M.J. Mitchell, Delivery technologies for cancer immunotherapy. *Nat Rev Drug Discov*, 2019. 18(3): p. 175-196.DOI: 10.1038/s41573-018-0006-z.
88. Coley, W.B., The Treatment of Inoperable Sarcoma by Bacterial Toxins (the Mixed Toxins of the Streptococcus erysipelas and the Bacillus prodigiosus). *Proc R Soc Med*, 1910. 3(Surg Sect): p. 1-48.
89. Met, O., K.M. Jensen, C.A. Chamberlain, M. Donia, and I.M. Svane, Principles of adoptive T cell therapy in cancer. *Semin Immunopathol*, 2019. 41(1): p. 49-58.DOI: 10.1007/s00281-018-0703-z.

90. Wang, Z., G. Wang, H. Lu, H. Li, M. Tang, and A. Tong, Development of therapeutic antibodies for the treatment of diseases. *Mol Biomed*, 2022. 3(1): p. 35.DOI: 10.1186/s43556-022-00100-4.
91. Morse, M.A., W.R. Gwin, 3rd, and D.A. Mitchell, Vaccine Therapies for Cancer: Then and Now. *Target Oncol*, 2021. 16(2): p. 121-152.DOI: 10.1007/s11523-020-00788-w.
92. Bruni, D., H.K. Angell, and J. Galon, The immune contexture and Immunoscore in cancer prognosis and therapeutic efficacy. *Nat Rev Cancer*, 2020. 20(11): p. 662-680.DOI: 10.1038/s41568-020-0285-7.
93. Yang, Y., Cancer immunotherapy: harnessing the immune system to battle cancer. *J Clin Invest*, 2015. 125(9): p. 3335-7.DOI: 10.1172/JCI83871.
94. Lee, Y.T., Y.J. Tan, and C.E. Oon, Molecular targeted therapy: Treating cancer with specificity. *Eur J Pharmacol*, 2018. 834: p. 188-196.DOI: 10.1016/j.ejphar.2018.07.034.
95. Zhong, L., Y. Li, L. Xiong, W. Wang, M. Wu, T. Yuan, W. Yang, C. Tian, Z. Miao, T. Wang, and S. Yang, Small molecules in targeted cancer therapy: advances, challenges, and future perspectives. *Signal Transduct Target Ther*, 2021. 6(1): p. 201.DOI: 10.1038/s41392-021-00572-w.
96. Delgado, M. and J.A. Garcia-Sanz, Therapeutic Monoclonal Antibodies against Cancer: Present and Future. *Cells*, 2023. 12(24).DOI: 10.3390/cells12242837.
97. Wathoni, N., L.E. Puluhulawa, I.M. Joni, M. Muchtaridi, A.F.A. Mohammed, K.M. Elamin, T. Milanda, and D. Gozali, Monoclonal antibody as a targeting mediator for nanoparticle targeted delivery system for lung cancer. *Drug Deliv*, 2022. 29(1): p. 2959-2970.DOI: 10.1080/10717544.2022.2120566.
98. Adams, G.P. and L.M. Weiner, Monoclonal antibody therapy of cancer. *Nat Biotechnol*, 2005. 23(9): p. 1147-57.DOI: 10.1038/nbt1137.
99. Kwilas, A.R., A. Ardiani, R.N. Donahue, D.T. Aftab, and J.W. Hodge, Dual effects of a targeted small-molecule inhibitor (cabozantinib) on immune-mediated killing of tumor cells and immune tumor microenvironment permissiveness when combined with a cancer vaccine. *J Transl Med*, 2014. 12: p. 294.DOI: 10.1186/s12967-014-0294-y.
100. Kudo-Saito, C., J. Schlom, K. Camphausen, C.N. Coleman, and J.W. Hodge, The requirement of multimodal therapy (vaccine, local tumor radiation, and reduction of suppressor cells) to eliminate established tumors. *Clin Cancer Res*, 2005. 11(12): p. 4533-44.DOI: 10.1158/1078-0432.CCR-04-2237.
101. Griffioen, A.W. and A.C. Dudley, The rising impact of angiogenesis research. *Angiogenesis*, 2022. 25(4): p. 435-437.DOI: 10.1007/s10456-022-09849-2.
102. Ohshio, Y., K. Teramoto, J. Hanaoka, N. Tezuka, Y. Itoh, T. Asai, Y. Daigo, and K. Ogasawara, Cancer-associated fibroblast-targeted strategy enhances antitumor immune responses in dendritic cell-based vaccine. *Cancer Sci*, 2015. 106(2): p. 134-42.DOI: 10.1111/cas.12584.
103. Lacouture, M. and V. Sibaud, Toxic Side Effects of Targeted Therapies and Immunotherapies Affecting the Skin, Oral Mucosa, Hair, and Nails. *Am J Clin Dermatol*, 2018. 19(Suppl 1): p. 31-39.DOI: 10.1007/s40257-018-0384-3.
104. Cerruti, F., G. Jocolle, C. Salio, L. Oliva, L. Paglietti, B. Alessandria, S. Mioletti, G. Donati, G. Numico, S. Cenci, and P. Cascio, Proteasome stress sensitizes malignant

pleural mesothelioma cells to bortezomib-induced apoptosis. *Sci Rep*, 2017. 7(1): p. 17626.DOI: 10.1038/s41598-017-17977-9.
105. Barbieri, F., R. Wurth, R.E. Favoni, A. Pattarozzi, M. Gatti, A. Ratto, A. Ferrari, A. Bajetto, and T. Florio, Receptor tyrosine kinase inhibitors and cytotoxic drugs affect pleural mesothelioma cell proliferation: insight into EGFR and ERK1/2 as antitumor targets. *Biochem Pharmacol*, 2011. 82(10): p. 1467-77.DOI: 10.1016/j.bcp.2011.07.073.
106. Jung, T., B. Catalgol, and T. Grune, The proteasomal system. *Mol Aspects Med*, 2009. 30(4): p. 191-296.DOI: 10.1016/j.mam.2009.04.001.
107. Ciechanover, A., Proteolysis: from the lysosome to ubiquitin and the proteasome. *Nat Rev Mol Cell Biol*, 2005. 6(1): p. 79-87.DOI: 10.1038/nrm1552.
108. Marshall, R.S. and R.D. Vierstra, Dynamic Regulation of the 26S Proteasome: From Synthesis to Degradation. *Front Mol Biosci*, 2019. 6: p. 40.DOI: 10.3389/fmolb.2019.00040.
109. Hershko, A., H. Heller, S. Elias, and A. Ciechanover, Components of ubiquitin-protein ligase system. Resolution, affinity purification, and role in protein breakdown. *J Biol Chem*, 1983. 258(13): p. 8206-14.
110. Guo, H.J., N. Rahimi, and P. Tadi, *Biochemistry, Ubiquitination*, in *StatPearls*. 2024: Treasure Island (FL).
111. Ciechanover, A., Intracellular protein degradation: from a vague idea thru the lysosome and the ubiquitin-proteasome system and onto human diseases and drug targeting. *Cell Death Differ*, 2005. 12(9): p. 1178-90.DOI: 10.1038/sj.cdd.4401692.
112. Deng, L., T. Meng, L. Chen, W. Wei, and P. Wang, The role of ubiquitination in tumorigenesis and targeted drug discovery. *Signal Transduct Target Ther*, 2020. 5(1): p. 11.DOI: 10.1038/s41392-020-0107-0.
113. Glickman, M.H. and A. Ciechanover, The ubiquitin-proteasome proteolytic pathway: destruction for the sake of construction. *Physiol Rev*, 2002. 82(2): p. 373-428.DOI: 10.1152/physrev.00027.2001.
114. Nandi, D., P. Tahiliani, A. Kumar, and D. Chandu, The ubiquitin-proteasome system. *J Biosci*, 2006. 31(1): p. 137-55.DOI: 10.1007/BF02705243.
115. He, M., Z. Zhou, A.A. Shah, H. Zou, J. Tao, Q. Chen, and Y. Wan, The emerging role of deubiquitinating enzymes in genomic integrity, diseases, and therapeutics. *Cell Biosci*, 2016. 6: p. 62.DOI: 10.1186/s13578-016-0127-1.
116. Bashore, C., S. Prakash, M.C. Johnson, R.J. Conrad, I.A. Kekessie, S.J. Scales, N. Ishisoko, T. Kleinheinz, P.S. Liu, N. Popovych, A.T. Wecksler, L. Zhou, C. Tam, I. Zilberleyb, R. Srinivasan, R.A. Blake, A. Song, S.T. Staben, Y. Zhang, D. Arnott, W.J. Fairbrother, S.A. Foster, I.E. Wertz, C. Ciferri, and E.C. Dueber, Targeted degradation via direct 26S proteasome recruitment. *Nat Chem Biol*, 2023. 19(1): p. 55-63.DOI: 10.1038/s41589-022-01218-w.
117. Borissenko, L. and M. Groll, 20S proteasome and its inhibitors: crystallographic knowledge for drug development. *Chem Rev*, 2007. 107(3): p. 687-717.DOI: 10.1021/cr0502504.
118. Liu, C.W., X. Li, D. Thompson, K. Wooding, T.L. Chang, Z. Tang, H. Yu, P.J. Thomas, and G.N. DeMartino, ATP binding and ATP hydrolysis play distinct roles in the

function of 26S proteasome. *Mol Cell*, 2006. 24(1): p. 39-50.DOI: 10.1016/j.molcel.2006.08.025.
119. Inobe, T. and A. Matouschek, Paradigms of protein degradation by the proteasome. *Curr Opin Struct Biol*, 2014. 24: p. 156-64.DOI: 10.1016/j.sbi.2014.02.002.
120. King, R.W., R.J. Deshaies, J.M. Peters, and M.W. Kirschner, How proteolysis drives the cell cycle. *Science*, 1996. 274(5293): p. 1652-9.DOI: 10.1126/science.274.5293.1652.
121. Tu, Y., C. Chen, J. Pan, J. Xu, Z.G. Zhou, and C.Y. Wang, The Ubiquitin Proteasome Pathway (UPP) in the regulation of cell cycle control and DNA damage repair and its implication in tumorigenesis. *Int J Clin Exp Pathol*, 2012. 5(8): p. 726-38.
122. Fribley, A., Q. Zeng, and C.Y. Wang, Proteasome inhibitor PS-341 induces apoptosis through induction of endoplasmic reticulum stress-reactive oxygen species in head and neck squamous cell carcinoma cells. *Mol Cell Biol*, 2004. 24(22): p. 9695-704.DOI: 10.1128/MCB.24.22.9695-9704.2004.
123. Han, Y.H., S.Z. Kim, S.H. Kim, and W.H. Park, Reactive oxygen species and glutathione level changes by a proteasome inhibitor, MG132, partially affect calf pulmonary arterial endothelial cell death. *Drug Chem Toxicol*, 2010. 33(4): p. 403-9.DOI: 10.3109/01480540903524350.
124. Janen, S.B., H. Chaachouay, and C. Richter-Landsberg, Autophagy is activated by proteasomal inhibition and involved in aggresome clearance in cultured astrocytes. *Glia*, 2010. 58(14): p. 1766-74.DOI: 10.1002/glia.21047.
125. Ding, W.X., H.M. Ni, W. Gao, T. Yoshimori, D.B. Stolz, D. Ron, and X.M. Yin, Linking of autophagy to ubiquitin-proteasome system is important for the regulation of endoplasmic reticulum stress and cell viability. *Am J Pathol*, 2007. 171(2): p. 513-24.DOI: 10.2353/ajpath.2007.070188.
126. Fribley, A. and C.Y. Wang, Proteasome inhibitor induces apoptosis through induction of endoplasmic reticulum stress. *Cancer Biol Ther*, 2006. 5(7): p. 745-8.DOI: 10.4161/cbt.5.7.2971.
127. Dang, F., L. Nie, and W. Wei, Ubiquitin signaling in cell cycle control and tumorigenesis. *Cell Death Differ*, 2021. 28(2): p. 427-438.DOI: 10.1038/s41418-020-00648-0.
128. Yu, H., L. Lin, Z. Zhang, H. Zhang, and H. Hu, Targeting NF-kappaB pathway for the therapy of diseases: mechanism and clinical study. *Signal Transduct Target Ther*, 2020. 5(1): p. 209.DOI: 10.1038/s41392-020-00312-6.
129. Li, H., X. Niu, D. Zhang, M.H. Qu, and K. Yang, The role of the canonical nf-kappab signaling pathway in the development of acute liver failure. *Biotechnol Genet Eng Rev*, 2023. 39(2): p. 775-795.DOI: 10.1080/02648725.2022.2162999.
130. Sun, S.C., The noncanonical NF-kappaB pathway. *Immunol Rev*, 2012. 246(1): p. 125-40.DOI: 10.1111/j.1600-065X.2011.01088.x.
131. Baldwin, A.S., Control of oncogenesis and cancer therapy resistance by the transcription factor NF-kappaB. *J Clin Invest*, 2001. 107(3): p. 241-6.DOI: 10.1172/JCI11991.
132. Mitchell, S., J. Vargas, and A. Hoffmann, Signaling via the NFkappaB system. *Wiley Interdiscip Rev Syst Biol Med*, 2016. 8(3): p. 227-41.DOI: 10.1002/wsbm.1331.

133. Pakjoo, M., S.E. Ahmadi, M. Zahedi, N. Jaafari, R. Khademi, A. Amini, and M. Safa, Interplay between proteasome inhibitors and NF-kappaB pathway in leukemia and lymphoma: a comprehensive review on challenges ahead of proteasome inhibitors. *Cell Commun Signal*, 2024. 22(1): p. 105.DOI: 10.1186/s12964-023-01433-5.
134. Wang, Z., ErbB Receptors and Cancer. *Methods Mol Biol*, 2017. 1652: p. 3-35.DOI: 10.1007/978-1-4939-7219-7_1.
135. Palumbo, C., M. Benvenuto, C. Focaccetti, L. Albonici, L. Cifaldi, A. Rufini, D. Nardozi, V. Angiolini, A. Bei, L. Masuelli, and R. Bei, Recent findings on the impact of ErbB receptors status on prognosis and therapy of head and neck squamous cell carcinoma. *Front Med (Lausanne)*, 2023. 10: p. 1066021.DOI: 10.3389/fmed.2023.1066021.
136. Ullah, R., Q. Yin, A.H. Snell, and L. Wan, RAF-MEK-ERK pathway in cancer evolution and treatment. *Semin Cancer Biol*, 2022. 85: p. 123-154.DOI: 10.1016/j.semcancer.2021.05.010.
137. Morgos, D.T., C. Stefani, D. Miricescu, M. Greabu, S. Stanciu, S. Nica, S. Stanescu, II, D.G. Balan, A.E. Balcangiu-Stroescu, E.C. Coculescu, D.E. Georgescu, and R.I. Nica, Targeting PI3K/AKT/mTOR and MAPK Signaling Pathways in Gastric Cancer. *Int J Mol Sci*, 2024. 25(3).DOI: 10.3390/ijms25031848.
138. Vivanco, I. and C.L. Sawyers, The phosphatidylinositol 3-Kinase AKT pathway in human cancer. *Nat Rev Cancer*, 2002. 2(7): p. 489-501.DOI: 10.1038/nrc839.
139. Zhao, W.L., Targeted therapy in T-cell malignancies: dysregulation of the cellular signaling pathways. *Leukemia*, 2010. 24(1): p. 13-21.DOI: 10.1038/leu.2009.223.
140. Kumagai, S., S. Koyama, and H. Nishikawa, Antitumour immunity regulated by aberrant ERBB family signalling. *Nat Rev Cancer*, 2021. 21(3): p. 181-197.DOI: 10.1038/s41568-020-00322-0.
141. Destro, A., G.L. Ceresoli, M. Falleni, P.A. Zucali, E. Morenghi, P. Bianchi, C. Pellegrini, N. Cordani, V. Vaira, M. Alloisio, A. Rizzi, S. Bosari, and M. Roncalli, EGFR overexpression in malignant pleural mesothelioma. An immunohistochemical and molecular study with clinico-pathological correlations. *Lung Cancer*, 2006. 51(2): p. 207-15.DOI: 10.1016/j.lungcan.2005.10.016.
142. Yang, L., H. Fang, J. Jiang, Y. Sha, Z. Zhong, and F. Meng, EGFR-targeted pemetrexed therapy of malignant pleural mesothelioma. *Drug Deliv Transl Res*, 2022. 12(10): p. 2527-2536.DOI: 10.1007/s13346-021-01094-2.
143. Klampatsa, A., D.Y. Achkova, D.M. Davies, A.C. Parente-Pereira, N. Woodman, J. Rosekilly, G. Osborne, T. Thayaparan, A. Bille, M. Sheaf, J.F. Spicer, J. King, and J. Maher, Intracavitary 'T4 immunotherapy' of malignant mesothelioma using pan-ErbB re-targeted CAR T-cells. *Cancer Lett*, 2017. 393: p. 52-59.DOI: 10.1016/j.canlet.2017.02.015.
144. Kurai, J., H. Chikumi, K. Hashimoto, M. Takata, T. Sako, K. Yamaguchi, N. Kinoshita, M. Watanabe, H. Touge, H. Makino, T. Igishi, H. Hamada, S. Yano, and E. Shimizu, Therapeutic antitumor efficacy of anti-epidermal growth factor receptor antibody, cetuximab, against malignant pleural mesothelioma. *Int J Oncol*, 2012. 41(5): p. 1610-8.DOI: 10.3892/ijo.2012.1607.

145. Graham, D.K., D. DeRyckere, K.D. Davies, and H.S. Earp, The TAM family: phosphatidylserine sensing receptor tyrosine kinases gone awry in cancer. *Nat Rev Cancer*, 2014. 14(12): p. 769-85.DOI: 10.1038/nrc3847.
146. Zhu, C., Y. Wei, and X. Wei, AXL receptor tyrosine kinase as a promising anti-cancer approach: functions, molecular mechanisms and clinical applications. *Mol Cancer*, 2019. 18(1): p. 153.DOI: 10.1186/s12943-019-1090-3.
147. Ou, W.B., C. Hubert, J.M. Corson, R. Bueno, D.L. Flynn, D.J. Sugarbaker, and J.A. Fletcher, Targeted inhibition of multiple receptor tyrosine kinases in mesothelioma. *Neoplasia*, 2011. 13(1): p. 12-22.DOI: 10.1593/neo.101156.
148. Corno, C., L. Gatti, C. Lanzi, N. Zaffaroni, D. Colombo, and P. Perego, Role of the Receptor Tyrosine Kinase Axl and its Targeting in Cancer Cells. *Curr Med Chem*, 2016. 23(15): p. 1496-512.DOI: 10.2174/0929867323666160405112954.
149. Tai, K.Y., Y.S. Shieh, C.S. Lee, S.G. Shiah, and C.W. Wu, Axl promotes cell invasion by inducing MMP-9 activity through activation of NF-kappaB and Brg-1. *Oncogene*, 2008. 27(29): p. 4044-55.DOI: 10.1038/onc.2008.57.
150. Zagorska, A., P.G. Traves, E.D. Lew, I. Dransfield, and G. Lemke, Diversification of TAM receptor tyrosine kinase function. *Nat Immunol*, 2014. 15(10): p. 920-8.DOI: 10.1038/ni.2986.
151. Nieto, M.A., Epithelial-Mesenchymal Transitions in development and disease: old views and new perspectives. *Int J Dev Biol*, 2009. 53(8-10): p. 1541-7.DOI: 10.1387/ijdb.072410mn.
152. Ou, W.B., J.M. Corson, D.L. Flynn, W.P. Lu, S.C. Wise, R. Bueno, D.J. Sugarbaker, and J.A. Fletcher, AXL regulates mesothelioma proliferation and invasiveness. *Oncogene*, 2011. 30(14): p. 1643-52.DOI: 10.1038/onc.2010.555.
153. Song, W., H. Wang, M. Lu, X. Ni, N. Bahri, S. Zhu, L. Chen, Y. Wu, J. Qiu, J.A. Fletcher, and W.B. Ou, AXL Inactivation Inhibits Mesothelioma Growth and Migration via Regulation of p53 Expression. *Cancers (Basel)*, 2020. 12(10).DOI: 10.3390/cancers12102757.
154. Patel, V., M.J. Keating, W.G. Wierda, and V. Gandhi, Preclinical combination of TP-0903, an AXL inhibitor and B-PAC-1, a procaspase-activating compound with ibrutinib in chronic lymphocytic leukemia. *Leuk Lymphoma*, 2016. 57(6): p. 1494-7.DOI: 10.3109/10428194.2015.1102243.
155. Iida, M., N.K. McDaniel, K.L. Kostecki, N.B. Welke, C.A. Kranjac, P. Liu, C. Longhurst, J.Y. Bruce, S. Hong, R. Salgia, and D.L. Wheeler, AXL regulates neuregulin1 expression leading to cetuximab resistance in head and neck cancer. *BMC Cancer*, 2022. 22(1): p. 447.DOI: 10.1186/s12885-022-09511-6.
156. Balaji, K., S. Vijayaraghavan, L. Diao, P. Tong, Y. Fan, J.P. Carey, T.N. Bui, S. Warner, J.V. Heymach, K.K. Hunt, J. Wang, L.A. Byers, and K. Keyomarsi, AXL Inhibition Suppresses the DNA Damage Response and Sensitizes Cells to PARP Inhibition in Multiple Cancers. *Mol Cancer Res*, 2017. 15(1): p. 45-58.DOI: 10.1158/1541-7786.MCR-16-0157.

157. Zhai, X., D. Pu, R. Wang, J. Zhang, Y. Lin, Y. Wang, N. Zhai, X. Peng, Q. Zhou, and L. Li, Gas6/AXL pathway: immunological landscape and therapeutic potential. *Front Oncol*, 2023. 13: p. 1121130.DOI: 10.3389/fonc.2023.1121130.
158. Worthmuller, J. and C. Ruegg, The Crosstalk between FAK and Wnt Signaling Pathways in Cancer and Its Therapeutic Implication. *Int J Mol Sci*, 2020. 21(23).DOI: 10.3390/ijms21239107.
159. Owens, L.V., L. Xu, R.J. Craven, G.A. Dent, T.M. Weiner, L. Kornberg, E.T. Liu, and W.G. Cance, Overexpression of the focal adhesion kinase (p125FAK) in invasive human tumors. *Cancer Res*, 1995. 55(13): p. 2752-5.
160. Owens, L.V., L. Xu, G.A. Dent, X. Yang, G.C. Sturge, R.J. Craven, and W.G. Cance, Focal adhesion kinase as a marker of invasive potential in differentiated human thyroid cancer. *Ann Surg Oncol*, 1996. 3(1): p. 100-5.DOI: 10.1007/BF02409059.
161. Tremblay, L., W. Hauck, A.G. Aprikian, L.R. Begin, A. Chapdelaine, and S. Chevalier, Focal adhesion kinase (pp125FAK) expression, activation and association with paxillin and p50CSK in human metastatic prostate carcinoma. *Int J Cancer*, 1996. 68(2): p. 164-71.DOI: 10.1002/(sici)1097-0215(19961009)68:2<169::aid-ijc4>3.0.co;2-w.
162. Lark, A.L., C.A. Livasy, B. Calvo, L. Caskey, D.T. Moore, X. Yang, and W.G. Cance, Overexpression of focal adhesion kinase in primary colorectal carcinomas and colorectal liver metastases: immunohistochemistry and real-time PCR analyses. *Clin Cancer Res*, 2003. 9(1): p. 215-22.
163. Judson, P.L., X. He, W.G. Cance, and L. Van Le, Overexpression of focal adhesion kinase, a protein tyrosine kinase, in ovarian carcinoma. *Cancer*, 1999. 86(8): p. 1551-6.DOI: 10.1002/(sici)1097-0142(19991015)86:6<1551::aid-cncr23>3.0.co;2-p.
164. Worthmuller, J., W. Blum, L. Pecze, V. Salicio, and B. Schwaller, Calretinin promotes invasiveness and EMT in malignant mesothelioma cells involving the activation of the FAK signaling pathway. *Oncotarget*, 2018. 9(91): p. 36256-36272.DOI: 10.18632/oncotarget.26332.
165. Pifer, P.M., L. Yang, M. Kumar, T. Xie, M. Frederick, A. Hefner, B. Beadle, D. Molkentine, J. Molkentine, A. Dhawan, M. Abdelhakiem, A.A. Osman, B.J. Leibowitz, J.N. Myers, C.R. Pickering, V.C. Sandulache, J. Heymach, and H.D. Skinner, FAK Drives Resistance to Therapy in HPV-Negative Head and Neck Cancer in a p53-Dependent Manner. *Clin Cancer Res*, 2024. 30(1): p. 187-197.DOI: 10.1158/1078-0432.CCR-23-0964.
166. Yoon, H., J.P. Dehart, J.M. Murphy, and S.T. Lim, Understanding the roles of FAK in cancer: inhibitors, genetic models, and new insights. *J Histochem Cytochem*, 2015. 63(2): p. 114-28.DOI: 10.1369/0022155414561498.
167. Alamoud, K.A. and M.A. Kukuruzinska, Emerging Insights into Wnt/beta-catenin Signaling in Head and Neck Cancer. *J Dent Res*, 2018. 97(6): p. 665-673.DOI: 10.1177/0022034518771923.
168. Kanteti, R., T. Mirzapoiazova, J.J. Riehm, I. Dhanasingh, B. Mambetsariev, J. Wang, P. Kulkarni, G. Kaushik, P. Seshacharyulu, M.P. Ponnusamy, H.L. Kindler, M.W. Nasser, S.K. Batra, and R. Salgia, Focal adhesion kinase a potential therapeutic target

for pancreatic cancer and malignant pleural mesothelioma. *Cancer Biol Ther*, 2018. 19(4): p. 316-327.DOI: 10.1080/15384047.2017.1416937.
169. Hu, H.H., S.Q. Wang, H.L. Shang, H.F. Lv, B.B. Chen, S.G. Gao, and X.B. Chen, Roles and inhibitors of FAK in cancer: current advances and future directions. *Front Pharmacol*, 2024. 15: p. 1274209.DOI: 10.3389/fphar.2024.1274209.
170. Sherman, D.J. and J. Li, Proteasome Inhibitors: Harnessing Proteostasis to Combat Disease. *Molecules*, 2020. 25(3).DOI: 10.3390/molecules25030671.
171. Screen, M., M. Britton, S.L. Downey, M. Verdoes, M.J. Voges, A.E. Blom, P.P. Geurink, M.D. Risseeuw, B.I. Florea, W.A. van der Linden, A.A. Pletnev, H.S. Overkleeft, and A.F. Kisselev, Nature of pharmacophore influences active site specificity of proteasome inhibitors. *J Biol Chem*, 2010. 285(51): p. 40125-34.DOI: 10.1074/jbc.M110.160606.
172. Thibaudeau, T.A. and D.M. Smith, A Practical Review of Proteasome Pharmacology. *Pharmacol Rev*, 2019. 71(2): p. 170-197.DOI: 10.1124/pr.117.015370.
173. Davies, F., R. Rifkin, C. Costello, G. Morgan, S. Usmani, R. Abonour, A. Palumbo, D. Romanus, R. Hajek, E. Terpos, D. Cherepanov, D.M. Stull, H. Huang, X. Leleu, J. Berdeja, H.C. Lee, K. Weisel, M. Thompson, M. Boccadoro, J. Zonder, G. Cook, N. Puig, J. Vela-Ojeda, E. Farrelly, A. Raju, M. Blazer, and A. Chari, Real-world comparative effectiveness of triplets containing bortezomib (B), carfilzomib (C), daratumumab (D), or ixazomib (I) in relapsed/refractory multiple myeloma (RRMM) in the US. *Ann Hematol*, 2021. 100(9): p. 2325-2337.DOI: 10.1007/s00277-021-04534-8.
174. Guerrero-Garcia, T.A., S. Gandolfi, J.P. Laubach, T. Hideshima, D. Chauhan, C. Mitsiades, K.C. Anderson, and P.G. Richardson, The power of proteasome inhibition in multiple myeloma. *Expert Rev Proteomics*, 2018. 15(12): p. 1033-1052.DOI: 10.1080/14789450.2018.1543595.
175. PubChem. Bethesda (MD): National Library of Medicine (US), N.C.f.B.I. *PubChem Compound Summary for CID 387447, Bortezomib*. 2004. Available from: https://pubchem.ncbi.nlm.nih.gov/compound/Bortezomib.
176. Robak, P. and T. Robak, Bortezomib for the Treatment of Hematologic Malignancies: 15 Years Later. *Drugs R D*, 2019. 19(2): p. 73-92.DOI: 10.1007/s40268-019-0269-9.
177. Ma, Y. and L.M. Hendershot, The role of the unfolded protein response in tumour development: friend or foe? *Nat Rev Cancer*, 2004. 4(12): p. 966-77.DOI: 10.1038/nrc1505.
178. Brown, J.M., Tumor hypoxia in cancer therapy. *Methods Enzymol*, 2007. 435: p. 297-321.DOI: 10.1016/S0076-6879(07)35015-5.
179. Ding, W.X., H.M. Ni, W. Gao, Y.F. Hou, M.A. Melan, X. Chen, D.B. Stolz, Z.M. Shao, and X.M. Yin, Differential effects of endoplasmic reticulum stress-induced autophagy on cell survival. *J Biol Chem*, 2007. 282(7): p. 4702-4710.DOI: 10.1074/jbc.M609267200.
180. Roufayel, R., K. Younes, A. Al-Sabi, and N. Murshid, BH3-Only Proteins Noxa and Puma Are Key Regulators of Induced Apoptosis. *Life (Basel)*, 2022. 12(2).DOI: 10.3390/life12020256.
181. Li, C., R. Li, J.R. Grandis, and D.E. Johnson, Bortezomib induces apoptosis via Bim and Bik up-regulation and synergizes with cisplatin in the killing of head and neck

squamous cell carcinoma cells. *Mol Cancer Ther*, 2008. 7(6): p. 1647-55.DOI: 10.1158/1535-7163.MCT-07-2444.
182. Qian, S., Z. Wei, W. Yang, J. Huang, Y. Yang, and J. Wang, The role of BCL-2 family proteins in regulating apoptosis and cancer therapy. *Front Oncol*, 2022. 12: p. 985363.DOI: 10.3389/fonc.2022.985363.
183. Selimovic, D., B.B. Porzig, A. El-Khattouti, H.E. Badura, M. Ahmad, F. Ghanjati, S. Santourlidis, Y. Haikel, and M. Hassan, Bortezomib/proteasome inhibitor triggers both apoptosis and autophagy-dependent pathways in melanoma cells. *Cell Signal*, 2013. 25(1): p. 308-18.DOI: 10.1016/j.cellsig.2012.10.004.
184. Tseng, L.M., C.Y. Liu, K.C. Chang, P.Y. Chu, C.W. Shiau, and K.F. Chen, CIP2A is a target of bortezomib in human triple negative breast cancer cells. *Breast Cancer Res*, 2012. 14(2): p. R68.DOI: 10.1186/bcr3175.
185. Yi, H., L. Liang, H. Wang, S. Luo, L. Hu, Y. Wang, X. Shen, L. Xiao, Y. Zhang, H. Peng, C. Dai, L. Yuan, R. Li, F. Gong, Z. Li, M. Ye, J. Liu, H. Zhou, J. Zhang, and X. Xiao, Albendazole inhibits NF-kappaB signaling pathway to overcome tumor stemness and bortezomib resistance in multiple myeloma. *Cancer Lett*, 2021. 520: p. 307-320.DOI: 10.1016/j.canlet.2021.08.009.
186. Tan, C.R.C., S. Abdul-Majeed, B. Cael, and S.K. Barta, Clinical Pharmacokinetics and Pharmacodynamics of Bortezomib. *Clin Pharmacokinet*, 2019. 58(2): p. 157-168.DOI: 10.1007/s40262-018-0679-9.
187. Mohan, M., A. Matin, and F.E. Davies, Update on the optimal use of bortezomib in the treatment of multiple myeloma. *Cancer Manag Res*, 2017. 9: p. 51-63.DOI: 10.2147/CMAR.S105163.
188. Cavo, M., Current status of bortezomib in the treatment of multiple myeloma. *Curr Hematol Malig Rep*, 2007. 2(2): p. 128-37.DOI: 10.1007/s11899-007-0018-y.
189. Mateos, M.V., P. Sonneveld, V. Hungria, A.K. Nooka, J.A. Estell, W. Barreto, P. Corradini, C.K. Min, E. Medvedova, K. Weisel, C. Chiu, J.M. Schecter, H. Amin, X. Qin, J. Ukropec, R. Kobos, and A. Spencer, Daratumumab, Bortezomib, and Dexamethasone Versus Bortezomib and Dexamethasone in Patients With Previously Treated Multiple Myeloma: Three-year Follow-up of CASTOR. *Clin Lymphoma Myeloma Leuk*, 2020. 20(8): p. 509-518.DOI: 10.1016/j.clml.2019.09.623.
190. Lu, S. and J. Wang, The resistance mechanisms of proteasome inhibitor bortezomib. *Biomark Res*, 2013. 1(1): p. 13.DOI: 10.1186/2050-7771-1-13.
191. Khan, S.U., K. Fatima, S. Aisha, and F. Malik, Unveiling the mechanisms and challenges of cancer drug resistance. *Cell Commun Signal*, 2024. 22(1): p. 109.DOI: 10.1186/s12964-023-01302-1.
192. Benvenuto, M., S. Ciuffa, C. Focaccetti, D. Sbardella, S. Fazi, M. Scimeca, G.R. Tundo, G. Barillari, M. Segni, E. Bonanno, V. Manzari, A. Modesti, L. Masuelli, M. Coletta, and R. Bei, Proteasome inhibition by bortezomib parallels a reduction in head and neck cancer cells growth, and an increase in tumor-infiltrating immune cells. *Sci Rep*, 2021. 11(1): p. 19051.DOI: 10.1038/s41598-021-98450-6.

193. Fu, Z., C. Lu, C. Zhang, and B. Qiao, PSMA5 promotes the tumorigenic process of prostate cancer and is related to bortezomib resistance. *Anticancer Drugs*, 2019. 30(7): p. e0773.DOI: 10.1097/CAD.0000000000000773.
194. Liu, Y., X. Wang, T. Zhu, N. Zhang, L. Wang, T. Huang, Y. Cao, W. Li, and J. Zhang, Resistance to bortezomib in breast cancer cells that downregulate Bim through FOXA1 O-GlcNAcylation. *J Cell Physiol*, 2019. 234(10): p. 17527-17537.DOI: 10.1002/jcp.28376.
195. Lenz, H.J., Clinical update: proteasome inhibitors in solid tumors. *Cancer Treat Rev*, 2003. 29 Suppl 1: p. 41-8.DOI: 10.1016/s0305-7372(03)00082-3.
196. Caravita, T., P. de Fabritiis, A. Palumbo, S. Amadori, and M. Boccadoro, Bortezomib: efficacy comparisons in solid tumors and hematologic malignancies. *Nat Clin Pract Oncol*, 2006. 3(7): p. 374-87.DOI: 10.1038/ncponc0555.
197. Kohler, S., S. Marschenz, U. Grittner, T. Alexander, F. Hiepe, and A. Meisel, Bortezomib in antibody-mediated autoimmune diseases (TAVAB): study protocol for a unicentric, non-randomised, non-placebo controlled trial. *BMJ Open*, 2019. 9(1): p. e024523.DOI: 10.1136/bmjopen-2018-024523.
198. Zajaczkowska, R., M. Kocot-Kepska, W. Leppert, A. Wrzosek, J. Mika, and J. Wordliczek, Mechanisms of Chemotherapy-Induced Peripheral Neuropathy. *Int J Mol Sci*, 2019. 20(6).DOI: 10.3390/ijms20061451.
199. Burkhart, T., M.C.L. Keith, C.A.G. Lenneman, and R.R. Fernando, Bortezomib-Induced Cardiac Tamponade in a 49-Year-Old Man. *Tex Heart Inst J*, 2018. 45(4): p. 260-263.DOI: 10.14503/THIJ-17-6242.
200. Pancheri, E., V. Guglielmi, G.M. Wilczynski, M. Malatesta, P. Tonin, G. Tomelleri, D. Nowis, and G. Vattemi, Non-Hematologic Toxicity of Bortezomib in Multiple Myeloma: The Neuromuscular and Cardiovascular Adverse Effects. *Cancers (Basel)*, 2020. 12(9).DOI: 10.3390/cancers12092540.
201. Zhang, J., P.L. Yang, and N.S. Gray, Targeting cancer with small molecule kinase inhibitors. *Nat Rev Cancer*, 2009. 9(1): p. 28-39.DOI: 10.1038/nrc2559.
202. Thawani, R., M. Repetto, C. Keddy, K. Nicholson, K. Jones, K. Nusser, C.Z. Beach, G. Harada, A. Drilon, and M.A. Davare, TKI type switching overcomes ROS1 L2086F in ROS1 fusion-positive cancers. *NPJ Precis Oncol*, 2024. 8(1): p. 175.DOI: 10.1038/s41698-024-00663-1.
203. Catlett, I.M., U. Aras, L. Hansen, Y. Liu, D. Bei, I.G. Girgis, and B. Murthy, First-in-human study of deucravacitinib: A selective, potent, allosteric small-molecule inhibitor of tyrosine kinase 2. *Clin Transl Sci*, 2023. 16(1): p. 151-164.DOI: 10.1111/cts.13435.
204. Martin, G., Novel Therapies in Plaque Psoriasis: A Review of Tyrosine Kinase 2 Inhibitors. *Dermatol Ther (Heidelb)*, 2023. 13(2): p. 417-435.DOI: 10.1007/s13555-022-00878-9.
205. Sibaud, V., M. Beylot-Barry, C. Protin, E. Vigarios, C. Recher, and L. Ysebaert, Dermatological Toxicities of Bruton's Tyrosine Kinase Inhibitors. *Am J Clin Dermatol*, 2020. 21(6): p. 799-812.DOI: 10.1007/s40257-020-00535-x.

206. Jiao, Q., L. Bi, Y. Ren, S. Song, Q. Wang, and Y.S. Wang, Advances in studies of tyrosine kinase inhibitors and their acquired resistance. *Mol Cancer*, 2018. 17(1): p. 36.DOI: 10.1186/s12943-018-0801-5.
207. Johnson, M., M.C. Garassino, T. Mok, and T. Mitsudomi, Treatment strategies and outcomes for patients with EGFR-mutant non-small cell lung cancer resistant to EGFR tyrosine kinase inhibitors: Focus on novel therapies. *Lung Cancer*, 2022. 170: p. 41-51.DOI: 10.1016/j.lungcan.2022.05.011.
208. PubChem. Bethesda (MD): National Library of Medicine (US), N.C.f.B.I. *PubChem Compound Summary for CID 10184653, Afatinib*. 2004. Available from: https://pubchem.ncbi.nlm.nih.gov/compound/Afatinib.
209. Dungo, R.T. and G.M. Keating, Afatinib: first global approval. *Drugs*, 2013. 73(13): p. 1503-15.DOI: 10.1007/s40265-013-0111-6.
210. Yarden, Y., The EGFR family and its ligands in human cancer. signalling mechanisms and therapeutic opportunities. *Eur J Cancer*, 2001. 37 Suppl 4: p. S3-8.DOI: 10.1016/s0959-8049(01)00230-1.
211. Scaltriti, M. and J. Baselga, The epidermal growth factor receptor pathway: a model for targeted therapy. *Clin Cancer Res*, 2006. 12(18): p. 5268-72.DOI: 10.1158/1078-0432.CCR-05-1554.
212. Wieduwilt, M.J. and M.M. Moasser, The epidermal growth factor receptor family: biology driving targeted therapeutics. *Cell Mol Life Sci*, 2008. 65(10): p. 1566-84.DOI: 10.1007/s00018-008-7440-8.
213. Wang, S. and J. Li, Second-generation EGFR and ErbB tyrosine kinase inhibitors as first-line treatments for non-small cell lung cancer. *Onco Targets Ther*, 2019. 12: p. 6535-6548.DOI: 10.2147/OTT.S198945.
214. van der Wekken, A.J., A. Saber, T.J. Hiltermann, K. Kok, A. van den Berg, and H.J. Groen, Resistance mechanisms after tyrosine kinase inhibitors afatinib and crizotinib in non-small cell lung cancer, a review of the literature. *Crit Rev Oncol Hematol*, 2016. 100: p. 107-16.DOI: 10.1016/j.critrevonc.2016.01.024.
215. Okita, R., K. Shimizu, Y. Nojima, T. Yukawa, A. Maeda, S. Saisho, and M. Nakata, Lapatinib enhances trastuzumab-mediated antibody-dependent cellular cytotoxicity via upregulation of HER2 in malignant mesothelioma cells. *Oncol Rep*, 2015. 34(6): p. 2864-70.DOI: 10.3892/or.2015.4314.
216. Wei, Q., P. Li, T. Yang, J. Zhu, L. Sun, Z. Zhang, L. Wang, X. Tian, J. Chen, C. Hu, J. Xue, L. Ma, T. Shimura, J. Fang, J. Ying, P. Guo, and X. Cheng, The promise and challenges of combination therapies with antibody-drug conjugates in solid tumors. *J Hematol Oncol*, 2024. 17(1): p. 1.DOI: 10.1186/s13045-023-01509-2.
217. Agatsuma, N., Y. Yasuda, and H. Ozasa, Malignant Pleural Mesothelioma Harboring Both G719C and S768I Mutations of EGFR Successfully Treated with Afatinib. *J Thorac Oncol*, 2017. 12(9): p. e141-e143.DOI: 10.1016/j.jtho.2017.04.028.
218. Wolff, A.C., M.E.H. Hammond, K.H. Allison, B.E. Harvey, P.B. Mangu, J.M.S. Bartlett, M. Bilous, I.O. Ellis, P. Fitzgibbons, W. Hanna, R.B. Jenkins, M.F. Press, P.A. Spears, G.H. Vance, G. Viale, L.M. McShane, and M. Dowsett, Human Epidermal Growth Factor Receptor 2 Testing in Breast Cancer: American Society of Clinical

Oncology/College of American Pathologists Clinical Practice Guideline Focused Update. *J Clin Oncol*, 2018. 36(20): p. 2105-2122.DOI: 10.1200/JCO.2018.77.8738.
219. Schildgen, V., O. Pabst, R.L. Tillmann, J. Lusebrink, O. Schildgen, C. Ludwig, M. Brockmann, and E. Stoelben, Low frequency of EGFR mutations in pleural mesothelioma patients, Cologne, Germany. *Appl Immunohistochem Mol Morphol*, 2015. 23(2): p. 118-25.DOI: 10.1097/PDM.0b013e3182a3645e.
220. PubChem. Bethesda (MD): National Library of Medicine (US), N.C.f.B.I. *PubChem Compound Summary for CID 56839178*. 2004. Available from: https://pubchem.ncbi.nlm.nih.gov/compound/Dubermatinib.
221. Yang, H., H.R. Lawrence, A. Kazi, H. Gevariya, R. Patel, Y. Luo, U. Rix, E. Schonbrunn, N.J. Lawrence, and S.M. Sebti, Dual Aurora A and JAK2 kinase blockade effectively suppresses malignant transformation. *Oncotarget*, 2014. 5(10): p. 2947-61.DOI: 10.18632/oncotarget.1615.
222. Huelse, J.M., D.M. Fridlyand, S. Earp, D. DeRyckere, and D.K. Graham, MERTK in cancer therapy: Targeting the receptor tyrosine kinase in tumor cells and the immune system. *Pharmacol Ther*, 2020. 213: p. 107577.DOI: 10.1016/j.pharmthera.2020.107577.
223. DeRyckere, D., J.M. Huelse, H.S. Earp, and D.K. Graham, TAM family kinases as therapeutic targets at the interface of cancer and immunity. *Nat Rev Clin Oncol*, 2023. 20(11): p. 755-779.DOI: 10.1038/s41571-023-00813-7.
224. Zhang, Y., E.N. Arner, A. Rizvi, J.E. Toombs, H. Huang, S.L. Warner, J.M. Foulks, and R.A. Brekken, AXL Inhibitor TP-0903 Reduces Metastasis and Therapy Resistance in Pancreatic Cancer. *Mol Cancer Ther*, 2022. 21(1): p. 38-47.DOI: 10.1158/1535-7163.MCT-21-0293.
225. ClinicalTrials.gov. *A Phase 1a / 1b, First-in-human, Open-label, Dose-escalation, Safety, Pharmacokinetic, and Pharmacodynamic Study of Oral TP-0903 Administered Daily for 21 Days to Patients With Advanced Solid Tumors*. 2016. Available from: https://clinicaltrials.gov/study/NCT02729298?a=14&tab=history#document-section-card.
226. Engelsen, A.S.T., M.L. Lotsberg, R. Abou Khouzam, J.P. Thiery, J.B. Lorens, S. Chouaib, and S. Terry, Dissecting the Role of AXL in Cancer Immune Escape and Resistance to Immune Checkpoint Inhibition. *Front Immunol*, 2022. 13: p. 869676.DOI: 10.3389/fimmu.2022.869676.
227. Tang, Y., H. Zang, Q. Wen, and S. Fan, AXL in cancer: a modulator of drug resistance and therapeutic target. *J Exp Clin Cancer Res*, 2023. 42(1): p. 148.DOI: 10.1186/s13046-023-02726-w.
228. Terenziani, R., S. Zoppi, C. Fumarola, R. Alfieri, and M. Bonelli, Immunotherapeutic Approaches in Malignant Pleural Mesothelioma. *Cancers (Basel)*, 2021. 13(11).DOI: 10.3390/cancers13112793.
229. PubChem. Bethesda (MD): National Library of Medicine (US), N.C.f.B.I. *PubChem Compound Summary for CID 78260, 1,2,4,5-Benzenetetramine tetrahydrochloride*. 2004. Available from: https://pubchem.ncbi.nlm.nih.gov/compound/1_2_4_5-Benzenetetramine-tetrahydrochloride.

230. Zhang, H., H. Shao, V.M. Golubovskaya, H. Chen, W. Cance, A.A. Adjei, and G.K. Dy, Efficacy of focal adhesion kinase inhibition in non-small cell lung cancer with oncogenically activated MAPK pathways. *Br J Cancer*, 2016. 115(2): p. 203-11.DOI: 10.1038/bjc.2016.190.
231. Catalano, A., M. Romano, I. Robuffo, L. Strizzi, and A. Procopio, Methionine aminopeptidase-2 regulates human mesothelioma cell survival: role of Bcl-2 expression and telomerase activity. *Am J Pathol*, 2001. 159(2): p. 721-31.DOI: 10.1016/S0002-9440(10)61743-9.
232. Reale, F.R., T.W. Griffin, J.M. Compton, S. Graham, P.L. Townes, and A. Bogden, Characterization of a human malignant mesothelioma cell line (H-MESO-1): a biphasic solid and ascitic tumor model. *Cancer Res*, 1987. 47(12): p. 3199-205.
233. Goodglick, L.A., C.A. Vaslet, N.J. Messier, and A.B. Kane, Growth factor responses and protooncogene expression of murine mesothelial cell lines derived from asbestos-induced mesotheliomas. *Toxicol Pathol*, 1997. 25(6): p. 565-73.DOI: 10.1177/019262339702500605.
234. Benvenuto, M., L. Masuelli, E. De Smaele, M. Fantini, R. Mattera, D. Cucchi, E. Bonanno, E. Di Stefano, G.V. Frajese, A. Orlandi, I. Screpanti, A. Gulino, A. Modesti, and R. Bei, In vitro and in vivo inhibition of breast cancer cell growth by targeting the Hedgehog/GLI pathway with SMO (GDC-0449) or GLI (GANT-61) inhibitors. *Oncotarget*, 2016. 7(8): p. 9250-70.DOI: 10.18632/oncotarget.7062.
235. Benvenuto, M., R. Mattera, J.I. Sticca, P. Rossi, C. Cipriani, M.G. Giganti, A. Volpi, A. Modesti, L. Masuelli, and R. Bei, Effect of the BH3 Mimetic Polyphenol (-)-Gossypol (AT-101) on the in vitro and in vivo Growth of Malignant Mesothelioma. *Front Pharmacol*, 2018. 9: p. 1269.DOI: 10.3389/fphar.2018.01269.
236. Masuelli, L., M. Benvenuto, V. Izzi, E. Zago, R. Mattera, B. Cerbelli, V. Potenza, S. Fazi, S. Ciuffa, I. Tresoldi, E. Lucarelli, A. Modesti, and R. Bei, In vivo and in vitro inhibition of osteosarcoma growth by the pan Bcl-2 inhibitor AT-101. *Invest New Drugs*, 2020. 38(3): p. 675-689.DOI: 10.1007/s10637-019-00827-y.
237. Masuelli, L., E. Di Stefano, M. Fantini, R. Mattera, M. Benvenuto, L. Marzocchella, P. Sacchetti, C. Focaccetti, R. Bernardini, I. Tresoldi, V. Izzi, M. Mattei, G.V. Frajese, F. Lista, A. Modesti, and R. Bei, Resveratrol potentiates the in vitro and in vivo anti-tumoral effects of curcumin in head and neck carcinomas. *Oncotarget*, 2014. 5(21): p. 10745-62.DOI: 10.18632/oncotarget.2534.
238. Long, S., Y. Wang, Y. Chen, T. Fang, Y. Yao, and K. Fu, Pan-cancer analysis of cuproptosis regulation patterns and identification of mTOR-target responder in clear cell renal cell carcinoma. *Biol Direct*, 2022. 17(1): p. 28.DOI: 10.1186/s13062-022-00340-y.
239. Brauns, S.C., G. Dealtry, P. Milne, R. Naude, and M. Van de Venter, Caspase-3 activation and induction of PARP cleavage by cyclic dipeptide cyclo(Phe-Pro) in HT-29 cells. *Anticancer Res*, 2005. 25(6B): p. 4197-202.
240. D'Amours, D., F.R. Sallmann, V.M. Dixit, and G.G. Poirier, Gain-of-function of poly(ADP-ribose) polymerase-1 upon cleavage by apoptotic proteases: implications for apoptosis. *J Cell Sci*, 2001. 114(Pt 20): p. 3771-8.DOI: 10.1242/jcs.114.20.3771.

241. Podhorecka, M., A. Skladanowski, and P. Bozko, H2AX Phosphorylation: Its Role in DNA Damage Response and Cancer Therapy. *J Nucleic Acids*, 2010. 2010.DOI: 10.4061/2010/920161.
242. Rogakou, E.P., W. Nieves-Neira, C. Boon, Y. Pommier, and W.M. Bonner, Initiation of DNA fragmentation during apoptosis induces phosphorylation of H2AX histone at serine 139. *J Biol Chem*, 2000. 275(13): p. 9390-5.DOI: 10.1074/jbc.275.13.9390.
243. Di Lernia, G., P. Leone, A.G. Solimando, A. Buonavoglia, I. Saltarella, R. Ria, P. Ditonno, N. Silvestris, L. Crudele, A. Vacca, and V. Racanelli, Bortezomib Treatment Modulates Autophagy in Multiple Myeloma. *J Clin Med*, 2020. 9(2).DOI: 10.3390/jcm9020552.
244. Belloni, D., L. Veschini, C. Foglieni, G. Dell'Antonio, F. Caligaris-Cappio, M. Ferrarini, and E. Ferrero, Bortezomib induces autophagic death in proliferating human endothelial cells. *Exp Cell Res*, 2010. 316(6): p. 1010-8.DOI: 10.1016/j.yexcr.2009.11.005.
245. Jiang, P. and N. Mizushima, LC3- and p62-based biochemical methods for the analysis of autophagy progression in mammalian cells. *Methods*, 2015. 75: p. 13-8.DOI: 10.1016/j.ymeth.2014.11.021.
246. Kang, R., H.J. Zeh, M.T. Lotze, and D. Tang, The Beclin 1 network regulates autophagy and apoptosis. *Cell Death Differ*, 2011. 18(4): p. 571-80.DOI: 10.1038/cdd.2010.191.
247. Chen, X., C. Shi, M. He, S. Xiong, and X. Xia, Endoplasmic reticulum stress: molecular mechanism and therapeutic targets. *Signal Transduct Target Ther*, 2023. 8(1): p. 352.DOI: 10.1038/s41392-023-01570-w.
248. Ron, D. and P. Walter, Signal integration in the endoplasmic reticulum unfolded protein response. *Nat Rev Mol Cell Biol*, 2007. 8(7): p. 519-29.DOI: 10.1038/nrm2199.
249. Ibrahim, I.M., D.H. Abdelmalek, and A.A. Elfiky, GRP78: A cell's response to stress. *Life Sci*, 2019. 226: p. 156-163.DOI: 10.1016/j.lfs.2019.04.022.
250. Hu, H., M. Tian, C. Ding, and S. Yu, The C/EBP Homologous Protein (CHOP) Transcription Factor Functions in Endoplasmic Reticulum Stress-Induced Apoptosis and Microbial Infection. *Front Immunol*, 2018. 9: p. 3083.DOI: 10.3389/fimmu.2018.03083.
251. Heintz, N.H., Y.M. Janssen-Heininger, and B.T. Mossman, Asbestos, lung cancers, and mesotheliomas: from molecular approaches to targeting tumor survival pathways. *Am J Respir Cell Mol Biol*, 2010. 42(2): p. 133-9.DOI: 10.1165/rcmb.2009-0206TR.
252. Wang, Y., A.K. Rishi, V.T. Puliyappadamba, S. Sharma, H. Yang, A. Tarca, Q.P. Dou, F. Lonardo, J.C. Ruckdeschel, H.I. Pass, and A. Wali, Targeted proteasome inhibition by Velcade induces apoptosis in human mesothelioma and breast cancer cell lines. *Cancer Chemother Pharmacol*, 2010. 66(3): p. 455-66.DOI: 10.1007/s00280-009-1181-8.
253. Tomasetti, M., M. Amati, L. Santarelli, R. Alleva, and J. Neuzil, Malignant mesothelioma: biology, diagnosis and therapeutic approaches. *Curr Mol Pharmacol*, 2009. 2(2): p. 190-206.DOI: 10.2174/1874467210902020190.

254. Urso, L., I. Cavallari, E. Sharova, F. Ciccarese, G. Pasello, and V. Ciminale, Metabolic rewiring and redox alterations in malignant pleural mesothelioma. *Br J Cancer*, 2020. 122(1): p. 52-61.DOI: 10.1038/s41416-019-0661-9.
255. Chia, P.L., S. Parakh, P. Russell, H.K. Gan, K. Asadi, V. Gebski, C. Murone, M. Walkiewicz, Z. Liu, B. Thapa, F.E. Scott, A.M. Scott, and T. John, Expression of EGFR and conformational forms of EGFR in malignant pleural mesothelioma and its impact on survival. *Lung Cancer*, 2021. 153: p. 35-41.DOI: 10.1016/j.lungcan.2020.12.028.
256. Singh, A.S., R. Heery, and S.G. Gray, In Silico and In Vitro Analyses of LncRNAs as Potential Regulators in the Transition from the Epithelioid to Sarcomatoid Histotype of Malignant Pleural Mesothelioma (MPM). *Int J Mol Sci*, 2018. 19(5).DOI: 10.3390/ijms19051297.
257. Beasley, M.B., F. Galateau-Salle, and S. Dacic, Pleural mesothelioma classification update. *Virchows Arch*, 2021. 478(1): p. 59-72.DOI: 10.1007/s00428-021-03031-7.
258. Moberg, H.L., I. Gramer, I. Schofield, L. Blackwood, D. Killick, S.L. Priestnall, and A. Guillen, Clinical presentation, treatment and outcome of canine malignant mesothelioma: A retrospective study of 34 cases. *Vet Comp Oncol*, 2022. 20(1): p. 304-312.DOI: 10.1111/vco.12777.
259. Gray, S.G., D.A. Fennell, L. Mutti, and K.J. O'Byrne, In arrayed ranks: array technology in the study of mesothelioma. *J Thorac Oncol*, 2009. 4(3): p. 411-25.DOI: 10.1097/JTO.0b013e3181951ce8.
260. Zalcman, G., J. Mazieres, J. Margery, L. Greillier, C. Audigier-Valette, D. Moro-Sibilot, O. Molinier, R. Corre, I. Monnet, V. Gounant, F. Riviere, H. Janicot, R. Gervais, C. Locher, B. Milleron, Q. Tran, M.P. Lebitasy, F. Morin, C. Creveuil, J.J. Parienti, A. Scherpereel, and I. French Cooperative Thoracic, Bevacizumab for newly diagnosed pleural mesothelioma in the Mesothelioma Avastin Cisplatin Pemetrexed Study (MAPS): a randomised, controlled, open-label, phase 3 trial. *Lancet*, 2016. 387(10026): p. 1405-1414.DOI: 10.1016/S0140-6736(15)01238-6.
261. Brigand, C., O. Monneuse, F. Mohamed, A.C. Sayag-Beaujard, S. Isaac, F.N. Gilly, and O. Glehen, Peritoneal mesothelioma treated by cytoreductive surgery and intraperitoneal hyperthermic chemotherapy: results of a prospective study. *Ann Surg Oncol*, 2006. 13(3): p. 405-12.DOI: 10.1245/ASO.2006.05.041.
262. Favoni, R.E. and T. Florio, Combined chemotherapy with cytotoxic and targeted compounds for the management of human malignant pleural mesothelioma. *Trends Pharmacol Sci*, 2011. 32(8): p. 463-79.DOI: 10.1016/j.tips.2011.03.011.
263. Alessandrini, L., T. Perin, S. Kadare, L. Del Pup, L. Memeo, A. Steffan, L. Colarossi, M. Berretta, P. De Paoli, and V. Canzonieri, Cancer Targeted Therapy Strategy: The Pathologist's Perspectives. *Curr Cancer Drug Targets*, 2018. 18(5): p. 410-420.DOI: 10.2174/1568009618666171129145703.
264. Disselhorst, M.J. and P. Baas, Chemotherapy options versus "novel" therapies: how should we treat patients with malignant pleural mesothelioma. *Transl Lung Cancer Res*, 2020. 9(Suppl 1): p. S77-S85.DOI: 10.21037/tlcr.2020.01.16.

265. Palumbo, C., R. Bei, A. Procopio, and A. Modesti, Molecular targets and targeted therapies for malignant mesothelioma. *Curr Med Chem*, 2008. 15(9): p. 855-67.DOI: 10.2174/092986708783955446.
266. Cantini, L., R. Hassan, D.H. Sterman, and J. Aerts, Emerging Treatments for Malignant Pleural Mesothelioma: Where Are We Heading? *Front Oncol*, 2020. 10: p. 343.DOI: 10.3389/fonc.2020.00343.
267. Porpodis, K., P. Zarogoulidis, E. Boutsikou, A. Papaioannou, N. Machairiotis, K. Tsakiridis, N. Katsikogiannis, B. Zaric, B. Perin, H. Huang, I. Kougioumtzi, D. Spyratos, and K. Zarogoulidis, Malignant pleural mesothelioma: current and future perspectives. *J Thorac Dis*, 2013. 5 Suppl 4(Suppl 4): p. S397-406.DOI: 10.3978/j.issn.2072-1439.2013.08.08.
268. Yamamoto, S. and N. Egashira, Pathological Mechanisms of Bortezomib-Induced Peripheral Neuropathy. *Int J Mol Sci*, 2021. 22(2).DOI: 10.3390/ijms22020888.
269. Sullivan, I. and D. Planchard, Next-Generation EGFR Tyrosine Kinase Inhibitors for Treating EGFR-Mutant Lung Cancer beyond First Line. *Front Med (Lausanne)*, 2016. 3: p. 76.DOI: 10.3389/fmed.2016.00076.
270. Velcheti, V., Y. Kasai, A.K. Viswanathan, J. Ritter, and R. Govindan, Absence of mutations in the epidermal growth factor receptor (EGFR) kinase domain in patients with mesothelioma. *J Thorac Oncol*, 2009. 4(4): p. 559.DOI: 10.1097/JTO.0b013e31819c8661.
271. Sang, Y.B., J.H. Kim, C.G. Kim, M.H. Hong, H.R. Kim, B.C. Cho, and S.M. Lim, The Development of AXL Inhibitors in Lung Cancer: Recent Progress and Challenges. *Front Oncol*, 2022. 12: p. 811247.DOI: 10.3389/fonc.2022.811247.
272. Heffler, M., V.M. Golubovskaya, J. Conroy, S. Liu, D. Wang, W.G. Cance, and K.B. Dunn, FAK and HAS inhibition synergistically decrease colon cancer cell viability and affect expression of critical genes. *Anticancer Agents Med Chem*, 2013. 13(4): p. 584-94.DOI: 10.2174/1871520611313040008.
273. Sartore-Bianchi, A., F. Gasparri, A. Galvani, L. Nici, J.W. Darnowski, D. Barbone, D.A. Fennell, G. Gaudino, C. Porta, and L. Mutti, Bortezomib inhibits nuclear factor-kappaB dependent survival and has potent in vivo activity in mesothelioma. *Clin Cancer Res*, 2007. 13(19): p. 5942-51.DOI: 10.1158/1078-0432.CCR-07-0536.
274. Venkatakrishnan, K., M. Rader, R.K. Ramanathan, S. Ramalingam, E. Chen, W. Riordan, W. Trepicchio, M. Cooper, M. Karol, L. von Moltke, R. Neuwirth, M. Egorin, and G. Chatta, Effect of the CYP3A inhibitor ketoconazole on the pharmacokinetics and pharmacodynamics of bortezomib in patients with advanced solid tumors: a prospective, multicenter, open-label, randomized, two-way crossover drug-drug interaction study. *Clin Ther*, 2009. 31 Pt 2: p. 2444-58.DOI: 10.1016/j.clinthera.2009.11.012.
275. Sazonova, E.V., S.V. Petrichuk, G.S. Kopeina, and B. Zhivotovsky, A link between mitotic defects and mitotic catastrophe: detection and cell fate. *Biol Direct*, 2021. 16(1): p. 25.DOI: 10.1186/s13062-021-00313-7.
276. Walter, R.F.H., S.R. Sydow, E. Berg, J. Kollmeier, D.C. Christoph, S. Christoph, W.E.E. Eberhardt, T. Mairinger, J. Wohlschlaeger, K.W. Schmid, and F.D. Mairinger,

Bortezomib sensitivity is tissue dependent and high expression of the 20S proteasome precludes good response in malignant pleural mesothelioma. *Cancer Manag Res*, 2019. 11: p. 8711-8720.DOI: 10.2147/CMAR.S194337.
277. Busacca, S., A.D. Chacko, A. Klabatsa, K. Arthur, M. Sheaff, D. Barbone, L. Mutti, V.K. Gunasekharan, J.J. Gorski, M. El-Tanani, V.C. Broaddus, G. Gaudino, and D.A. Fennell, BAK and NOXA are critical determinants of mitochondrial apoptosis induced by bortezomib in mesothelioma. *PLoS One*, 2013. 8(6): p. e65489.DOI: 10.1371/journal.pone.0065489.
278. Kao, C., A. Chao, C.L. Tsai, W.C. Chuang, W.P. Huang, G.C. Chen, C.Y. Lin, T.H. Wang, H.S. Wang, and C.H. Lai, Bortezomib enhances cancer cell death by blocking the autophagic flux through stimulating ERK phosphorylation. *Cell Death Dis*, 2014. 5(11): p. e1510.DOI: 10.1038/cddis.2014.468.
279. Bonsignore, G., S. Martinotti, and E. Ranzato, Endoplasmic Reticulum Stress and Cancer: Could Unfolded Protein Response Be a Druggable Target for Cancer Therapy? *Int J Mol Sci*, 2023. 24(2).DOI: 10.3390/ijms24021566.
280. Hetz, C., K. Zhang, and R.J. Kaufman, Mechanisms, regulation and functions of the unfolded protein response. *Nat Rev Mol Cell Biol*, 2020. 21(8): p. 421-438.DOI: 10.1038/s41580-020-0250-z.
281. Dalton, L.E., H.J. Clarke, J. Knight, M.H. Lawson, J. Wason, D.A. Lomas, W.J. Howat, R.C. Rintoul, D.M. Rassl, and S.J. Marciniak, The endoplasmic reticulum stress marker CHOP predicts survival in malignant mesothelioma. *Br J Cancer*, 2013. 108(6): p. 1340-7.DOI: 10.1038/bjc.2013.66.
282. Zhang, L., J.E. Littlejohn, Y. Cui, X. Cao, C. Peddaboina, and W.R. Smythe, Characterization of bortezomib-adapted I-45 mesothelioma cells. *Mol Cancer*, 2010. 9: p. 110.DOI: 10.1186/1476-4598-9-110.
283. Wang, G., F. Fan, C. Sun, and Y. Hu, Looking into Endoplasmic Reticulum Stress: The Key to Drug-Resistance of Multiple Myeloma? *Cancers (Basel)*, 2022. 14(21).DOI: 10.3390/cancers14215340.
284. Xu, D., H. Yang, Z. Yang, S. Berezowska, Y. Gao, S.Q. Liang, T.M. Marti, S.R.R. Hall, P. Dorn, G.J. Kocher, R.A. Schmid, and R.W. Peng, Endoplasmic Reticulum Stress Signaling as a Therapeutic Target in Malignant Pleural Mesothelioma. *Cancers (Basel)*, 2019. 11(10).DOI: 10.3390/cancers11101502.
285. Chia, P.L., A.M. Scott, and T. John, Epidermal growth factor receptor (EGFR)-targeted therapies in mesothelioma. *Expert Opin Drug Deliv*, 2019. 16(4): p. 441-451.DOI: 10.1080/17425247.2019.1598374.
286. Kesarwala, A.H., M.M. Samrakandi, and D. Piwnica-Worms, Proteasome inhibition blocks ligand-induced dynamic processing and internalization of epidermal growth factor receptor via altered receptor ubiquitination and phosphorylation. *Cancer Res*, 2009. 69(3): p. 976-83.DOI: 10.1158/0008-5472.CAN-08-2938.
287. Luan, H., T.A. Bailey, R.J. Clubb, B.C. Mohapatra, A.M. Bhat, S. Chakraborty, N. Islam, I. Mushtaq, M.D. Storck, S.M. Raja, V. Band, and H. Band, CHIP/STUB1 Ubiquitin Ligase Functions as a Negative Regulator of ErbB2 by Promoting Its Early

Post-Biosynthesis Degradation. *Cancers (Basel)*, 2021. 13(16).DOI: 10.3390/cancers13163936.
288. Huynh, T.K., C.Y. Ho, C.H. Tsai, C.K. Wang, Y.J. Chen, D.T. Bau, C.Y. Tu, T.S. Li, and W.C. Huang, Proteasome Inhibitors Suppress ErbB Family Expression through HSP90-Mediated Lysosomal Degradation. *Int J Mol Sci*, 2019. 20(19).DOI: 10.3390/ijms20194812.
289. Chen, K.F., P.Y. Yeh, K.H. Yeh, Y.S. Lu, S.Y. Huang, and A.L. Cheng, Down-regulation of phospho-Akt is a major molecular determinant of bortezomib-induced apoptosis in hepatocellular carcinoma cells. *Cancer Res*, 2008. 68(16): p. 6698-707.DOI: 10.1158/0008-5472.CAN-08-0257.
290. Mimura, N., T. Hideshima, T. Shimomura, R. Suzuki, H. Ohguchi, O. Rizq, S. Kikuchi, Y. Yoshida, F. Cottini, J. Jakubikova, D. Cirstea, G. Gorgun, J. Minami, Y.T. Tai, P.G. Richardson, T. Utsugi, A. Iwama, and K.C. Anderson, Selective and potent Akt inhibition triggers anti-myeloma activities and enhances fatal endoplasmic reticulum stress induced by proteasome inhibition. *Cancer Res*, 2014. 74(16): p. 4458-69.DOI: 10.1158/0008-5472.CAN-13-3652.
291. Ni, M., Y. Zhang, and A.S. Lee, Beyond the endoplasmic reticulum: atypical GRP78 in cell viability, signalling and therapeutic targeting. *Biochem J*, 2011. 434(2): p. 181-8.DOI: 10.1042/BJ20101569.
292. Hyoda, K., T. Hosoi, N. Horie, Y. Okuma, K. Ozawa, and Y. Nomura, PI3K-Akt inactivation induced CHOP expression in endoplasmic reticulum-stressed cells. *Biochem Biophys Res Commun*, 2006. 340(1): p. 286-90.DOI: 10.1016/j.bbrc.2005.12.007.
293. He, Y., M.M. Sun, G.G. Zhang, J. Yang, K.S. Chen, W.W. Xu, and B. Li, Targeting PI3K/Akt signal transduction for cancer therapy. *Signal Transduct Target Ther*, 2021. 6(1): p. 425.DOI: 10.1038/s41392-021-00828-5.
294. Masuelli, L., M. Benvenuto, E. Di Stefano, R. Mattera, M. Fantini, G. De Feudis, E. De Smaele, I. Tresoldi, M.G. Giganti, A. Modesti, and R. Bei, Curcumin blocks autophagy and activates apoptosis of malignant mesothelioma cell lines and increases the survival of mice intraperitoneally transplanted with a malignant mesothelioma cell line. *Oncotarget*, 2017. 8(21): p. 34405-34422.DOI: 10.18632/oncotarget.14907.
295. Masuelli, L., M. Benvenuto, R. Mattera, E. Di Stefano, E. Zago, G. Taffera, I. Tresoldi, M.G. Giganti, G.V. Frajese, G. Berardi, A. Modesti, and R. Bei, In Vitro and In Vivo Anti-tumoral Effects of the Flavonoid Apigenin in Malignant Mesothelioma. *Front Pharmacol*, 2017. 8: p. 373.DOI: 10.3389/fphar.2017.00373.
296. Harber, J., T. Kamata, C. Pritchard, and D. Fennell, Matter of TIME: the tumor-immune microenvironment of mesothelioma and implications for checkpoint blockade efficacy. *J Immunother Cancer*, 2021. 9(9).DOI: 10.1136/jitc-2021-003032.
297. Hegmans, J.P., A. Hemmes, H. Hammad, L. Boon, H.C. Hoogsteden, and B.N. Lambrecht, Mesothelioma environment comprises cytokines and T-regulatory cells that suppress immune responses. *Eur Respir J*, 2006. 27(6): p. 1086-95.DOI: 10.1183/09031936.06.00135305.
298. Klampatsa, A., S.M. O'Brien, J.C. Thompson, A.S. Rao, J.E. Stadanlick, M.C. Martinez, M. Liousia, E. Cantu, K. Cengel, E.K. Moon, S. Singhal, E.B. Eruslanov, and S.M.

Albelda, Phenotypic and functional analysis of malignant mesothelioma tumor-infiltrating lymphocytes. *Oncoimmunology*, 2019. 8(9): p. e1638211.DOI: 10.1080/2162402X.2019.1638211.

299. Pasello, G., G. Zago, F. Lunardi, L. Urso, I. Kern, G. Vlacic, F. Grosso, M. Mencoboni, G.L. Ceresoli, M. Schiavon, F. Pezzuto, A. Pavan, S.E. Vuljan, P. Del Bianco, P. Conte, F. Rea, and F. Calabrese, Malignant pleural mesothelioma immune microenvironment and checkpoint expression: correlation with clinical-pathological features and intratumor heterogeneity over time. *Ann Oncol*, 2018. 29(5): p. 1258-1265.DOI: 10.1093/annonc/mdy086.
300. Yang, H., S. Berezowska, P. Dorn, P. Zens, P. Chen, R.W. Peng, T.M. Marti, G.J. Kocher, R.A. Schmid, and S.R.R. Hall, Tumor-infiltrating lymphocytes are functionally inactivated by CD90+ stromal cells and reactivated by combined Ibrutinib and Rapamycin in human pleural mesothelioma. *Theranostics*, 2022. 12(1): p. 167-185.DOI: 10.7150/thno.61209.
301. Pellom, S.T., Jr., A. Singhal, and A. Shanker, Prospects of combining adoptive cell immunotherapy with bortezomib. *Immunotherapy*, 2017. 9(4): p. 305-308.DOI: 10.2217/imt-2017-0015.
302. Renrick, A.N., M.C. Thounaojam, M.T.P. de Aquino, E. Chaudhuri, J. Pandhare, C. Dash, and A. Shanker, Bortezomib Sustains T Cell Function by Inducing miR-155-Mediated Downregulation of SOCS1 and SHIP1. *Front Immunol*, 2021. 12: p. 607044.DOI: 10.3389/fimmu.2021.607044.
303. Fennell, D.A., C. McDowell, S. Busacca, G. Webb, B. Moulton, A. Cakana, K.J. O'Byrne, J.V. Meerbeeck, P. Donnellan, J. McCaffrey, and P. Baas, Phase II clinical trial of first or second-line treatment with bortezomib in patients with malignant pleural mesothelioma. *J Thorac Oncol*, 2012. 7(9): p. 1466-70.DOI: 10.1097/JTO.0b013e318260dfb9.
304. O'Brien, M.E., R.M. Gaafar, S. Popat, F. Grossi, A. Price, D.C. Talbot, T. Cufer, C. Ottensmeier, S. Danson, A. Pallis, B. Hasan, J.P. Van Meerbeeck, and P. Baas, Phase II study of first-line bortezomib and cisplatin in malignant pleural mesothelioma and prospective validation of progression free survival rate as a primary end-point for mesothelioma clinical trials (European Organisation for Research and Treatment of Cancer 08052). *Eur J Cancer*, 2013. 49(13): p. 2815-22.DOI: 10.1016/j.ejca.2013.05.008.
305. Jandial, D.A., W.E. Brady, S.B. Howell, H.A. Lankes, R.J. Schilder, J.H. Beumer, S.M. Christner, S. Strychor, M.A. Powell, A.R. Hagemann, K.N. Moore, J.L. Walker, P.A. DiSilvestro, L.R. Duska, P.M. Fracasso, and D.S. Dizon, A phase I pharmacokinetic study of intraperitoneal bortezomib and carboplatin in patients with persistent or recurrent ovarian cancer: An NRG Oncology/Gynecologic Oncology Group study. *Gynecol Oncol*, 2017. 145(2): p. 236-242.DOI: 10.1016/j.ygyno.2017.03.013.
306. Klanova, M., P. Klener, M. Trneny, J. Straub, and I. Spicka, Intrapleural bortezomib for the therapy of myelomatous pleural effusion: a case report. *Case Reports Immunol*, 2012. 2012: p. 978479.DOI: 10.1155/2012/978479.

307. Liu, J., R. Zhao, X. Jiang, Z. Li, and B. Zhang, Progress on the Application of Bortezomib and Bortezomib-Based Nanoformulations. *Biomolecules*, 2021. 12(1).DOI: 10.3390/biom12010051.
308. Guazzelli, A., P. Meysami, E. Bakker, C. Demonacos, A. Giordano, M. Krstic-Demonacos, and L. Mutti, BAP1 Status Determines the Sensitivity of Malignant Mesothelioma Cells to Gemcitabine Treatment. *Int J Mol Sci*, 2019. 20(2).DOI: 10.3390/ijms20020429.
309. Hirosawa, T., M. Ishida, K. Ishii, K. Kanehara, K. Kudo, S. Ohnuma, T. Kamei, F. Motoi, T. Naitoh, F.M. Selaru, and M. Unno, Loss of BAP1 expression is associated with genetic mutation and can predict outcomes in gallbladder cancer. *PLoS One*, 2018. 13(11): p. e0206643.DOI: 10.1371/journal.pone.0206643.
310. Gao, J., H.R. Li, C. Jin, J.H. Jiang, and J.Y. Ding, Strategies to overcome acquired resistance to EGFR TKI in the treatment of non-small cell lung cancer. *Clin Transl Oncol*, 2019. 21(10): p. 1287-1301.DOI: 10.1007/s12094-019-02075-1.
311. Huang, L. and L. Fu, Mechanisms of resistance to EGFR tyrosine kinase inhibitors. *Acta Pharm Sin B*, 2015. 5(5): p. 390-401.DOI: 10.1016/j.apsb.2015.07.001.
312. Barozzi, D. and C. Scielzo, Emerging Strategies in 3D Culture Models for Hematological Cancers. *Hemasphere*, 2023. 7(8): p. e932.DOI: 10.1097/HS9.0000000000000932.
313. Rolver, M.G., L.O. Elingaard-Larsen, and S.F. Pedersen, Assessing Cell Viability and Death in 3D Spheroid Cultures of Cancer Cells. *J Vis Exp*, 2019(148).DOI: 10.3791/59714.
314. Yu, H., M. Gao, Y. Ma, L. Wang, Y. Shen, and X. Liu, Inhibition of cell migration by focal adhesion kinase: Time-dependent difference in integrin-induced signaling between endothelial and hepatoblastoma cells. *Int J Mol Med*, 2018. 41(5): p. 2573-2588.DOI: 10.3892/ijmm.2018.3512.
315. Wang, D., L. Bi, J. Ran, L. Zhang, N. Xiao, and X. Li, Gas6/Axl signaling pathway promotes proliferation, migration and invasion and inhibits apoptosis in A549 cells. *Exp Ther Med*, 2021. 22(5): p. 1321.DOI: 10.3892/etm.2021.10756.
316. Pouliquen, D.L., B. Nawrocki-Raby, J. Nader, S. Blandin, M. Robard, P. Birembaut, and M. Gregoire, Evaluation of intracavitary administration of curcumin for the treatment of sarcomatoid mesothelioma. *Oncotarget*, 2017. 8(34): p. 57552-57573.DOI: 10.18632/oncotarget.15744.
317. Hocking, A.J., A.L. Farrall, S. Newhouse, P. Sordillo, K. Greco, C.S. Karapetis, B. Dougherty, and S. Klebe, Study protocol of a phase 1 clinical trial establishing the safety of intrapleural administration of liposomal curcumin: curcumin as a palliative treatment for malignant pleural effusion (IPAL-MPE). *BMJ Open*, 2021. 11(3): p. e047075.DOI: 10.1136/bmjopen-2020-047075.